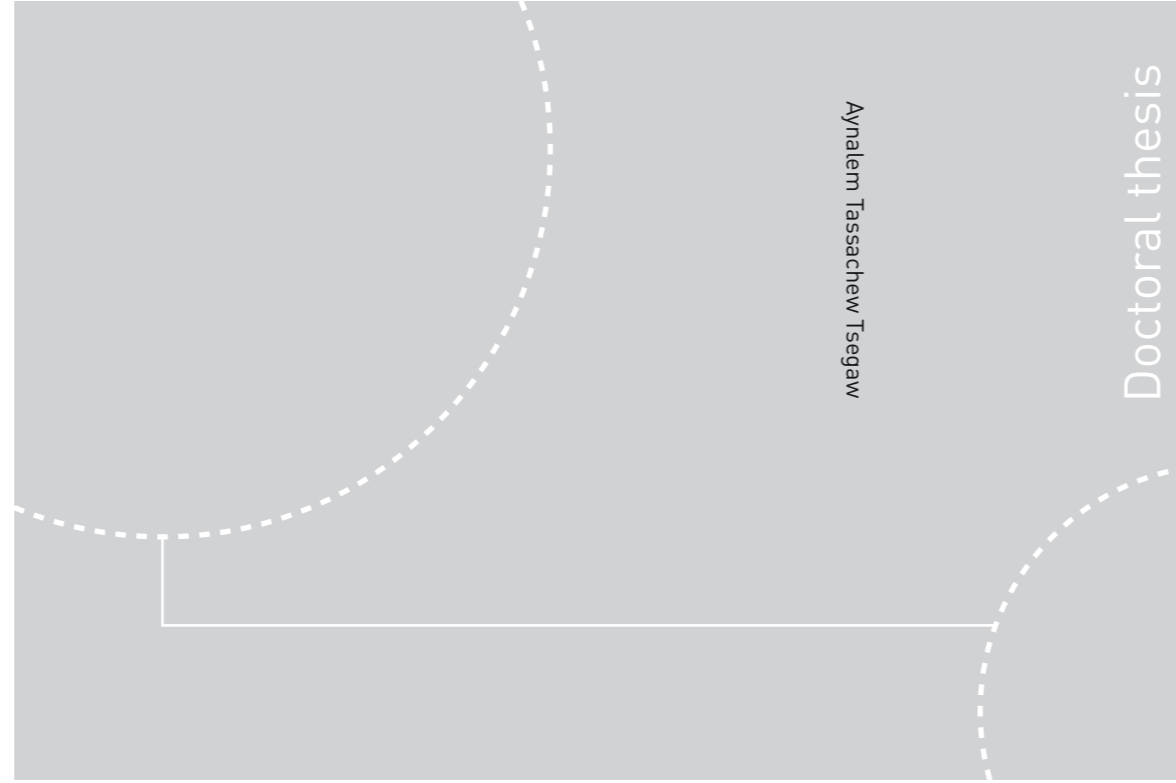


ISBN 978-82-326-4240-3 (printed ver.)  
ISBN 978-82-326-4241-0 (electronic ver.)  
ISSN 1503-8181



Doctoral theses at NTNU, 2019:322

Aynalem Tassachew Tsegaw

# Predicting flows in ungauged small rural catchments using hydrological modelling

 **NTNU**  
Norwegian University of  
Science and Technology

**NTNU**  
Norwegian University of Science and Technology  
Thesis for the Degree of  
Philosophiae Doctor  
Faculty of Engineering  
Department of Civil and Environmental  
Engineering

Doctoral theses at NTNU, 2019:322

 NTNU

 **NTNU**  
Norwegian University of  
Science and Technology

Aynalem Tassachew Tsegaw

# **Predicting flows in ungauged small rural catchments using hydrological modelling**

Thesis for the Degree of Philosophiae Doctor

Trondheim, November 2019

Norwegian University of Science and Technology  
Faculty of Engineering  
Department of Civil and Environmental Engineering

 **NTNU**  
Norwegian University of  
Science and Technology

**NTNU**

Norwegian University of Science and Technology

Thesis for the Degree of Philosophiae Doctor

Faculty of Engineering

Department of Civil and Environmental Engineering

© Aynalem Tassachew Tsegaw

ISBN 978-82-326-4240-3 (printed ver.)

ISBN 978-82-326-4241-0 (electronic ver.)

ISSN 1503-8181

Doctoral theses at NTNU, 2019:322

Printed by NTNU Grafisk senter

## **PREFACE**

The present thesis is submitted to the Norwegian University of Science and Technology (NTNU) for partial fulfilment of the requirements for the degree of Doctor of Philosophy (Ph.D.).

The research work in this thesis had been conducted at the Department of Civil and Environmental Engineering, NTNU, in Trondheim, mainly under the supervision of Professor Knut Alfredsen, NTNU. Research scientist Thomas Skaugen from Norwegian Water Resources and Energy Directorate (NVE) and Associate professor Tone Merete Muthanna, from the Department of Civil and Environmental Engineering, NTNU were the co-supervisors.

The research was financed as a 3-year Ph.D. position at the department of Civil and Environmental Engineering, NTNU, granted by the Research Council of Norway and several partners through the Centre for Research-based Innovation “Klima 2050 project” (project number 237859). In addition to the Klima 2050 project, the research work has got a financial support from the BINGO project (EU Horizon 2020, grant agreement 641739) for the research work related to hydrological impact of climate change on small catchments.

In accordance with the requirements of the Faculty of Engineering at NTNU, the present thesis comprises an introduction to the research work which is composed of three scientific papers.



## **ACKNOWLEDGMENT**

First and foremost, I would like to thank Almighty God for giving me the strength, knowledge, ability and opportunity to undertake this research work and to complete it satisfactorily. Without his blessings, this achievement would not have been possible.

Secondly, I would like to express my sincere gratitude to my supervisors: Professor Knut Alfredsen, Research Scientist Thomas Skaugen and Associate professor Tone Merete Muthana for the continuous support of my Ph.D. study, for their patience, motivation, and immense knowledge. Their guidance helped me in all the time of the research work and writing of this thesis.

Finally, I would like to thank my family: my parents (my mother: Kelemua G/Mariam and my father: Tassachew Tsegaw) and my brothers and sisters for supporting me throughout studying my Ph.D. degree, writing this thesis and my life in general.

## **ABSTRACT**

Flow data are important information for water resources management such as flood risk management, water utilization, and environmental impact assessment in a changing environment. However, most of the catchments that we are interested in are ungauged which makes a method to predict flow in ungauged catchments an important prerequisite. Reliable estimation of continuous streamflow in ungauged catchments has remained a fundamental challenge in hydrology, although significant insights have been gained in recent years. Flood is the most typical example of natural risk and causes significant economic damage worldwide. Flood risk will become more frequent in the future because of climate and land use changes and may cause increased impacts on human health and economic losses. Growing economic losses are evidence of the increasing intensity of floods draining from small catchments to small watercourses which are usually not sufficiently considered by the flood risk management approaches. Knowledge of hydrological impacts of climate change is essential to aid infrastructure owners in managing the impacts on existing and planned water infrastructures. To provide a meaningful climate impact results at ungauged small rural catchments, it is necessary to use high spatial and temporal resolutions of climate data that can be used to force high resolution hydrological models; however, rainfall-runoff modelling in such catchments is hampered by a lack of both observed discharge and precipitation data and high-resolution climate data. To address the challenges of flood risk management, a parsimonious continuous rainfall-runoff model (Distance Distribution Dynamics) with high resolution climate data has been used as the main tool to predict flow and to study impact of climate change; however, the parameters of the model cannot be obtained by calibration on the flow data and hence need to be obtained by regionalization.

The Distance Distribution Dynamics (DDD) model has been regionalized for 41 gauged small rural catchments in Norway (area  $\leq 50\text{km}^2$ ). Three regionalization methods: multiple regression, physical similarity (single-donor and pooling-group based methods) and a combination of the two methods, are used in this study. Seven independent catchments, which are not used in the regionalisation process, are used for validation of the regionalization methods. The combined method (multiple regression and pooling-group type of physical similarity) performs the best of all methods. The DDD model like many other rainfall-runoff models, underestimates floods in many cases in the continuous simulations. To improve the prediction of flood peaks in a continuous simulation, a dynamic river network method is conceptualized and implemented in the DDD model. The method is applied for 15 catchments in Norway and tested on 91 flood peaks. The performance of the method is evaluated using relative errors and mean absolute relative errors and the simulated flood peaks are improved significantly with the method. The mean absolute relative error of the simulated peaks is reduced from 32.9% (without dynamic river networks) to 15.7% (with dynamic river network method). The 0.75 and 0.25 quantiles of the relative errors of the simulated flood peaks are reduced from 41% to 23% and from 22% to 1% respectively. The regionalized DDD model with dynamic river network has been used to study the hydrological impacts of climate change on six ungauged small rural catchments in Bergen area of Norway using a new high-resolution regional climate projection with improved performance with regards to the precipitation distribution. The results show that in the future period (2070-2100), there will be an increase in the mean annual flow compared to the reference period (1981-2011). The maximum increase is 33.3%, and the minimum increase is 16.5%. The mean autumn, winter and spring flows show an increase for the study catchments and contributed significantly for the increase in mean annual flows, but there will be a decrease in the mean summer flows from the study catchments.

The maximum decrease in the mean summer flow is 35.2% and the minimum decrease is 7.2%. The results also show that the mean annual maximum flows (floods) increases by 28.9% to 38.3% in the future period. The results of the flood frequency analysis show that there will be an increase of floods (16.1% to 42.7%) with a return periods of 2, 5, 10, 20, 25, 50, 100 and 200 years in small rural catchments at Bergen area of Norway.

## CONTENTS

<b>PREFACE</b> .....	1
<b>ACKNOWLEDGMENT</b> .....	2
<b>ABSTRACT</b> .....	3
<b>LIST OF PUBLICATIONS</b> .....	7
<b>CHAPTER ONE</b> .....	8
<i>Introduction</i> .....	8
<i>Small catchments</i> .....	11
<i>Scope of the work</i> .....	12
<b>CHAPTER TWO</b> .....	13
<i>General methods</i> .....	13
<i>Methods in paper I</i> .....	15
<i>Methods in paper II</i> .....	17
<i>Methods in paper III</i> .....	19
<b>CHAPTER THREE</b> .....	23
<i>Summary of results by papers</i> .....	23
<i>Results of paper I</i> .....	23
<i>Results of paper II</i> .....	26
<i>Results of paper III</i> .....	29
<b>CHAPTER FOUR</b> .....	32
<i>Discussion and conclusion</i> .....	32
<i>Recommendations for further work</i> .....	35
<b>REFERENCES</b> .....	36

## LIST OF PUBLICATIONS

This thesis has three scientific papers of which two of them have been published on international peer reviewed journals and the third one is as a manuscript level. The papers are described below:

**Paper I: Predicting hourly flows at ungauged small rural catchments using a parsimonious hydrological model.**

Tsegaw, A. T., Alfredsen, K., Skaugen, T., & Muthanna, T. M. (2019). *Journal of Hydrology*, 573, 855-871. doi:<https://doi.org/10.1016/j.jhydrol.2019.03.090>

**Paper II: A dynamic river network method for the prediction of floods using a parsimonious rainfall-runoff model.**

Tsegaw, A. T., Alfredsen, K., Skaugen, T., & Muthanna, T. M. (2019). *Hydrology Research*, nh2019003. doi: <https://doi.org/10.2166/nh.2019.003>

**Paper III: Hydrological impacts of climate change on small ungauged catchments-results from a GCM-RCM-hydrologic model chain**

Tsegaw, A.T., Kristvik, Erle, Pontoppidan, M., Alfredsen, K., Muthanna, T. M.

*Manuscript*

## CHAPTER ONE

### *Introduction*

Flow data are important to address a range of water resource management challenges including water abstraction and flood risk management. Catchments, where no flow data are available, are termed ungauged and most catchments of the world are ungauged. There are operational and academic drivers for pursuing rainfall-runoff modelling of ungauged catchments (Günter, 2006). The former include design applications (spillways, culverts, and embankments), forecasting operations (flood warning and hydropower operation), and catchment management applications (water allocations, climate impact studies), the later are geared towards understanding the catchment functioning and how the individual processes combined to produce catchment response (Günter, 2006). For ungauged catchments, the parameters of rainfall-runoff models cannot be obtained by the calibration on the flow data and hence need to be obtained by other methods. Regionalization is the most widely used method to date, which relates parameters of the rainfall-runoff model to catchment characteristics (Saliha et al., 2011).

Flood is the most typical example of natural risk and causes significant economic damage worldwide. Flood risk will become more frequent in the future as a result of climate and land use changes and will cause increased impacts on human health and economic losses (Annamo & Kristiansen, 2012; Hall et al., 2014). Increasing intensity of floods on small rural watercourses (flash floods) which are usually not sufficiently considered by the flood risk management approaches and unplanned human settlements in flood-prone areas are among the major causes for increasing economic losses and number of fatalities (Borga et al., 2011; Di Baldassarre et al., 2010;

Jakubínský et al., 2014). For flood risk assessment and management, information about possible extreme floods, is essential and therefore, flood characteristics need to be derived to serve as a bases for inundation map, risk zoning or the design of flood defense infrastructure (Winter et al., 2019). While estimates usually refers to the flood magnitude, the severity of the flood is also defined by the duration and runoff volume of a flooding event (Brunner et al., 2017; Grimaldi et al., 2012; Lamb et al., 2016; Mediero et al., 2010). Uncertainty in the flood estimation methods from small catchments remains high and there is a need to develop and test improved methods for planning appropriate flood risk management strategies under the climate and land use changes (Faulkner et al., 2012).

Impacts of climate change on the ecology, human health and the economy are already apparent and will probably increase in the future. Infrastructure systems, which are required to be operational over very long-time scales are increasingly to experience the impact over their life time. In the future, climate change is expected to increase in the magnitude and hence frequency of extreme events like floods (Asadieh & Krakauer, 2017; Hirabayashi et al., 2013). Knowledge of hydrological impacts of climate change is essential to aid infrastructure owners manage the impacts on both the existing and planned infrastructures (Balston et al., 2017; Rääkkönen et al., 2017). To provide a meaningful climate impact results at small catchments, it is necessary to use high spatial and temporal resolutions of projected climate data that can be used as forcing in high resolution hydrological models (Lespinas et al., 2014; López-Moreno et al., 2013; Reynolds et al., 2015; Tofiq & Guven, 2014); however, getting a high temporal resolution climate data is a challenge.



Water resource management problems are increasingly approached using continuous time rainfall-runoff modelling, rather than the traditional statistical or event-based models (Swain & Patra, 2017; Winter et al., 2019). Continuous simulation methods of flood estimation are better than event-based methods because the event-based methods have the following limitations:

- (i) The return period of design rainfall is identical with the return period of the resulting flood magnitude, which remains questionable.
- (ii) The pre-event catchment state and the design rainfall duration are defined subjectively
- (iii) Not suitable for studying impacts of climate and land use changes on flood risks for proposing adaptation strategies.

Therefore, the continuous simulation methods are promising because of their potential to link the state of the catchment and processes ahead of the flooding event with the flood happening in the catchment to avoid subjective assumptions and to provide full hydrograph characteristics (Lamb et al., 2016). To use such methods for flood estimation at ungauged small rural catchments, we need to follow the following procedures:

- (i) Select an appropriate continuous hydrological model and regionalize the model parameters with high temporal resolution (e.g. hourly).
- (ii) Evaluate the model in predicting the observed flood peaks and improve the capability in simulating flood peaks by introducing appropriate method in the model.
- (iii) Use high resolution climate data to study impacts of climate change on flow and floods.

The International Prediction in Ungauged Basins (PUB) initiative recommends the use of an appropriate model structure for predicting flow in ungauged catchments (Blöschl et al., 2013), and the choice of appropriate model structure helps in reducing predictive uncertainty (Son & Sivapalan, 2007). Flash floods are usually localized disasters that occur in small catchments with response times of a few hours or even less and their high risk potential is related to their rapid occurrence and to the spatial dispersion of the areas which may be impacted by these floods (Borga et al., 2011; Borga et al., 2007). The short lead time and small area collectively enhance the difficulty of flood management in such catchments (Miao et al., 2016).

### *Small catchments*

In general, different definitions of small rural catchments exist worldwide. In Norway, Stenius (2012) considers catchments up to 50km<sup>2</sup> as small. Many small catchments are ungauged, and this condition makes flood estimation in such catchments difficult. Moreover, rainfall-runoff modelling in such catchments is hampered by a lack of both observed discharge and precipitation data (Fleig & Wilson, 2013).

It has been pointed out by Fleig and Wilson (2013) that the flood estimation in small catchments is particularly difficult due to the following reasons:

- (1) Flood peaks in small catchments are more susceptible to the influence of local features.
- (2) Local extreme precipitation events can result in higher peak flows relative to the average flow than in larger catchments.

- (3) Appropriately describing the local hydrological processes is crucial for reliable flood estimation which is difficult in small catchments.
- (4) Flow data are not available or not adequate for the calibration of hydrological models.
- (5) Observed flow data should be available in high temporal resolution, due to the fast response and flow fluctuation in small catchments. In particular, mean daily observations can differ considerably from observed instantaneous flood peaks in small fast responding catchments.
- (6) Observed precipitation data from representative station are rare and would be needed in high temporal resolution.

In Norway, the data availability has been improved for catchments smaller than 50km<sup>2</sup> (Stenius, 2012). Therefore, this PhD research work addresses some of the difficulties of estimating flood peaks in small ungauged rural catchments ( $\leq 50\text{km}^2$ ) using a continuous rainfall-runoff model to contribute for flood risk management under climate change.

### *Scope of the work*

This thesis focuses on flow and flood prediction methods and the applicability of the methods for climate impact studies at ungauged small rural catchments in Norway. The developed methods also provide support to flood risk assessment and planning of adaptation strategies to infrastructures (e.g. culverts and bridges) located at the outlet of the ungauged small rural catchments. More specifically, the thesis aims at answering the following research objectives:

- ❖ What are the best regionalization methods of Distance Distribution Dynamics (DDD) model parameters with hourly resolution to predict flow at ungauged small rural catchments in Norway?

- ❖ How can we predict observed flood peaks as accurate as possible in the continuous simulations using the DDD model?
- ❖ How does climate change affect the flow pattern and flood frequency at small ungauged rural catchments in Bergen area in western Norway in the future period (2070 – 2100) compared to the reference period (1981 – 2011)?

Three scientific research papers, appended in the appendix section of the thesis, are produced to address the research objectives.

## CHAPTER TWO

### *General methods*

In this Ph.D. research work, a parsimonious continuous rainfall-runoff model has been used as the main tool. A model can be considered as a simplified representation of a real world system (Devia et al., 2015). Physically based models, which use differential equations in describing a physical process in a catchment, need simplifications related to the identification of the parameter values, the uncertainties in the input and output observations and the point nature of physically based equations. Therefore, the best model might be the one which gives results close to reality with the use of a minimum numbers of parameters and reduced model complexity (Masseroni et al., 2016). Accordingly, in this thesis a continuous semi-distributed conceptual parsimonious rainfall-runoff model (Distance Distribution Dynamics) has been used. Figure 1 shows the structure of the DDD rainfall-runoff model.

The DDD model is written in the R programming language (R Core Team, 2017) and currently runs operationally with daily and three-hourly time steps at the Norwegian flood forecasting service at NVE. Subsurface and dynamic runoff are the two main modules of the model. The volume capacity of the subsurface water reservoir,  $M$  (mm), is shared between a saturated zone with volume  $S$  (mm) and an unsaturated zone with volume  $D$  (mm). If the saturated zone is high, the unsaturated volume has to be small (Skaugen & Onof, 2014). The actual water volume present in the unsaturated zone is described as  $Z$  (mm). The subsurface state variables are updated after evaluating whether the current soil moisture,  $Z(t)$ , together with the input of rain and snowmelt,  $G(t)$ , represent an excess of water over the field capacity,  $R$ , which is fixed at 30 % ( $R = 0.3$ ) of  $D(t)$  (Skaugen & Onof, 2014). If  $G(t) + Z(t) > R \cdot D(t)$ , then the excess water  $X(t)$  is added to  $S(t)$ . The DDD model has three main groups of parameters. The first group are those determined by model calibration against observed discharge, the second group are those estimated from observed hydro-meteorological data and the third group are those estimated from geographical data.

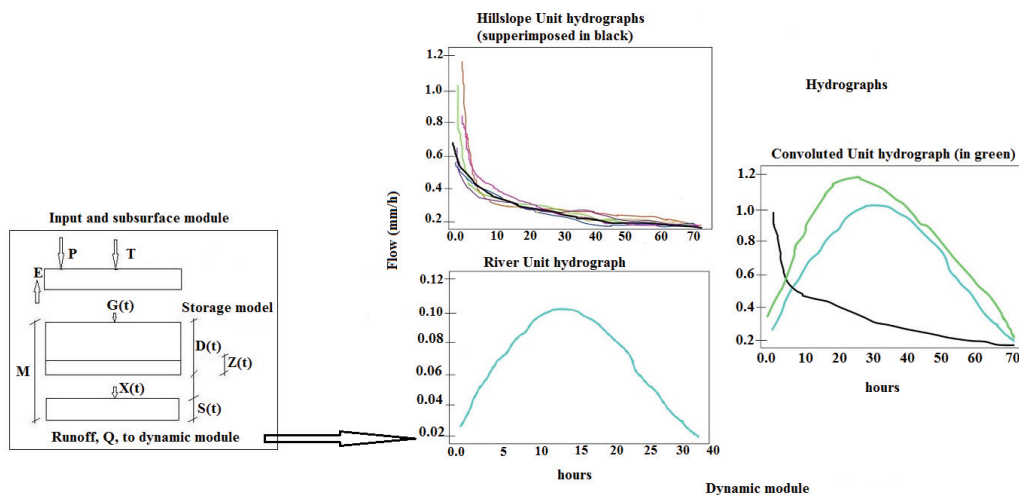


Figure 1. Structure of the Distance Distributions Dynamics model adapted from Skaugen and Onof (2014) . Left panel: the storage model and right panel: hydrographs of hillslope and river.

The methods used in addressing the research objectives are described into the following three sections and the location of the study catchments are presented in Fig.2.

### *Methods in paper I*

Forty-one gauged small rural catchments (area  $\leq 50\text{km}^2$ ), with an hourly discharge observation, have been selected from the Norwegian Water Resources and Energy Directorates (NVE) HYDRA II database and the following data have been prepared for calibration and validating the DDD model:

- a) The precipitation and temperature data, with hourly temporal resolution and 1km X 1km spatial resolution, have been extracted from the Norwegian Meteorological Institute data base (<http://thredds.met.no/thredds/catalog.html>) for the selected catchments.
- b) The second and third group of DDD model parameters have been computed from observed discharge (using an R-script) and from topography data (using a GIS).

After deriving the DDD model parameters which do not need calibration, and input climatological data (precipitation and temperature), the DDD model has been calibrated and evaluated with hourly time resolution for the 41 gauged small catchments in Norway. The uncertainty of the calibrated parameters has been analyzed before conducting the regionalization study.

Three methods of regionalization are evaluated for transferring the DDD model parameters needing regionalization from the 41 gauged catchments to the ungauged catchments. The methods

are multiple regression, physical similarity (single-donor and pooling-group types) and a combined method. The nine parameters needing regionalization are: maximum liquid water in snow, degree hour factor for snow melt, degree hour factor for refreezing, degree hour factor for evapotranspiration, celerity for river flow, shape parameter of  $\lambda$  (the parameter of the unit hydrograph of storage level), scale parameter of  $\lambda$ , shape parameter of  $\Lambda$  (the slope of change per time of the observed flow recession in log-log space) and scale parameter of  $\Lambda$ . For the regionalization, catchment descriptors (CDs) (from land use, topography and hydro-climatic data) have been extracted for the selected 41 catchments. In multiple regression method, equations which are used to relate the CDs with the model parameters are fitted to the calibrated model parameters of the 41 catchments. The physical similarity method transfers entire parameter sets from gauged to ungauged catchments instead of establishing links between model parameters and CDs. The 9 model parameters needing regionalization come from two groups with different estimation methods. In the combined method, the new parameter set is derived by combining regression and physical similarity methods (recession parameters estimated from multiple regression and calibrated parameters estimated from the pooling-group method of physical similarity). The regionalization methods are validated with seven independent catchments (test catchments) which are not used in the initial calibration of the DDD model. The 41 gauged study catchments and the 7 test catchments locations are shown in Fig.2.

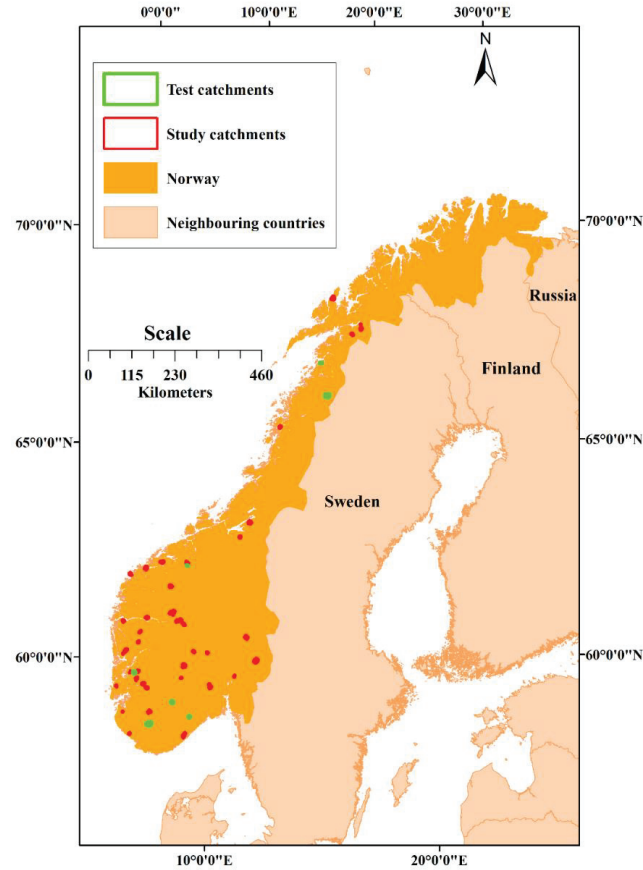


Fig.2 Locations of gauged small rural catchments used in the research paper I. The red study catchments are used to evaluate (calibrate and validate) DDD model and the green catchments are used for evaluating the regionalization methods.

### *Methods in paper II*

The performance of DDD model has been evaluated for predicting flood peaks using visual inspection of the observed and simulated flood hydrographs of the 41 study catchments defined in paper I. Even if the model performance is adequate in terms of Kling-Gupta Efficiency (KGE) and



BIAS (ratio of mean simulated to observed runoff) during calibration and validation, the DDD model, like many other rainfall-runoff models, underestimate flood peaks in the continuous simulation. To improve the prediction of the flood peaks, a dynamic river network method has been conceptualized and implemented in the DDD model. The performance of the model with dynamic river network routine has been evaluated in predicting flood peaks at a number of small catchments.

The river network indicates where the subsurface water flow becomes surface water flow. Stream networks in a catchment expand and contract as the catchment wets and dries, both seasonally and in response to individual precipitation events, and this dynamics of stream networks give an important information to the pattern and process of runoff generation (Godsey & Kirchner, 2014; Ward et al., 2018). The network system governs the dynamics of runoff for conditions where we have no overland flow from the hillslope in that there is a significant (orders of magnitude) difference in water celerity for flow through the soils and flow in the river network (Robinson et al., 1995). In case of overland flow, however, we can imagine a dynamic river network (and hence dynamic overland flow unit hydrograph) as a function of overland flow ( $OF$ ). To compute the dynamic hillslope overland flow unit hydrograph, a critical flux (an overland flow in cubic meter per second required to initiate and maintain a stream network) is introduced as a calibration parameter in the dynamic river network method. The critical flux is defined as the product of overland flow and critical supporting area (the minimum catchment area from which the generated overland flow is enough to initiate and maintain a stream network). Once the critical flux is calibrated for a catchment, the critical supporting area ( $A_c$ ) is dynamic for different overland flows i.e. the higher the overland flow, the lower the  $A_c$  and vice versa. To use the dynamic river network

method at ungauged small rural catchments, multiple regression is carried out to estimate the critical flux of the dynamic river network routine from the CDs. Figure 3 shows the expansion of a river network during flooding events.

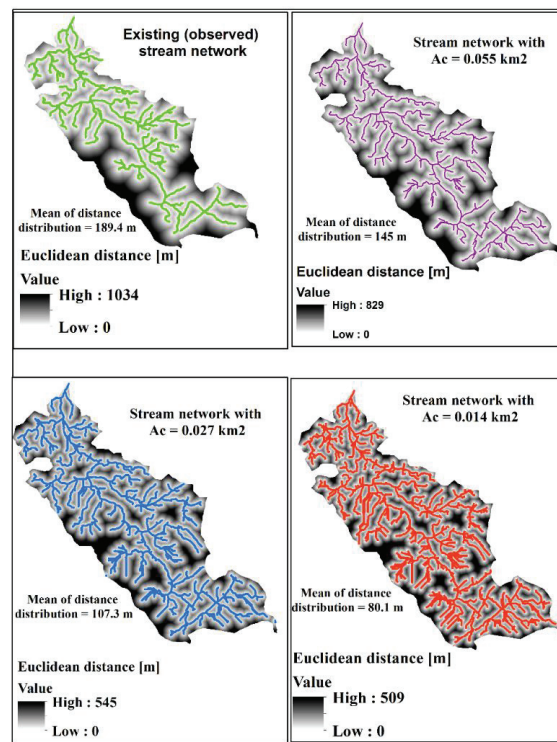


Fig.3 Expansion of observed river networks during flooding conditions in the dynamic river network method for prediction of floods. During flooding conditions, the  $A_c$  required to initiate and maintain stream becomes smaller than the  $A_c$  required for observed stream networks, and the mean of distances between points in the catchment to nearest river reach also becomes smaller.

### *Methods in paper III*

Six small ungauged rural catchments, upstream of culverts and buildings in the Bergen area in western Norway, have been selected for studying impacts of climate change on flow patterns and

frequency of floods. Figure 4 shows the locations of the ungauged small rural catchments. Bergen is selected because it is one of the locations in western Norway where heavy precipitation and associated flooding are major concerns under both present climate conditions and projected future scenarios, and it was also the BINGO project site (Pontoppidan et al., 2018; Pontoppidan et al., 2017).

The precipitation and temperature data used to drive the DDD model are obtained from a simulation performed by the Weather Research and Forecasting model (WRF) version 3.8.1 (Skamarock et al., 2008). The model is non-hydrostatic and widely used for weather forecasting and research purposes. The simulation has a spatial grid resolution of 4 km x 4 km and the precipitation and temperature are available every 3 hours. However, regional models, as WRF, inherit biases from the boundary conditions used to drive the model. These biases may lead to misrepresentation of important features in the models, e.g. the known bias of the North Atlantic storm track (Zappa et al., 2013) leads individual storms into central Europe instead of a more northern path along the Norwegian coast as observations suggest. Therefore, the global climate model NorESM1-M used as forcing data at the boundaries in WRF was corrected for such biases before the regional downscaling. This led to a more realistic representation of the North Atlantic storm track and the precipitation distribution in southern Norway (Pontoppidan et al., 2018). Ultimately this leads to a more local representation of precipitation and temperature.

The precipitation and temperature data, from the high-resolution (3 hours and 4km X 4km) climate model have been extracted for the selected catchments using an R-script both for the reference (1981 – 2011) and future (2070 – 2100) periods. To run the regionalized DDD model with the

climate data at the ungauged catchments, the DDD model parameters needing regionalization are computed for the selected catchments using the methods outlined in paper I and II. The climate data are forced to the DDD model for the two periods for generating time series of discharge. Finally, the changes in the flow patterns and flood frequencies between the reference and future periods are analyzed to assess the hydrological impacts of climate change on the study catchments.

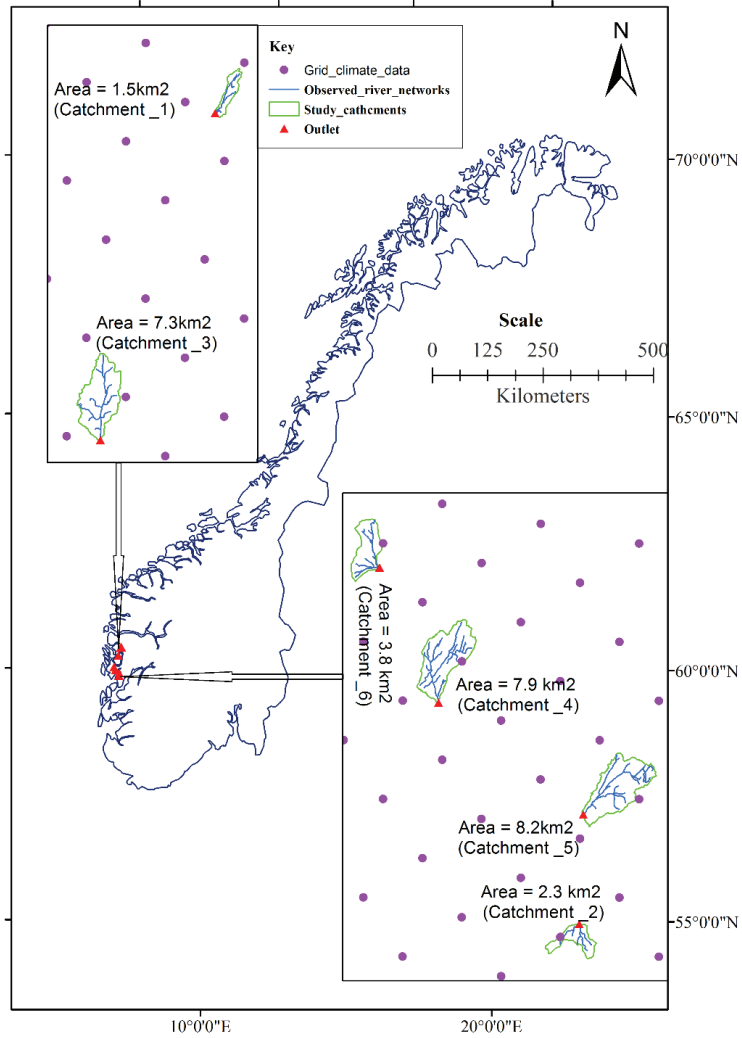


Fig.4 Locations of the study catchments and gridded climate data used in the climate impact study in paper III.

## CHAPTER THREE

The DDD model parameters have been regionalized for hourly simulation and then the model is improved with a dynamic river network method for predicting floods and finally it is used in a climate impact study in Bergen.

### *Summary of results by papers*

#### *Results of paper I*

#### **Paper I: Predicting hourly flows at ungauged small rural catchments using a parsimonious hydrological model**

All the three methods (the multiple regression, pooling-group, and combined methods) of regionalizations perform satisfactorily ( $0.5 \leq KGE < 0.75$ ). The model parameters which describe the recession characteristics of a hydrograph are estimated better by the regionalization methods than those estimated locally from short period of data for some test catchments. The combined method (which combines multiple regression and pooling-group) performs slightly better than the other methods. The satisfactory performance of the combined method shows that regionalization of the DDD model parameters is possible by combining multiple regression and physical similarity. The single-donor method did not perform satisfactorily. Table 1 presents the results of the performance and Fig.5 shows the observed and the simulated hydrographs using the regionalization methods for two of test catchments.

S.no	Test catchment	ID	Area (km <sup>2</sup> )	Regression method		Physical similarity method				Combined method							
				BIAS	KGE	Single donor	Pooling group (7 members)		Recession parameters from regression		Recession parameters from physical similarity						
							BIAS	KGE	BIAS	KGE	BIAS	KGE	BIAS	KGE			
1	Gravå	19.79	6.3	1.04	<b>0.67</b>	1.09	0.33	1.04	0.58	1.06	0.6	<b>1.03</b>	<b>0.67</b>	1.09	0.34	1.04	0.58
2	Knabåni	25.32	49.1	<b>0.8</b>	0.74	0.75	0.66	0.77	0.72	0.75	0.66	0.77	0.7	0.75	0.66	<b>0.8</b>	<b>0.75</b>
3	Kjemåvatn	163.7	36.6	<b>0.9</b>	0.75	<b>0.9</b>	0.59	0.87	0.67	0.88	0.75	<b>0.9</b>	<b>0.76</b>	<b>0.9</b>	0.59	<b>0.9</b>	0.66
4	M.Mardalsvatn	104.22	13.5	0.72	<b>0.65</b>	0.72	0.53	<b>0.74</b>	0.6	0.69	0.63	<b>0.74</b>	<b>0.65</b>	<b>0.74</b>	0.56	0.72	0.6
5	Fjellhaugen	42.16	7.3	0.83	<b>0.75</b>	0.79	0.63	0.79	0.72	0.79	0.72	0.79	0.72	0.8	0.71	<b>0.84</b>	<b>0.75</b>
6	Tjellingtjernbekken	18.11	2.1	1.47	0.44	1.51	0.2	1.46	0.34	1.46	0.45	<b>1.4</b>	<b>0.5</b>	1.49	0.26	1.49	0.31
7	Strånda	165.6	23.3	1.13	0.57	<b>1.06</b>	<b>0.6</b>	<b>1.06</b>	<b>0.6</b>	1.07	0.58	1.08	0.59	<b>1.06</b>	0.6	1.12	0.58
	<i>Mean</i>			<i>0.98</i>	<i>0.65</i>	<i>0.97</i>	<i>0.51</i>	<i>0.96</i>	<i>0.60</i>	<i>0.96</i>	<i>0.63</i>	<i>0.96</i>	<i>0.66</i>	<i>0.98</i>	<i>0.53</i>	<i>0.99</i>	<i>0.60</i>
	<i>Standard deviation</i>			<i>0.26</i>	<i>0.12</i>	<i>0.28</i>	<i>0.17</i>	<i>0.25</i>	<i>0.13</i>	<i>0.27</i>	<i>0.1</i>	<b><i>0.23</i></b>	<b><i>0.09</i></b>	<i>0.27</i>	<i>0.17</i>	<i>0.26</i>	<i>0.15</i>

Table: 1 Summary of comparisons of the regionalization methods using KGE and BIAS. The green shows the best KGE values (close to 1) while the blue shows the best BIAS value (close to 1).

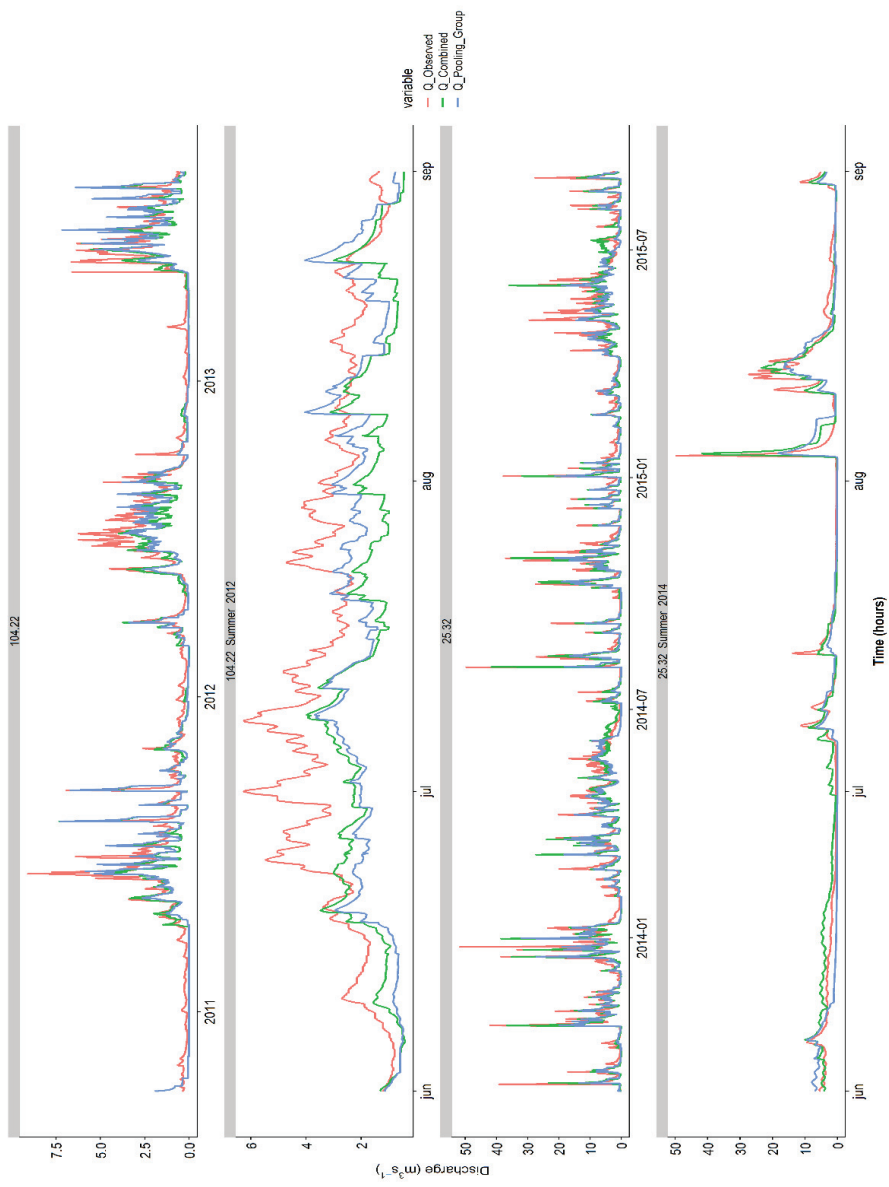


Fig.5 Observed and predicted hydrographs using pooling group and combined methods of regionalization at two test catchments. The top two hydrographs show for the catchment ID 104.22 and the bottom two for catchment ID 25.32 (the whole period and summer).



*Results of paper II*

**Paper II: A dynamic river network method for the predication of floods using a parsimonious rainfall-runoff model.**

The dynamic river network method is applied for 15 small rural catchments in Norway and tested on 91 flood peaks. The performance of DDD in terms of KGE and BIAS is the same with and without dynamic river network, but the relative errors and mean absolute relative errors of the simulated flood peaks have improved significantly in the simulations with dynamic river networks. The 0.75 and 0.25 quantiles of the relative errors of the simulated flood peaks are reduced from 41% to 23% and from 22% to 1% respectively. The mean absolute relative error of the simulated peaks is reduced from 32.9% to 15.7%. Figure 6 shows the flood peaks simulated using DDD with and without river dynamic network. Table 2 presents the observed and simulated floods with and without dynamic river networks.

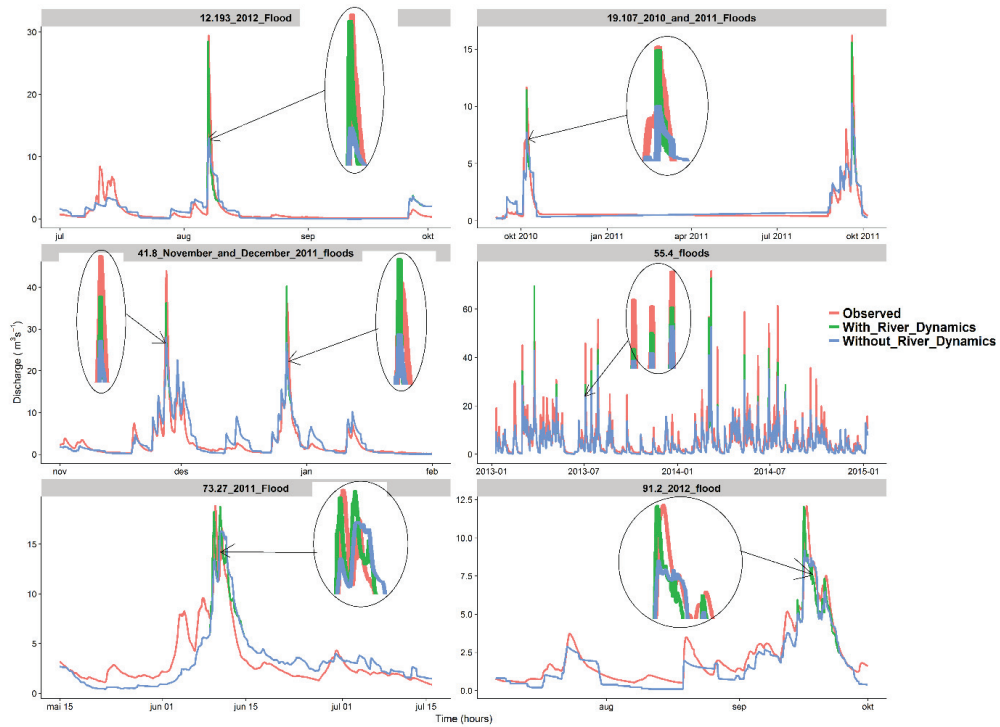


Fig.6 Samples of hydrographs of continuous simulations results of DDD rainfall-runoff models with flood peaks i.e. observed, simulated with and without dynamic river network for 6 of the 15 study catchments.

Cat_ID	Observed flood(s) in m <sup>3</sup> /s	Simulation period	Simulated value(s) of flood without river dynamics in m <sup>3</sup> /s	Performance of DDD model without river dynamics in calibration		Simulated value(s) of flood with river dynamics in m <sup>3</sup> /s	Performance of DDD model with river dynamics	
				KGE	BIAS		KGE	BIAS
12.193	<b>29.42</b>	2 years	<b>12.97</b>	0.64	1.2	<b>28.78</b>	0.65	1.2
19.107	<b>11.65 and 16.2</b>	3 years	<b>7.64 and 10.3</b>	0.8	0.93	<b>9.42 and 16.1</b>	0.81	0.94
41.8	<b>43.96 and 36.13</b>	2 years	<b>28.02 and 26.74</b>	0.77	0.84	<b>36.3 and 40.3</b>	0.77	0.84
73.27	<b>18.85</b>	3 years	<b>13.3</b>	0.71	0.76	<b>18.3</b>	0.71	0.76
91.2	<b>12.06</b>	2 years	<b>8.34</b>	0.71	0.8	<b>12.04</b>	0.71	0.8

**Table 2.** Observed and simulated floods using DDD with and without dynamic river network and the corresponding performance of the model for 5 sample catchments.

### *Results of paper III*

#### **Paper III: Hydrological impacts of climate change on small ungauged catchments**

Generally, the results of the six study catchments in Bergen show that there will be an increase in the mean annual flow and mean annual maximum floods in the future period. The results also show that there will be also an increase in the mean autumn, mean winter and mean spring flows and a decrease in the mean summer flow. The maximum increase in the mean annual flow is 33.3%, and the minimum increase is 16.5%. The increase in the mean autumn, winter and spring flows contributed significantly in the increase of the mean annual flow. The maximum decrease in the mean summer flow is 35.2% and the minimum decrease is 7.2%. The mean annual maximum floods increase by 28.9% to 38.3%. The floods with a return periods of 2, 5, 10, 20, 25, 50, 100 and 200 will increase by 16.1% to 42.7%. Figure 7 Shows distributions of the mean annual maximum and seasonal maximum flows. Table 3 shows the changes in floods with return periods ranging from 2 to 200 years.

Table 3. : Changes in floods with return periods of 2, 5, 10, 20, 25, 50, 100 and 200 years using Gumbel's Extreme Value Distribution for all study catchments.

T(years)	Change (%)					
	Cat_1	Cat_2	Cat_3	Cat_4	Cat_5	Cat_6
2	28.9	36.7	35.7	28.0	31.4	29.5
5	24.1	35.9	37.9	33.3	31.3	26.9
10	21.8	35.5	38.9	35.9	31.2	25.7
20	20.0	35.3	39.7	38.0	31.2	24.8
25	19.5	35.2	39.9	38.6	31.2	24.5
50	18.2	35.0	40.5	40.2	31.1	23.8
100	17.0	34.9	40.9	41.5	31.1	23.2
200	16.1	34.7	41.3	42.7	31.1	22.7

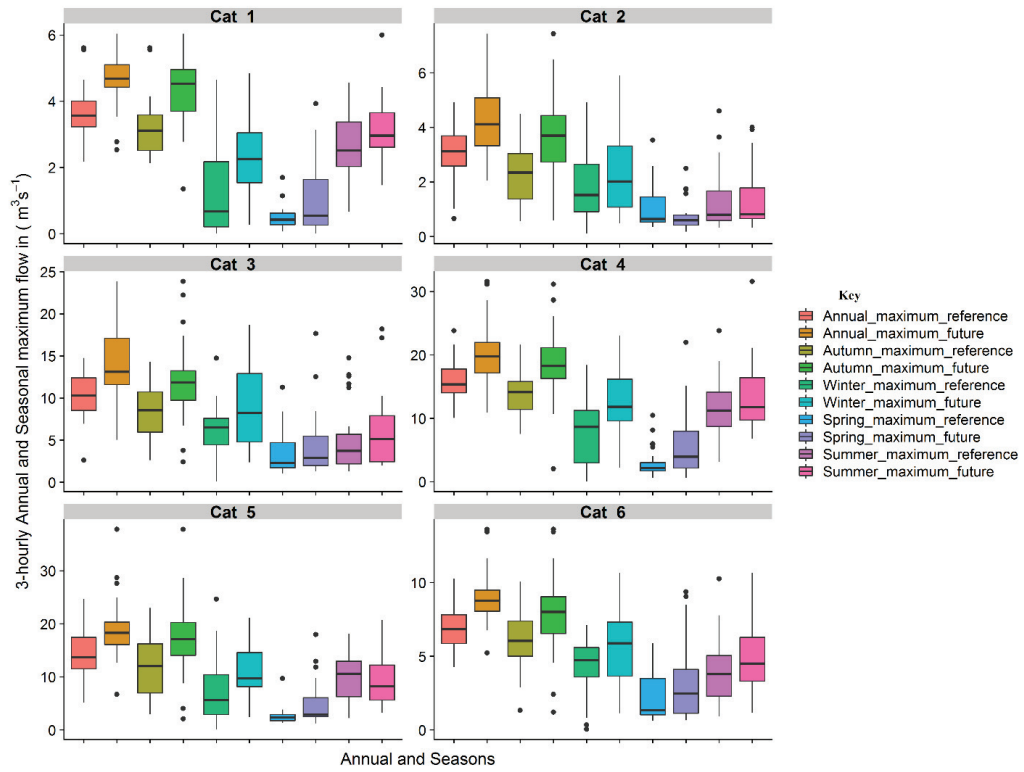


**Fig.5** Distributions of the annual and seasonal maximum flow values of the 30 years period both for the reference and future periods for all the study catchments.

## CHAPTER FOUR

### *Discussion and conclusion*

The continuous stream flow predictions at ungauged small rural catchments in Norway has been carried out using regionalizations of DDD model parameters. Since the regionalization process is inherently involved with catchment descriptors, it is not possible to establish a universal approach as the best method for all of the catchments. Therefore, a specific study needs to be done on any region of interest to identify the best regionalization method among rainfall runoff models (Razavi & Coulibaly, 2013). Accordingly, three regionalization methods using DDD model have been used in this study. The use of rainfall-runoff models causes uncertainties due to errors in computing local and regional model parameters, errors in the relationship between local parameters and catchment descriptors and because of the uniqueness of the catchment (Wagner & Wheater, 2006). Therefore, the DDD model parameters uncertainty is evaluated before regionalizing the parameters, and it was found that the uncertainty is small.

All the three methods of regionalizations performed satisfactorily ( $0.5 \leq KGE < 0.75$ ) in predicting continuous flow series at ungauged small rural catchments in Norway. The combined method of regionalization performs slightly better than multiple-regression and physical-similarity methods. The best performance of combined method is the result of combining the advantages of physical similarity in transferring the calibrated parameters and multiple regression in the transfer of recession parameters (Arsenault & Brissette, 2014; Kokkonen et al., 2003; McIntyre et al., 2005; Oudin et al., 2010; Parajka et al., 2005). The recession parameters describe the integrated information of how different factors influence the flow process (Fiorotto & Caroni, 2013). Recession parameters are used in the DDD model to estimate the subsurface storage capacity

(Skaugen & Mengistu, 2016), and they can also be used to model streamflow recession for regionalization and prediction (Stoelzle et al., 2013). Regression procedures for estimating hydrograph recession parameters generally work well (Vogel & Kroll, 1996), which is supported by our findings in that the recession parameters estimated using multiple regression are slightly better than those estimated by physical similarity.

Dynamic river networks and hence dynamic overland unit hydrographs are introduced and implemented in the DDD rainfall-runoff model to improve the prediction of flood peaks. The dynamic river network method expands the observed river networks during excess overland flow events which generate floods. The expansion means that the  $A_c$  required to initiate and maintain a stream decreases. Smaller  $A_c$  results in smaller mean distance distribution ( $D_m$ ) of the points in the catchment to the nearest river reach. The smaller  $D_m$  value results in shorter travel times of points in the catchment to the nearest river reach. The shorter travel time distribution generates overland unit hydrographs (OUHs) with a higher peak and shorter scale for the hillslopes. The dynamic OUHs are superpositioned with the other four subsurface unit hydrographs of DDD to give a single dynamic unit hydrograph of a catchment during flooding events. D'Odorico and Rigon (2003) found that shorter hillslope distances result in shorter travel times and hence higher flood peaks which supports our finding.

The study of the hydrological impacts of climate change on ungauged small rural catchments in Bergen, Norway shows that there will be an increase in the mean annual flows. The increase in the mean annual flow is due to the increase in the mean autumn, winter and spring flows in the future period (2070-2100) compared to the reference period (1981 - 2011). In the future period, there will



be a decrease in the mean summer flows. The mean annual maximum flow increases in the future period. The finding that mean annual maximum flows (floods) increases by 28.9% to 38.3% in our study is supported by different studies. Lawrence and Hisdal (2011) have done ensemble modelling based on locally adjusted precipitation and temperature data from 13 regional climate scenarios to assess likely changes in hydrological floods between a reference period (1960 – 1990) and two future periods (2021-2050) and (2071 - 2100), for the 115 catchments distributed throughout Norway. Their results showed that western regions of Norway (where Bergen is located) is associated with the largest percentage increases in the magnitude of the mean annual floods (> 20%). Lawrence and Hisdal (2011) also pointed out that increase in autumn and winter rainfall throughout Norway will increase the magnitude of peak flows during these seasons and at areas already dominated by autumn and winter floods, the projected increases in floods magnitude will be large which aligns with our findings. Lawrence (2016) used ensembles of regional climate projections from EURO-CORDEX together with HBV model to assess possible effects of climate change on floods on 115 catchments in Norway for two future periods (20131-2016 and 2071-2100). The assessment result shows that the minimum increase in the 200 years flood for catchments less than 100km<sup>2</sup> at Møre og Romsdal, Sogn og Fjordane, and Hordaland counties is 20% which is generally in agreement with our findings.

This thesis provides a methods for prediciting continous stream flow and floods at ungauged small rural catchments (area  $\leq$  50km<sup>2</sup>). The developed methods have been tested in the hydrologic impacts of climate change on ungauged small rural cathcments in Bergen, Norway. The findings of the impacts study are in agreement with the results of previous studies conducted by different reseachers. Therefore, the thesis contributes for flood risk mangments in small rural catchments

and offers promising methods which could be adapted and tested for application in Norway and other parts of the world after addressing the limitations.

### *Recommendations for further work*

For efficient flood risk management at ungauged small rural catchments using the DDD model in the changing environment (e.g. under climate and land use changes), the following topics are recommended as future research works:

- Evaluate different approaches and recommend the best approach to be used in computing the distance distribution of points in the catchment to the nearest river reach in the DDD model (e.g. Euclidean distances used in this thesis against distances along the steepest descent path).
- Evaluate different approaches and recommend the best approach in estimating the actual evapotranspiration routine in the DDD model ( e.g. the degree day model used in this thesis against energy balance method).
- The spatial variability of the critical support area,  $A_c$ , has been observed when  $A_c$  at the head of the observed stream network is analysed using GIS. Therefore, a more detailed investigation, supported by field work should be carried out to assess how the combination of these factors control  $A_c$  and hence critical flux,  $F_c$ . The field work could include mapping of the slope, geology, vegetation cover and soil of a catchment at the head of first order streams of observed river networks and mapping of the pattern of expansion of first order streams during flooding events.
- Generate continuous flow data using the methods developed in this thesis (hydrographs generated by the regionalized DDD model) at ungauged small rural catchments and then

calibrate a distributed hydrological model and study impacts of land use changes on flow and floods.

- When several high temporal (e.g. hourly) and spatial resolution (e.g. 1km x 1km) regional climate models are available in the future, conduct uncertainty analysis of impacts of climate change on ungauged small rural catchments.

## REFERENCES

- Annamo, E., & Kristiansen, G. (2012). *Challenges in Flood Risk Management Planning: An example of a Flood Risk Management Plan for the Finnish-Norwegian River Tana Oslo, Norway*: Norwegian Water Resources and Energy Directorate.
- Arsenault, R., & Brissette, F. P. (2014). Continuous streamflow prediction in ungauged basins: The effects of equifinality and parameter set selection on uncertainty in regionalization approaches. *Water Resources Research*, 50(7), 6135-6153. doi:10.1002/2013WR014898
- Asadieh, B., & Krakauer, N. Y. (2017). Global change in streamflow extremes under climate change over the 21st century. *Hydrol. Earth Syst. Sci.*, 21(11), 5863-5874. doi:10.5194/hess-21-5863-2017
- Balston, J., Li, S., Iankov, I., Kellett, J., & Wells, G. (2017). Quantifying the Financial Impact of Climate Change on Australian Local Government Roads. *Infrastructures*, 2(1), 2.
- Blöschl, G., Sivapalan, M., Wagener, T., Viglione, A., & Savenije, H. (2013). *Runoff Prediction in Ungauged Basins: Synthesis across Processes, Places and Scales* (G. Blöschl, M. Sivapalan, T. Wagener, A. Viglione, & H. Savenije Eds.). Cambridge: Cambridge University Press.
- Borga, M., Anagnostou, E. N., Blöschl, G., & Creutin, J. D. (2011). Flash flood forecasting, warning and risk management: the HYDRATE project. *Environmental Science & Policy*, 14(7), 834-844. doi:<https://doi.org/10.1016/j.envsci.2011.05.017>

- Borga, M., Boscolo, P., Zanon, F., & Sangati, M. (2007). Hydrometeorological analysis of the 29 August 2003 flash flood in the eastern Italian Alps. *Journal of Hydrometeorology*, 8(5), 1049-1067. doi:10.1175/JHM593.1
- Brunner, M. I., Viviroli, D., Sikorska, A. E., Vannier, O., Favre, A.-C., & Seibert, J. (2017). Flood type specific construction of synthetic design hydrographs. *Water Resources Research*, 53(2), 1390-1406. doi:10.1002/2016wr019535
- D'Odorico, P., & Rigon, R. (2003). Hillslope and channel contributions to the hydrologic response. *Water Resources Research*, 39(5). doi:doi:10.1029/2002WR001708
- Devia, G. K., Ganasri, B. P., & Dwarakish, G. S. (2015). A Review on Hydrological Models. *Aquatic Procedia*, 4, 1001-1007. doi:<https://doi.org/10.1016/j.aqpro.2015.02.126>
- Di Baldassarre, G., Montanari, A., Lins, H., Koutsoyiannis, D., Brandimarte, L., & Blöschl, G. (2010). Flood fatalities in Africa: From diagnosis to mitigation. *Geophysical Research Letters*, 37(22). doi:10.1029/2010gl045467
- Faulkner, D., Kjeldsen, T., Packman, J., & Stewart, L. (2012). *Estimating flood peaks and hydrographs for small catchments: Phase 1* UK: Environment Agency, Horizon House, Deanery Road, Bristol BS1 5AH.
- Fiorotto, V., & Caroni, E. (2013). A new approach to master recession curve analysis. *Hydrological Sciences Journal*, 58(5), 966-975. doi:10.1080/02626667.2013.788248
- Fleig, A. K., & Wilson, D. (2013). *Flood estimation in small catchments*. Norwegian Water Resources and Energy Directorate, Report no. 60-2013.
- Godsey, S. E., & Kirchner, J. W. (2014). Dynamic, discontinuous stream networks: hydrologically driven variations in active drainage density, flowing channels and stream order. *Hydrological Processes*, 28(23), 5791-5803. doi:doi:10.1002/hyp.10310
- Grimaldi, S., Petroselli, A., & Serinaldi, F. (2012). Design hydrograph estimation in small and ungauged watersheds: continuous simulation method versus event-based approach. *Hydrological Processes*, 26(20), 3124-3134. doi:10.1002/hyp.8384
- Günter, B. (2006). Rainfall-Runoff Modeling of Ungauged Catchments *Encyclopedia of Hydrological Sciences*.

- Hall, J., Arheimer, B., Borga, M., Brázdil, R., Claps, P., Kiss, A., . . . Blöschl, G. (2014). Understanding flood regime changes in Europe: a state-of-the-art assessment. *Hydrol. Earth Syst. Sci.*, *18*(7), 2735-2772. doi:10.5194/hess-18-2735-2014
- Hirabayashi, Y., Roobavannan, M., Koirala, S., Konoshima, L., Yamazaki, D., Watanabe, S., . . . Kanae, S. (2013). Global flood risk under climate change. *Nature Climate Change*, *3*, 816-821. doi:10.1038/nclimate1911
- Jakubínský, J., Bacova, R., Svobodova, E., Kubicek, P., & Herber, V. (2014). *Small watershed management as a tool of flood risk prevention* (Vol. 364).
- Kokkonen, T., Jakeman, A., Young, P., Koivusalo, H., Blöschl, G., Vertessy, R., . . . Zhang, L. (2003). Predicting daily flows in ungauged catchments: model regionalization from catchment descriptors at the Coweeta Hydrologic Laboratory, North Carolina. *Hydrological Processes*, *17*(11), 2219-2238. doi:10.1002/hyp.1329
- Lamb, R., Faulkner, D., Wass, P., & Cameron, D. (2016). Have applications of continuous rainfall–runoff simulation realized the vision for process-based flood frequency analysis? *Hydrological Processes*, *30*(14), 2463-2481. doi:10.1002/hyp.10882
- Lawrence, D. (2016). *Klimaendring og framtidige flommer i Norge*. Oslo: Norges vassdrags-og energidirektorat.
- Lawrence, D., & Hisdal, H. (2011). *Hydrological projections for floods in Norway under a future climate*. Oslo: Norwegian Water Resources and Energy Directorate.
- Lespinas, F., Ludwig, W., & Heussner, S. (2014). *Hydrological and climatic uncertainties associated with modeling the impact of climate change on water resources of small Mediterranean coastal rivers* (Vol. 511).
- López-Moreno, J. I., Zabalza, J., Vicente-Serrano, S., Revuelto, J., Gilaberte-Búrdalo, M., Azorin-Molina, C., . . . Tague, C. (2013). *Impact of climate and land use change on water availability and reservoir management: Scenarios in the Upper Aragon River, Spanish Pyrenees* (Vol. 493).
- Masseroni, D., Cislighi, A., Camici, S., Massari, C., & Brocca, L. (2016). A reliable rainfall–runoff model for flood forecasting: review and application to a semi-urbanized watershed at high flood risk in Italy. *Hydrology Research*, *48*(3), 726-740. doi:10.2166/nh.2016.037

- McIntyre, N., Lee, H., Wheeler, H., Young, A., & Wagener, T. (2005). Ensemble predictions of runoff in ungauged catchments. *Water Resources Research*, 41(12), n/a-n/a. doi:10.1029/2005WR004289
- Mediero, L., Jiménez-Álvarez, A., & Garrote, L. (2010). Design flood hydrographs from the relationship between flood peak and volume. *Hydrol. Earth Syst. Sci.*, 14(12), 2495-2505. doi:10.5194/hess-14-2495-2010
- Miao, Q., Yang, D., Yang, H., & Li, Z. (2016). Establishing a rainfall threshold for flash flood warnings in China's mountainous areas based on a distributed hydrological model. *Journal of Hydrology*, 541, 371-386. doi:10.1016/j.jhydrol.2016.04.054
- Oudin, L., Kay, A., Andréassian, V., & Perrin, C. (2010). Are seemingly physically similar catchments truly hydrologically similar? *Water Resources Research*, 46(11), n/a-n/a. doi:10.1029/2009WR008887
- Parajka, J., Merz, R., Bloeschl, G., & Parajka, J. (2005). A comparison of regionalisation methods for catchment model parameters. *Hydrology and Earth System Sciences Discussions*, 2(2), 509-542. doi:10.5194/hessd-2-509-2005
- Pontoppidan, M., Kolstad, E. W., Sobolowski, S., & King, M. P. (2018). Improving the Reliability and Added Value of Dynamical Downscaling via Correction of Large-Scale Errors: A Norwegian Perspective. *Journal of Geophysical Research: Atmospheres*, 123(21), 11,875-811,888. doi:doi:10.1029/2018JD028372
- Pontoppidan, Marie, Reuder, J., Mayer, S., & Kolstad, E. W. (2017). Downscaling an intense precipitation event in complex terrain: the importance of high grid resolution. *Tellus A: Dynamic Meteorology and Oceanography*, 69(1), 1271561. doi:10.1080/16000870.2016.1271561
- R Core Team. (2017). R: A Language and Environment for Statistical Computing. doi:<http://www.R-project.org/>
- Razavi, T., & Coulibaly, P. (2013). Streamflow Prediction in Ungauged Basins: Review of Regionalization Methods. *Journal of Hydrologic Engineering*, 18(8), 958-975. doi:10.1061/(ASCE)HE.1943-5584.0000690

- Reynolds, L. V., Shafroth, P. B., & Poff, N. L. (2015). Modeled intermittency risk for small streams in the Upper Colorado River Basin under climate change. *Journal of Hydrology*, 523, 768-780. doi:10.1016/j.jhydrol.2015.02.025
- Robinson, J. S., Sivapalan, M., & Snell, J. D. (1995). On the relative roles of hillslope processes, channel routing, and network geomorphology in the hydrologic response of natural catchments. *Water Resources Research*, 31(12), 3089-3101. doi:doi:10.1029/95WR01948
- Räikkönen, M., Molarius, R., Mäki, K., Forssén, K., Petiet, P., & Nieuwenhuijs, A. (2017). Creating Stakeholder Value through Risk Mitigation Measures in the Context of Disaster Management. *Infrastructures*, 2(4), 14.
- Saliha, A. H., Awulachew, S. B., Cullmann, J., & Horlacher, H.-B. (2011). Estimation of flow in ungauged catchments by coupling a hydrological model and neural networks: case study. *Hydrology Research*, 42(5), 386-400. doi:10.2166/nh.2011.157
- Skamarock, W. C., Klemp, J. B., Dudhia, J., Gill, D. O., Barker, D. M., & co-authors, a. (2008). A description of the advanced research WRF version 3. *Technical Report (June)*, 113.
- Skaugen, T., & Mengistu, Z. (2016). Estimating catchment-scale groundwater dynamics from recession analysis &ndash; enhanced constraining of hydrological models. *Hydrology and Earth System Sciences*, 20(12), 4963-4981. doi:10.5194/hess-20-4963-2016
- Skaugen, T., & Onof, C. (2014). A rainfall-runoff model parameterized from GIS and runoff data. *Hydrological Processes*, 28(15), 4529-4542. doi:doi:10.1002/hyp.9968
- Son, K., & Sivapalan, M. (2007). *Improving model structure and reducing parameter uncertainty in conceptual water balance models through the use of auxiliary data* (Vol. 430).
- Stenius, S. (2012). *Vannføringsstasjoner i Norge med felt mindre enn 50 km<sup>2</sup>*. NVE Report 2012-5.
- Stoelzle, M., Stahl, K., & Weiler, M. (2013). Are streamflow recession characteristics really characteristic? *Hydrol. Earth Syst. Sci.*, 17(2), 817-828. doi:10.5194/hess-17-817-2013

- Swain, J. B., & Patra, K. C. (2017). Streamflow estimation in ungauged catchments using regionalization techniques. *Journal of Hydrology*, *554*, 420-433.  
doi:<https://doi.org/10.1016/j.jhydrol.2017.08.054>
- Tofiq, F. A., & Guven, A. (2014). Prediction of design flood discharge by statistical downscaling and General Circulation Models. *Journal of Hydrology*, *517*, 1145-1153.  
doi:<https://doi.org/10.1016/j.jhydrol.2014.06.028>
- Vogel, R. M., & Kroll, C. N. (1996). Estimation of baseflow recession constants. *Water Resources Management*, *10*(4), 303-320. doi:10.1007/BF00508898
- Wagener, T., & Wheater, H. S. (2006). Parameter estimation and regionalization for continuous rainfall-runoff models including uncertainty. *Journal of Hydrology*, *320*(1), 132-154.  
doi:10.1016/j.jhydrol.2005.07.015
- Ward, A. S., Schmadel, N. M., & Wondzell, S. M. (2018). Simulation of dynamic expansion, contraction, and connectivity in a mountain stream network. *Advances in Water Resources*, *114*, 64-82. doi:<https://doi.org/10.1016/j.advwatres.2018.01.018>
- Winter, B., Schneeberger, K., Dung, N. V., Huttenlau, M., Achleitner, S., Stötter, J., . . . Vorogushyn, S. (2019). A continuous modelling approach for design flood estimation on sub-daily time scale. *Hydrological Sciences Journal*, *64*(5), 539-554.  
doi:10.1080/02626667.2019.1593419
- Zappa, G., Shaffrey, L. C., & Hodges, K. I. (2013). The Ability of CMIP5 Models to Simulate North Atlantic Extratropical Cyclones. *Journal of Climate*, *26*(15), 5379-5396. doi:10.1175/jcli-d-12-00501.1





## **Appendix A: Research papers**



**Paper I:**

**Predicting hourly flows at ungauged small rural catchments using a  
parsimonious hydrological model.**

Tsegaw, A. T., Alfredsen, K., Skaugen, T., & Muthanna, T. M. (2019). *Journal of Hydrology*,  
573, 855-871. doi:<https://doi.org/10.1016/j.jhydrol.2019.03.090>





Contents lists available at ScienceDirect

Journal of Hydrology

journal homepage: [www.elsevier.com/locate/jhydrol](http://www.elsevier.com/locate/jhydrol)

Research papers

## Predicting hourly flows at ungauged small rural catchments using a parsimonious hydrological model

Aynalem T. Tsegaw<sup>a,\*</sup>, Knut Alfredsen<sup>a</sup>, Thomas Skaugen<sup>b</sup>, Tone M. Muthanna<sup>a</sup><sup>a</sup> Department of Civil and Environmental Engineering, Norwegian University of Science and Technology (NTNU), S.P. Andersensvei 5, N-7491 Trondheim, Norway<sup>b</sup> Hydrology Department, Norwegian Water Resources and Energy Directorate (NVE), PO Box 5091, Oslo 0301, Norway

## ARTICLE INFO

This manuscript was handled by Marco Borga, Editor-in-Chief, with the assistance of Yasuto Tachikawa, Associate Editor

## Keywords:

Small ungauged catchments  
Prediction of hourly flow  
Recession parameters  
Regionalizations  
Distance distribution dynamics (DDD)  
rainfall-runoff model

## ABSTRACT

Streamflow data is important for studies of water resources and flood management, but an inherent problem is that many catchments of interest are ungauged. The lack of data is particularly the case for small catchments, where flow data with high temporal resolution is needed. This paper presents an analysis of regionalizing parameters of the Distance Distribution Dynamics (DDD) rainfall-runoff model for predicting hourly flows at small-ungauged rural catchments. The performance of the model with hourly time resolution has been evaluated (calibrated and validated) for 41 small gauged catchments in Norway (areas from 1 km<sup>2</sup>–50 km<sup>2</sup>). The model parameters needing regionalization have been regionalized using three different methods: multiple regression, physical similarity (single-donor and pooling-group based methods), and a combination of the two methods. Seven independent catchments, which are not used in the evaluation, are used for validation of the regionalization methods. All the three methods (the multiple regression, pooling-group, and combined methods) perform satisfactorily ( $0.5 \leq KGE < 0.75$ ). The combined method (which combines multiple regression and pooling-group) performed slightly better than the other methods. Some model parameters, namely those describing recession characteristics, estimated by the regionalization methods, appear to be a better choice than those estimated locally from short period of hydro-meteorological data for some test catchments. The single-donor method did not perform satisfactorily. The satisfactory performance of the combined method shows that regionalization of DDD model parameters is possible by combining multiple regression and physical similarity methods.

## 1. Introduction

Streamflow is important information for water resources management applications such as flood risk management, water resources planning, and environmental impact assessment (Parajka et al., 2013; Westerberg et al., 2014). However, most of the catchments that we are interested in are ungauged which makes a method to predict flow in ungauged catchments an important prerequisite (Blöschl et al., 2013; Parajka et al., 2013; Tegegne and Kim, 2018). Reliable estimation of continuous streamflow in ungauged catchments has remained a fundamental challenge in hydrology, although significant insights have been gained in recent years (Steinschneider et al., 2014; Wagener and Wheater, 2006; Wagener et al., 2004). To solve the challenges posed by ungauged catchments, a number of predictive tools have been developed and tested [e.g. data driven models, such as multiple linear regression (MLR), autoregressive moving average (ARMA), and artificial

neural networks (ANNs); lumped models (e.g., Hydrologiska Byråns for Vattenbalansavdelning model (HBV)); distributed models (e.g., MIKE-SHE) and statistical regionalization] that allow objective and quantitative decision-making with respect to water resources management, but considerable uncertainties remain (Sivapalan et al., 2003). The International Prediction in Ungauged Basins (PUB) initiative recommends the use of an appropriate model structure for predicting flow in ungauged catchments (Blöschl et al., 2013), and the choice of appropriate model structure helps in reducing predictive uncertainty (Son and Sivapalan, 2007). Flash floods are usually localized disasters that occur in small catchments with response times of a few hours or even less (Borga et al., 2007). The short lead time and small area collectively enhance the difficulty of flood management in such catchments (Miao et al., 2016). In addition, small catchments and short time scales are the most under-observed and problematic in terms of prediction and design, and should be identified as a priority in water resource and flood

\* Corresponding author.

E-mail addresses: [aynaalem.t.tasachew@ntnu.no](mailto:aynaalem.t.tasachew@ntnu.no), [aynaalem.tasachew1982@gmail.com](mailto:aynaalem.tasachew1982@gmail.com) (A.T. Tsegaw), [knut.alfredsen@ntnu.no](mailto:knut.alfredsen@ntnu.no) (K. Alfredsen), [ths@nve.no](mailto:ths@nve.no) (T. Skaugen), [tone.muthanna@ntnu.no](mailto:tone.muthanna@ntnu.no) (T.M. Muthanna).

<https://doi.org/10.1016/j.jhydrol.2019.03.090>

Received 3 October 2018; Received in revised form 14 March 2019; Accepted 25 March 2019

Available online 29 March 2019

0022-1694/ © 2019 Elsevier B.V. All rights reserved.

management (Spence et al., 2013).

Water resource management problems are increasingly approached using continuous time rainfall-runoff modelling (Lamb and Kay, 2004; Swain and Patra, 2017), rather than the traditional statistical or event-based models. Simple concept models such as the rational formula and its more sophisticated derivatives are criticized for containing parameters which are difficult to estimate (e.g. the runoff coefficient) or for being founded upon questionable assumptions (e.g. identical return period for precipitation and resulting peak flow) (Viviroli et al., 2009). The advantage of continuous simulation approaches is that the catchment moisture state prior to the flow-producing rainfall event is implicitly incorporated within the modeling framework provided that the model produces reasonable simulations (Pathiraja et al., 2012). Furthermore, getting the right answers for the right reasons is crucial for getting the right answers at all, if conditions shift beyond the range of prior experience (due to extreme precipitation events, climate change, or shifts in land use) (Kirchner, 2006).

Catchment size has an effect in hydrological modelling, and hydrological responses of small catchments are likely to be different from and more variable than those of large catchments (Pilgrim et al., 1982). Small catchments need to be modelled using shorter time steps (Blöschl and Sivapalan, 1995; Bronstert, 2003; Vormoor and Skaugen, 2013; Wetterhall et al., 2011). Until the 1990s, hydrologists had to rely mostly on data with a daily time step, e.g. accumulated rainfall amounts recorded once a day by observers, and this caused limitations to the applicability of rainfall-runoff models for problems (e.g. flooding) needing short time steps (Blöschl and Sivapalan, 1995; Creutin and Obled, 1980). However, over the last two decades, the availability of hourly and even sub-hourly data is increasing in many countries, especially with the implementation of automatic rain gauge networks and rainfall radars (Berne and Krajewski, 2013; Creutin and Borga, 2003).

A rainfall-runoff model is one of the tools used to predict flows in ungauged catchments (Nruthya and Srinivas, 2015). This method requires estimation of the model parameters using regionalization (Zhang et al., 2014). There are different types of rainfall-runoff hydrological models and regionalization methods. One method may work well for one type of model and another method may work well for another model in different regions (Razavi and Coulibaly, 2013) because each model has its own unique characteristics and respective applications (Devi et al., 2015). Conceptual rainfall-runoff models, such as HBV and Identification of Unit Hydrographs and Component Flows from Rainfall, Evaporation and Stream Data (IHACRES) have emerged as the most frequently used models for estimating continuous stream flow at ungauged catchments (Razavi and Coulibaly, 2013). The three commonly used regionalization methods are regression, physical similarity and spatial proximity (Bao et al., 2012; Bárdossy, 2007; Merz and Blöschl, 2004; Oudin et al., 2008; Parajka et al., 2005). Some hydrologists have tried to compare and evaluate the methods, but the results are not consistent (Kay et al., 2006; McIntyre et al., 2005; Oudin et al., 2008; Young, 2006; Zhang and Chiew, 2009). Young (2006) regionalized the Probability Distributed Model (PDM) in 260 catchments in the UK and found that the regression method was more accurate than the spatial proximity method. Skaugen et al. (2015) regionalized the Distance Distribution Dynamics (DDD) model in 84 catchments ranging from small to large sizes in Norway using daily data and found that multiple regression equations performed well in predicting flows at ungauged catchments. Kay et al. (2006) tried to compare the performance of regression and physical similarity methods with two models [PDM and Time–Area Topographic Extension (TATE)] for 119 catchments across the UK but did not obtain consistent results. For the PDM, physical similarity was more accurate, but regression outperformed physical similarity for TATE. Merz and Blöschl (2004) found that the multiple regression method of regionalization at 308 catchments in Austria, using HBV model involving 11 calibration parameters, gave significantly poorer results than the spatial proximity method. Oudin et al.

(2008) used two lumped rainfall-runoff models with daily data on 913 French catchments and found that when a dense network of gauging stations is available, the spatial proximity method provides the best regionalization solution, while the regression method shows the least satisfactory results, and the physical similarity method is in between the two others in accuracy. Magette et al. (1976) used 21 catchments in USA in the regionalization of six selected parameters of the Kentucky Watershed Model (KWM) using hourly data and found that a multiple regression method was successful in estimating model parameters from catchment descriptors, but a simple linear regression model was unsuccessful. Kokkonen et al. (2003) used 13 catchments in North Carolina, USA, in the regionalization of six parameters of IHACRES model with daily data and found that the arithmetic mean method of regionalization gave poorer results than regression and similar hydrologic behavior methods.

The major goal of the international PUB initiative was to reduce the uncertainty in the prediction of runoff by shifting away from tools that require calibration and curve fitting to tools that need little or no calibration (parsimonious models) (Spence et al., 2013). The PUB synthesis book states that the starting point for predicting the runoff hydrograph in ungauged catchments using rainfall-runoff models is the choice of an appropriate model structure (Blöschl et al., 2013). Sivapalan et al. (2003) pointed out that for predicting flow at ungauged catchments, it is important to challenge and overcome the potential problem posed by the “uniqueness in place” (Beven, 2000) of catchments. It is hence important that the hydrologic models are parametrically efficient (parsimonious), and their parameters are identifiable from the available catchment data (Young and Romanowicz, 2004). DDD is a parsimonious rainfall-runoff model with few calibration parameters recently developed by Skaugen and Onof (2014), and many of its other parameters can be estimated from the topography and land use of a catchment (Skaugen and Onof, 2014). Previous experience in using DDD for estimation of flow at ungauged catchments with daily data showed satisfactory results (Skaugen et al., 2015). Since DDD is one of the hydrological models which has features acknowledged for prediction of flow at ungauged catchments, we used it in this study.

During the calibration of hydrological models, it is common and probable that multiple calibration periods yield multiple optimum parameter sets. Different sets of optimum parameter values may yield similar performances, and this is designated as “equifinality” (Beven, 2006). Since conceptual hydrological models can be viewed as an empirically derived combination of mathematical operators describing the main features of an idealized hydrological cycle, one cannot rely on a uniquely determined model parameter set or model prediction (Kuczera and Parent, 1998). Consequently, attention should be given to uncertainties in hydrological modelling. Prediction uncertainties in hydrological modelling arise from a variety of sources, such as errors associated with input data and data for calibration, imperfection in model structure, calibration accuracy and uncertainty in model parameters (Benke et al., 2008; Jin et al., 2010; Montanari, 2011). In this study, uncertainty of the calibrated model parameters has been addressed.

Most of the regionalization methods applied so far are based on daily temporal resolution in catchments ranging from small to large sizes (Masih et al., 2010; Merz et al., 2006). Hailegeorgis et al. (2015) and Viviroli and Seibert (2015) have done regionalization studies with hourly resolution, but the studies are not specific to small catchments. Response times of small catchments are typically less than 24 h, and thus for flood forecasting purposes, hydrological models are required to provide simulations at high temporal resolution (Reynolds et al., 2017). Therefore, regionalization of model parameters for small catchments with sub-daily time resolution is important.

In this study, we have regionalized the DDD model parameters for small catchments with hourly time resolution in order to predict flows at ungauged rural small catchments in Norway. The specific research objectives are:

1. To evaluate the performance of the DDD rainfall-runoff hydrological model on rural small catchments with hourly temporal resolution (areas from 1 km<sup>2</sup>–50 km<sup>2</sup>). It includes the selection of parameters to calibrate, or to fix, the model goodness of fit and uncertainties in the calibration parameters.
2. To evaluate multiple regression-based regionalization against a physical similarity-based regionalization method.
3. To analyze and assess whether there is a combined regression and physical similarity method for regionalizing DDD model parameters.

## 2. Study area and data

Forty-one gauged small rural catchments located across Norway are used in the study. We selected the catchments from the Norwegian Water Resources and Energy Directorate (NVE) HYDRA II database of gauged catchments. Our definition of a small catchment follows that of Fleig and Wilson (2013) with an upper area limit of 50 km<sup>2</sup>. The number of catchments is limited by the availability of hydro-meteorological data with the required temporal resolution of 1 h and a length of record that makes calibration possible. Seven additional gauged catchments, which are not used in the model calibration, have been used in validation. Fig. 1 shows the location of the study and test catchments.

Time series of precipitation, temperature and discharge are the main input data for running and calibrating the DDD model. Precipitation and temperature are based on a 1 × 1 km gridded product of the Norwegian Meteorological Institute (<http://thredds.met.no/thredds/catalog.html>) with hourly temporal resolution (Lussana et al., 2016). Since the data is available from 2010 onwards, we have used a total of five years of data for calibration and validation. The DDD model uses distributed precipitation and temperature data as input for the model's 10 elevation zones extracted from the hypsographic curve of a catchment. The elevation of the center of each temperature and precipitation grid cell has been extracted from the 10 × 10 m digital elevation model (DEM) of Norway. For the model elevation zone that contains more than one grid cell, mean of the values of temperature and precipitation is used. Hourly discharge data have been obtained from the Norwegian Water Resources and Energy Directorate (NVE) HYDRA II database.

The constant model parameters during the simulation period are derived from an analysis of hydro-meteorological, topographical and land use data for a catchment using GIS. The source of the topography and land use data is the Norwegian Mapping Authority ([www.statkart.no](http://www.statkart.no)). The 10 × 10 m DEM, the river network and the 1: 50 000 scale land use data have been retrieved and used in the study. The DEM has been re-conditioned to the naturally occurring river network using the DEM reconditioning tool from Arc Hydro to create a hydrologically correct terrain model that can improve the accuracy of watershed modeling (Li, 2014). The re-conditioned DEM is further used to determine the distance distributions of hill slopes and river networks as needed by DDD.

## 3. Methodology

### 3.1. Model structure

The DDD model is written in R programming language (R Core and Team, 2017) and currently runs operationally with daily and three-hourly time steps at the Norwegian flood forecasting service at NVE. Subsurface and dynamic runoff are the two main modules of the model.

The volume capacity of the subsurface water reservoir,  $W$  (mm), is shared between a saturated zone with volume  $S$  (mm) and an unsaturated zone with volume  $D$  (mm). If the saturated zone is high, the unsaturated volume has to be small (Skaugen and Onof, 2014). The actual water volume present in the unsaturated zone is described as  $Z$  (mm). The subsurface state variables are updated after evaluating

whether the current soil moisture,  $Z(t)$ , together with the input of rain and snowmelt,  $G(t)$ , represent an excess of water over the field capacity,  $R$ , which is fixed at 30% ( $R = 0.3$ ) of  $D(t)$  (Skaugen and Onof, 2014). If  $G(t) + Z(t) > R \cdot D(t)$ , then the excess water  $X(t)$  is added to  $S(t)$ .

$$\text{Excess water } X(t) = \text{Max} \left\{ \frac{G(t) + Z(t)}{D(t)} - R, 0 \right\} D(t) \quad (1)$$

$$\text{Groundwater } \frac{dS}{dt} = X(t) - Q(t) \quad (2)$$

$$\text{Soil water content } \frac{dZ}{dt} = G(t) - X(t) - Ea(t) \quad (3)$$

$$\text{Soil water zone } \frac{dD}{dt} = -\frac{dS}{dt} \quad (4)$$

$$\text{Potential evapotranspiration } Ep = cea * T \quad (5)$$

$$\text{Actual evapotranspiration } Ea = Ep * \frac{S + Z}{W} \quad (6)$$

$Q(t)$  is runoff, and  $Ea(t)$  is the actual evapotranspiration which is estimated as a function of potential evapotranspiration and the level of storage. A degree hour factor ( $cea$ ) is positive for positive temperature ( $T$ ) and zero for negative temperature.  $Ea$  is drawn from  $Z$ . This is indeed a simplification, but experience from Skaugen and Onof (2014) shows that the evapotranspiration routine in DDD calculates similar values to the approach used in HBV (Bergström, 1976). A recession analysis of the observed runoff from the catchment is used to estimate the catchment scale fluctuations of storage (the capacity of the subsurface water reservoir,  $W$ , see Skaugen and Mengistu, 2016).

The dynamics of runoff in DDD has been derived from the catchment features using a GIS combined with runoff recession analysis. The method for describing the runoff dynamics of a catchment is built on the distance distribution derived from the catchment topography. The distances from the points in the catchment to the nearest river reach are calculated for marsh and soil (non-marsh) parts of a hillslope. Previous studies in more than 120 catchments in Norway showed that the exponential distribution described the hillslope distance distribution well, and the normal distribution described well the distances between points in the river network and outlet of a catchment (Skaugen and Mengistu, 2016; Skaugen and Onof, 2014). Fig. 2 shows a map of the distance distributions of the marsh and soil (non-marsh) parts of the hillslope and river network for the Valen catchment and the corresponding empirical cumulative distribution functions. Fig. 3 shows the structure of the DDD model. All GIS work is done with ArcMap 10.3, and the recession analysis is done using the R script.

In the model, water is conveyed through the soils to the river network by waves with celerity determined by the actual storage,  $S(t)$ , in the catchment (Skaugen and Mengistu, 2016; Skaugen and Onof, 2014). The celerity associated with the different levels of subsurface storage is estimated by assuming exponential recessions with parameter  $\Lambda$  in the equation  $Q(t) = Q_0 \Lambda e^{-\Lambda(t-t_0)}$ , where  $Q_0$  is the peak discharge immediately before the recession starts.  $\Lambda$  is the slope of change per time ( $t$ ) of the recession in the log-log space and calculated using Eq. (7). The distribution of  $\Lambda$  is modeled using a two-parameter gamma distribution.

$$\Lambda(t) = \frac{\log(Q(t)) - \log(Q(t + \Delta t))}{\Delta t} \quad (7)$$

The celerity,  $v$ , is calculated as a function of  $\Lambda$  using Eq. (8).

$$v = \frac{\Lambda d_{mean}}{\Delta t} \quad (8)$$

$d_{mean}$  is the mean of the distances from points in the catchment to the nearest river. The capacity of the subsurface reservoir  $W$  (mm), is divided into storage levels  $i$  corresponding to the quantiles of the distribution of  $\Lambda$  under the assumption that the higher the storage, the higher the value of  $\Lambda$ . Each storage level is further assigned a celerity



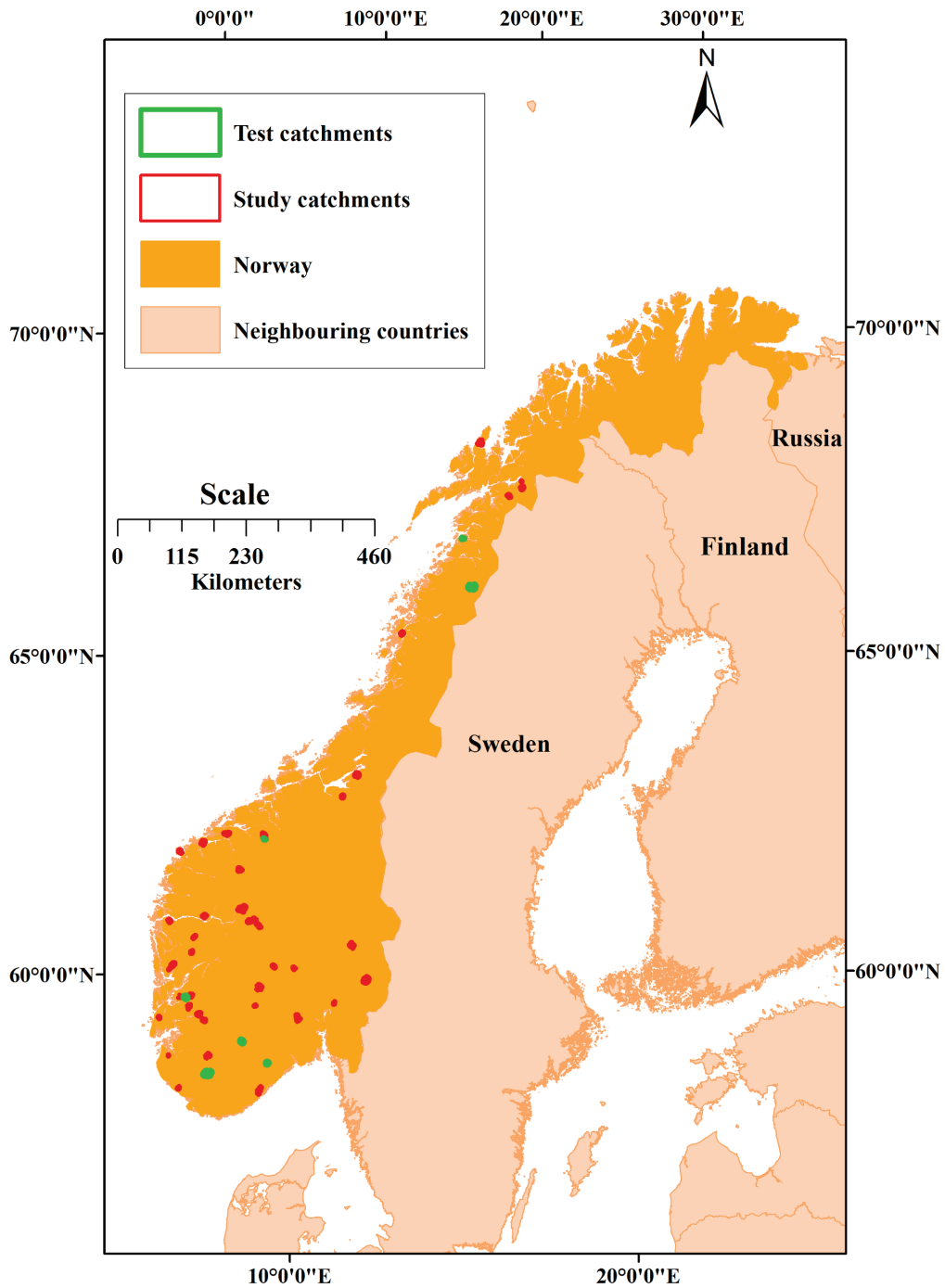


Fig. 1. Locations of the study and test catchments used in Norway.

$v_i = \frac{\lambda_i d_{mean}}{\Delta t}$  (see Eq. (8)), where  $\lambda_i$  is the parameter of the unit hydrograph for the individual storage level  $i$ , and estimated such that the runoff from several storage levels will give a unit hydrograph equal to

the exponential unit hydrograph with a parameter  $\Lambda_i$ . With the assumption that the recession and its distribution carry information on the distribution of catchment-scale storage, we can consider that the

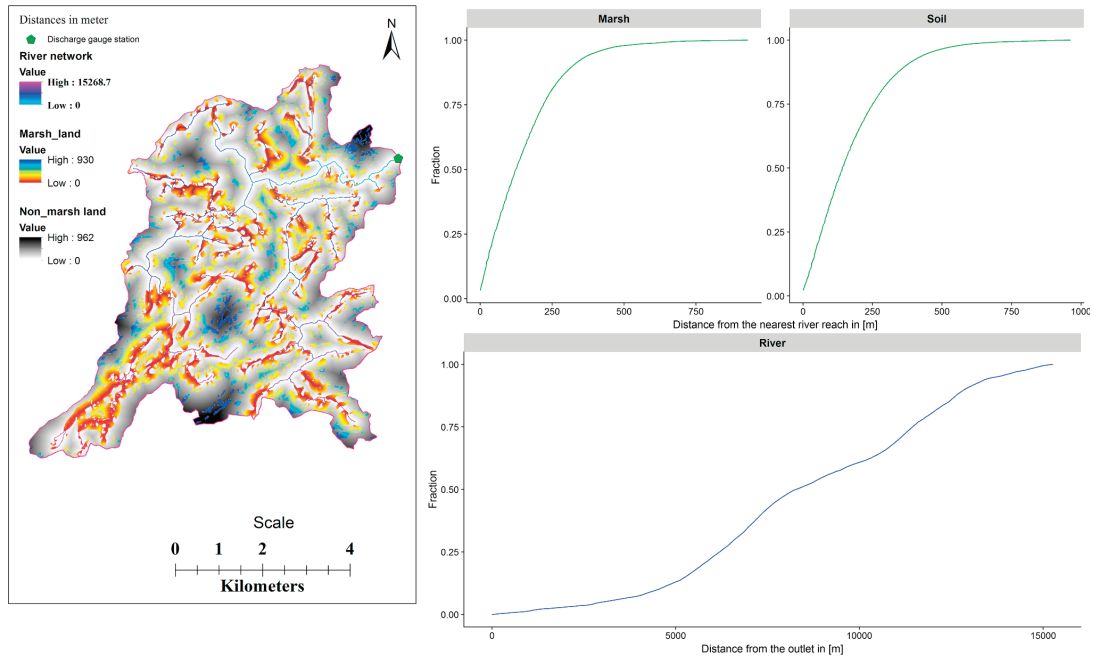


Fig. 2. Map of distance distribution of marsh, non-marsh (soil) part of hill slope and river network and the corresponding empirical cumulative distribution functions for catchment Valen.

temporal distribution of catchment-scale storage,  $S(t)$ , is a scaled version to that of  $\Lambda$ .  $S(t)$  is calculated using Eq. (9), and its distribution is modelled using a two-parameter gamma distribution.

$$S(t) = \frac{Q(t)}{1 - e^{-\lambda(t)}} \quad (9)$$

### 3.2. Model parameters and calibration

The model has three main groups of parameters. The first group are those determined by model calibration against observed discharge (the upper 5 in Table 1), the second group are those estimated from observed hydro-meteorological data (the lower 4 in Table 1 and the upper 3 in Table 2), and the third group are those estimated from geographical data (all in Table 2 except the upper 3). The calibration of the

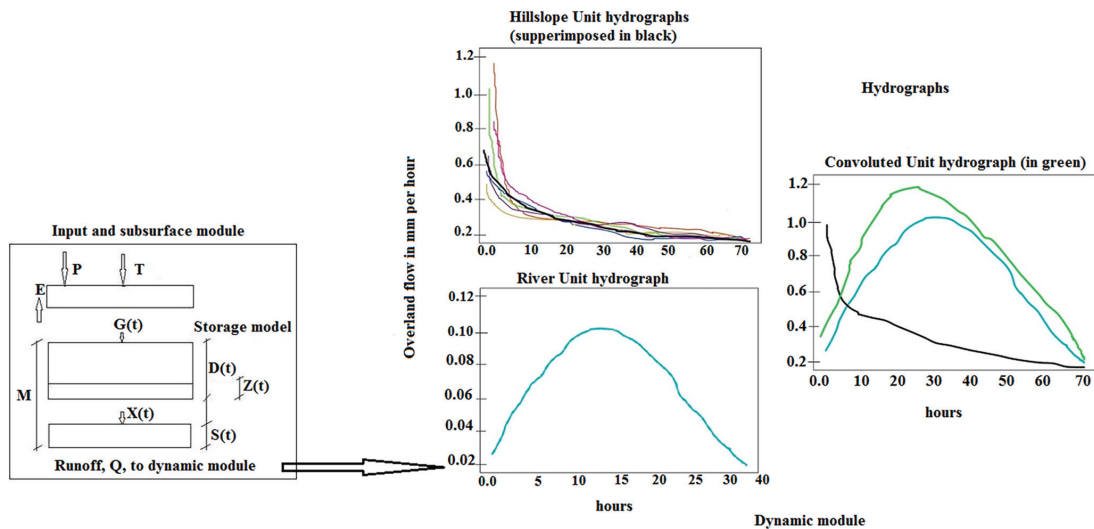


Fig. 3. Structure of the Distance Distributions Dynamics model adapted from Skaugen and Onof (2014). Left panel: the storage model and right panel: hydrographs of hillslope and river.

**Table 1**  
List of nine model parameters needing regionalization.

Parameters	Description of the parameter	Method of estimation	Unit	Intervals of calibration
pro	Maximum liquid water content of snow	Calibration	fraction	0.03 – 0.1
cx	Degree hour factor for snow melt	Calibration	mm °C <sup>-1</sup> h <sup>-1</sup>	0.05 – 1.0
CFR	Degree hour factor for refreezing	Calibration	mm °C <sup>-1</sup> h <sup>-1</sup>	0.001 – 0.01
cea	Degree hour factor for evapotranspiration	Calibration	mm °C <sup>-1</sup> h <sup>-1</sup>	0.01 – 0.1
rv	Celerity for river flow	Calibration	meter/second	0.5 – 1.5
Gshape	Shape parameter of $\lambda$	Recession analysis of observed runoff	Positive real number	not calibration parameter
Gscale	Scale parameter of $\lambda$	Recession analysis of observed runoff	Positive real number	not calibration parameter
GshInt	Shape parameter of $\Lambda$	Recession analysis of observed runoff	Positive real number	not calibration parameter
Gsclnt	Scale parameter of $\Lambda$	Recession analysis of observed runoff	Positive real number	not calibration parameter

model is performed using the probability particle swarm optimization (PPSO) algorithm (Lu and Han, 2011). The Kling-Gupta efficiency criteria (KGE) has been used as an objective function for the calibration (Gupta et al., 2009), and the KGE and BIAS (ratio of the mean of simulated to observed discharge) have been used to evaluate the calibrated results. In addition, the hydrographs of all catchments are visually inspected.

The calibration intervals of the parameters are set based on literature and experience in using the DDD model (Skaugen and Mengistu, 2016; Sælthun, 1996). Since cea and degree hour factor for snow melt (Cx) are sensitive to the temporal resolution, we used the DDD model calibration results from 84 catchments with daily time step (Skaugen et al., 2015) as a starting point, and literature review for setting the intervals of hourly time step. The mean celerity for river flow (rv) has a standard value of 1 m/s in using DDD with catchments ranging from small to large sizes (Skaugen and Mengistu, 2016) with daily time steps, but it has been calibrated with an interval of plus or minus 0.5 m/s of the standard value for hourly resolution. From experience and field measurements, we have set the calibration interval of maximum liquid water content of snow (pro) between 3% and 10% (Fierz et al., 2009; Saloranta, 2012).

For the 41 study catchments, we have calibrated the model on 2–3 years of data and validated on 1–2 years. The selection of the period is mainly based on the availability of flow and gridded precipitation and temperature data. The gridded precipitation data in Norway is highly uncertain due to rugged terrain and few precipitation stations in elevated areas. The data used does not include the correction for undercatch due to the wind, and the relation between the precipitation and elevation is introduced only locally around the station locations. As a result, the predicted precipitation field may potentially underestimate the actual precipitation, especially at higher elevations where the

station network is sparser such as at the mountainous region of the southern part of Norway (Frauenfelder et al., 2017; Lussana et al., 2018). Accordingly, we introduced a precipitation correction factor to take this into account so that the long-term water balance is correct. The correction factor is applied to those catchments that give BIAS less than 0.8, and the correction factor is the ratio of long-term mean annual discharge to mean of simulated discharge. For purely ungauged catchments, the long-term mean annual discharge is estimated from a gridded map of average annual runoff for Norway for the period 1961–1990 (Beldring et al., 2003). The threshold temperature for rain or snow and snow melt are fixed with a value of 0.5 °C and 0.0 °C, respectively, based on literature (Saloranta, 2012; Skaugen, 1998). This is done to avoid regressed parameters that do not have a clear physical relationship with any of the catchment descriptors, but which can be fixed on a physical or an empirical basis. Removing parameters from calibration also strengthens the parsimony of the model. Table 1 lists the nine model parameters needing regionalization (five calibrated and four estimated from recession analysis), and Table 2 lists the non-regionalized model parameters. The snow routine in DDD has two non-regionalized parameters. The shape parameter (a0) and the decorrelation length (d) of the gamma distribution of snow and snow water equivalent (SWE) (Skaugen and Weltzien, 2016) are estimated from the previous calibration of 84 catchments in Norway (Skaugen et al., 2015).

### 3.3. Uncertainty analysis of calibrated parameters

We calibrated the model using probability particle swarm optimization (PPSO) algorithm with 500 calibration runs for each study catchment and sampled sets of parameters from the calibration runs for uncertainty analysis. To select behavioral sets of parameters, we used a threshold KGE value of 70th percentile (a value below which at least

**Table 2**  
Non-regionalized model parameters which are unique to the local catchment of interest.

Symbol of parameters	Description of the Parameter	Method of estimation
a0	Parameter for new spatial distribution of SWE, shape parameter	From spatial distribution of observed precipitation
d	Parameter for new spatial distribution of SWE, decorrelation length	From spatial distribution of observed precipitation
MAD	Long term mean annual discharge	From long term observed mean annual flow data
area	Catchment area	GIS
maxLbog	Maximum distance of marsh land portion of hillslope	GIS
midLbog	Mean distance of marsh land portion of hillslope	GIS
bogfrac	Areal fraction of marsh land from the total land uses	GIS
zsoil	Areal fraction of DD for soils (what area with distance zero to the river)	GIS
zbog	Areal fraction of distance distribution for marsh land (what area with distance zero to the river)	GIS
midFl	Mean distance (from distance distribution) for river network	GIS
stdFl	Standard deviation of distance (from distance distribution) for river network	GIS
maxFl	Maximum distance (from distance distribution) for river network	GIS
maxDl	Maximum distance (from distance distribution) of non-marsh land (soils) of hill slope	GIS
midDL	Mean distance (from distance distribution) of non-marsh land (soils) of hill slope	GIS
midGl	Mean distance (from distance distribution) for Glacial	GIS
stdGl	Standard deviation of distance (from distance distribution) for Glacial	GIS
maxGl	Maximum distance (from distance distribution) for Glacial	GIS
Hypsographic curve	11 values describing the quantiles 0, 10, 20, 30, 40, 50, 60, 70, 80, 90, 100	GIS

**Table 3**  
Statistics of the catchment descriptors (CDs) of the study catchments used in the regionalization.

S.no	Catchment Descriptors	Symbol	Minimum	Maximum	Average	Unit
1	Topographic					
1.1	Area	A	1	50.7	28.2	km <sup>2</sup>
1.2	Mean of grid to grid slope	M <sub>g</sub>	8	64.8	28.4	%
1.3	Mean of elevation	M <sub>e</sub>	59.6	1372	654	m
1.4	Mean of non-marsh land distance from the river	M <sub>s</sub>	131.1	434.2	236.7	m
1.5	Mean of marsh land distance from the river	M <sub>m</sub>	0	389.4	140.1	m
1.6	Mean of river length from the outlet	M <sub>r</sub>	421.3	11422.5	5459.6	m
1.7	Standard deviation of river length from the outlet	S <sub>r</sub>	262	5583.6	2531.2	m
1.8	River Slope	R <sub>s</sub>	7.5	146	49	m/km
2	Land Uses					
2.1	Lake	L	0	13.6	5.63	%
2.2	Effective lake	L <sub>e</sub>	0	11	2.3	%
2.3	Bare mountain	B	0	93.7	48.2	%
2.4	Cultivated land	C	0	35	1.8	%
2.5	Forest	F	0	94.3	32.7	%
2.6	Marsh land	M	0	28.9	4.6	%
2.7	Urban	U	0	1.5	0.1	%
2.8	Glacial	G	0	5.1	0.3	%
3	Hydro-meteorological					
3.1	Mean annual precipitation	M <sub>p</sub>	679	3090	1543	mm
3.2	Mean annual temperature	M <sub>t</sub>	−2.5	7.2	2.6	°C
3.3	Specific discharge	S <sub>q</sub>	11.3	150.8	58	l/(s*km <sup>2</sup> )

70% of the values lie) from the 500 runs for each study catchment. Evaluating several thousand calibration runs with an hourly resolution at 41 study catchments is computationally costly. To check whether the 500 runs used in the calibration give different behavioral sets from several thousand calibration runs, we ran the model with 2000 runs at one catchment, and 5000 and 10,000 runs at another catchment. All the study catchments are run with the behavioral sets of parameters, but the results are presented only for four randomly selected catchments. For each timestep, we sampled the number of discharge values equal to the number of behavioral parameter sets for each catchment, and the minimum and maximum discharges are used to estimate the width of the uncertainty bounds.

#### 3.4. Regionalization methods

We used 41 catchments with KGE greater than or equal to 0.55 for the regionalization of the model parameters. For the three regionalization methods used in this study, 19 catchment descriptors (CDs) readily available from catchment data are used at the start and later refined based on their significance in estimating model parameters (Table 3). Since the selected catchments are widely spread across Norway, the spatial proximity method of regionalization may not be favored and is not considered in this study (Oudin et al., 2008). Validation of the regionalization methods is done assuming a selected number of gauged catchments to be ungauged and then comparing simulated runoff (using the regionalized parameters) with observed runoff.

##### 3.4.1. Multiple regression method

The multiple regression equations, which are used to relate the CDs with the model parameters, are fitted to the calibrated model parameters of the 41 catchments. We used a stepwise regression procedure for building the regression model. We build the model from 19 candidate CDs by entering and removing CDs in a stepwise manner into the regression model until there is no convincing reason to enter or remove any more. Before starting to use the step wise procedure, we removed a CD which is highly correlated with another CD(s). To identify the correlation between the CDs, we have plotted the scatter plot matrix of the CDs (predictors). When R-Squared of correlation between two CDs is greater than or equal to 0.5, they are considered as highly correlated. The stepwise procedure is described in detail as follows:

- i) We set a significance level of 0.2 for deciding when to enter into and remove from the stepwise model. We set the significance level so that it is not too difficult to enter CDs into the model and not too easy to remove CDs from the model.
- ii) We fit each of the one-predictor models that regress each model parameter with all CDs one by one. Example: celerity of river flow (rv) against bare mountain (B), rv against forest (F), etc.
- iii) Of those predictors (CDs) whose *P*-value is less than 0.2, the first predictor introduced to the stepwise model is the CD that has the smallest *P*-value. Accordingly, bare mountain is the first predictor for celerity of river flow.
- iv) If no predictor (CD) has a *P*-value less than 0.2, stop fitting the regression model (CFR is a typical example for this step).
- v) Now, we fit each of the two-predictor models that include the first CD as a predictor. Example: rv on B and R<sub>s</sub>, rv on B and U, etc.
- vi) Of those predictors whose *P*-value is less than 0.2, the second predictor put in the stepwise model is the predictor that has the smallest *P*-value. For the celerity of river flow (rv), river slope was deemed the “best” second predictor, and it is therefore entered into the stepwise model.
- vii) Now, since the bare mountain was the first predictor, we step back and see if entering river slope into the stepwise model somehow affects the significance of the bare mountain predictor. That is, check whether the *P*-value of bare mountain is less than 0.2 or not. If the *P*-value is less than 0.2, the first predictor (bare mountain) is retained in the stepwise model.
- viii) Continue the steps as described above until adding an additional predictor does not yield a *P*-value below the significant level chosen.

Both linear and non-linear (logarithmic) forms of the response variables (model parameters needing regionalization) and predictors (CDs) are tested in the regression model. If the non-linear values contribute significantly, then the non-linear form is retained in the model with the transformed value.

##### 3.4.2. Physical similarity method

The physical similarity method relies on the assumption that the same parameter set should be successful in physically similar catchments (Merz and Blöschl, 2004; Oudin et al., 2008; Parajka et al., 2005; Zhang and Chiew, 2009). The transfer can be made from one or several

donor catchments on the basis of a chosen similarity method (McIntyre et al., 2005). The method transfers entire parameter sets from gauged to ungauged catchments instead of establishing links between model parameters and CDs. In this study, we used two types of physical similarity methods i.e. single-donor based, and pooling-group based. We used 12 CDs (2 hydro-climatic, 4 land uses, 3 topographic and 3 that can describe the runoff dynamic processes in DDD). The CDs used are: area, mean elevation, mean of soil (non-marsh land) distance from a river, mean of marsh land distance from the river, mean of river distance from outlet, river slope, effective lake percentage, forest, urban, mean annual precipitation, specific discharge and bare mountain.

For the single-donor type, we used a rank accumulated method of physical similarity in selecting a donor catchment to a test catchment (Oudin et al., 2008; Zhang and Chiew, 2009). For each CD, the catchment with the most similar descriptor to the test catchment is assigned rank 1, the catchment with the second most similar descriptor is assigned rank 2, and so on. When two or more catchments have the same value of CDs with the test catchment, they have been assigned the same rank. The rank numbers of CDs have been added for each of the study catchments. Each CD used for regionalization is given equal weight in the ranking system (Oudin et al., 2008). All the 41 catchments are considered in the selection of the most similar catchment to each of the 7 test catchments. The single gauged catchment with the smallest total rank is used as a donor catchment.

In the pooling-group type, the parameters for an ungauged site are estimated from the calibrated parameters of a pooling-group, i.e., a set of gauged catchments considered to be most similar to the target ungauged catchment in terms of some set of CDs (Kay et al., 2006, 2007). Kay et al. (2006) defined physical similarity by Euclidean distance in a space of CDs that was determined for each model parameter as shown in Eq.10.

$$dist_{a,b} = \sqrt{\sum_{j=1}^J \left( \frac{X_{a,j} - X_{b,j}}{\sigma_{x,j}} \right)^2} \quad (10)$$

where  $j$  indicates one of a total of  $J$  CDs (12 in this study),  $X_{a,j}$  is the value of that CD at the  $a^{\text{th}}$  test catchment,  $X_{b,j}$  is the value of the CD at  $b^{\text{th}}$  study catchment, and  $\sigma_{x,j}$  is the standard deviation of the CD across all the  $N$  study catchments (41 in this study). Kay et al. (2007) suggests that around a 10-member pooling group is preferable to a much larger number, particularly when many CDs are used to define Euclidean distance for the pooling group.  $K(7$  in this study) closest neighbors (minimum distance) are selected to create a pooling group for the test catchments.

After identifying the pooling group, the estimate of the model parameter at the test catchment  $a$  ( $\alpha_a^{PG}$ ) is calculated as a weighted average of the corresponding parameters from the study catchments in the pooling group. Kay et al. (2007) stated that it is more appropriate to write the expression for the model parameter as a weighted average of the estimated parameter values,  $\alpha_m$ , for all catchments ( $N$ ) as shown in Eq. (11).

$$\alpha_a^{PG} = \frac{\sum_{m=1}^N h_{am} \alpha_m}{\sum_{m=1}^N h_{am}} \quad (11)$$

Catchments not in the pooling group are given a weight  $h_{am}$  equal to zero, but those in the pooling are assigned weights to reflect their importance which is based on the distance measure  $dist_{a,b}$  as defined in Eq. (10). The weights of the pooling group members are estimated by Eq. (12).

$$h_{am} = 1 - S_{am} \quad (12)$$

where

$$S_{am} = \begin{cases} dist_{a,b}/dist_{a,max} & \text{for linearly decreasing weights} \\ (dist_{a,b}/dist_{a,max})^2 & \text{for quadratically decreasing weights} \end{cases}$$

Where  $dist_{a,max}$  is set to be 10% larger than the maximum distance of a pooling group member from the test catchment,  $a$ . In this study, we used a linear weight assigning method.

#### 3.4.3. Combined method

The 9 model parameters needing regionalization come from two groups with different estimation methods. In the combined method, the new parameter set is derived by combining regression and physical similarity methods, i.e., when regression is used for the first group, physical similarity is used for the second group and vice versa.

## 4. Results

### 4.1. Calibration

To evaluate the performance of the DDD model in calibration and validation, we used the KGE, BIAS and visual inspection of hydrographs. The model performs satisfactorily ( $0.5 \leq KGE < 0.9$ ) both for the study (for calibration and validation) and for the test catchments (for calibration). The minimum and maximum KGE values during calibration of the study catchments are 0.55 and 0.89 respectively while the median is 0.71. The minimum and maximum KGE values during validation are 0.4 and 0.88 respectively while the median is 0.66. The median BIAS value for calibration and validation is 0.88. As stated in Thiemeig et al. (2013),  $0.75 \leq KGE < 0.9$  is good,  $0.5 \leq KGE < 0.75$  is intermediate and  $0.0 \leq KGE < 0.5$  is poor. When validating, 5, 27 and 9 study catchments show poor, intermediate and good KGE values respectively. Except for one catchment, all test catchments give satisfactory calibration results. The visual inspection of the hydrographs shows underestimation of floods caused by heavy precipitation.

### 4.2. Uncertainty of calibrated parameters

From parameter samples of different sizes at two of the study catchments, the frequency histograms and dot plots of the behavioral calibrated parameters show the same optimal value for the different sizes. Fig. 4(a) and (b) show the histogram and dot plot for one calibrated parameter (celerity of river flow), respectively. The results show that we have the same value of optimal parameter at 500, 5000 and 10,000 iterations, and hence a sample size of 500 appears to be sufficient for the uncertainty analysis of calibrated parameters.

The frequency histograms of behavioral calibrated parameters for the 41 study catchments are analyzed. The results of histograms (pro, cea, rv and cx) for the four randomly selected study catchments are shown in Fig. 5(a) to (d). The histograms show that the calibrated parameters have a well-identifiable modal value. The parameters max out the calibration interval except for rv. For each timestep, we used discharge values simulated from 170, 156, 183 and 179 behavioral parameter sets in the calibration period to plot the uncertainty bounds for the catchments with identification numbers (ID) 6.10, 19.107, 73.27 and 123.29 respectively. Examples of simulated ranges and observed discharges are shown in Fig. 6.

### 4.3. Regionalization results

#### 4.3.1. Regression method

The multiple regression equations are shown in Eqs. (13)–(20). The overall multiple regression model for CFR is statistically insignificant, hence the mean of the 41 calibrated catchments (0.007) has been used as the regionalized model parameter. For catchments with a CD value of zero in a logarithmic expression, a value of 1 has been assigned. The units of the model parameters are presented in Table 1. There is a probability that parameters estimated using the multiple regression equations can lie outside of the calibration intervals. In this case, we will use the nearest boundary value from the calibration interval.

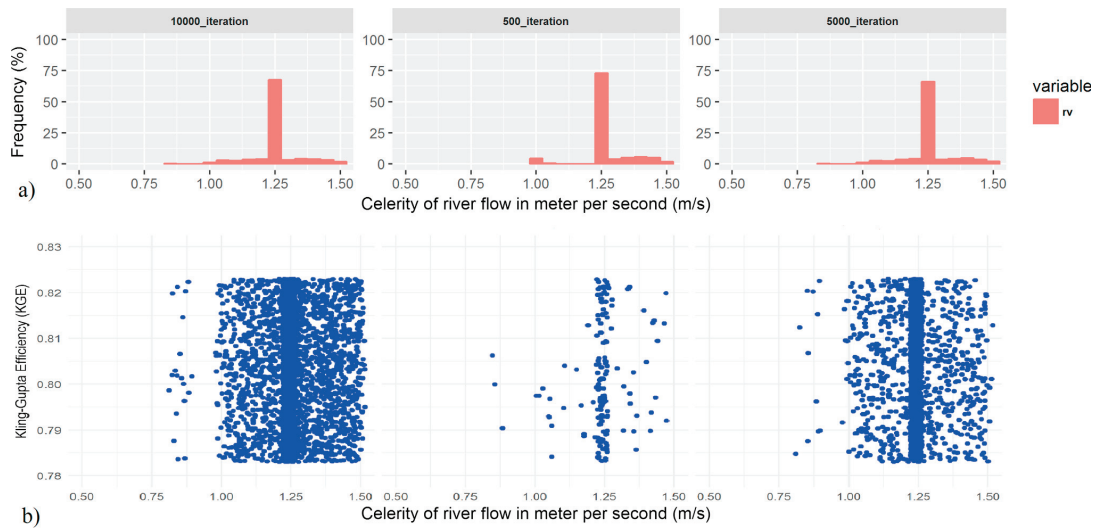


Fig. 4. Frequency histogram and dot plot of celerity of river flow for three different sample sizes at the study catchment with identification number 19.107.

$$Pro = 0.017 + 0.026\log(M_m) - 0.066\log(M_e) + 0.038\log(M_r) + 0.013\log(M_c) - 0.029U \quad (13)$$

$$Cx = \exp(-4.2 + 0.41\log(M_e) + 0.87\log(M_p) - 0.95\log(M_s)) \quad (14)$$

$$Cea = \exp(-8.78 + 0.28\log(M_e) + 1.17\log(M_p) - 0.26\log(M_m) + 0.22\log(M_r) + 0.003F) \quad (15)$$

$$rv = 0.83 + 0.05\log(R_s) + 0.003B \quad (16)$$

$$Gscale = \exp(-5.12 - 0.12L_e + 0.22\ln(S_q) + 0.3\log(M_e)) \quad (17)$$

$$Gshape = 0.82 + 0.0005M_p - 0.009S_q \quad (18)$$

$$GshI = 2.047Gshape - 0.658 \quad (19)$$

$$GscI = 0.49Gscale - 0.0014 \quad (20)$$

The standardized residuals of the regression model for the response variables show a distribution close to normal (Fig. 7). Fig. 7 shows that few large and small values deviate from the approximated straight line of normal probability plot while many of the residuals lie along the straight line. Fig. 8 shows the actual (calibrated and estimated from observed hydro-meteorological data) and predicted values of the response variables with the multiple regression model. The standard error of estimate is a measure of the accuracy of the regression model predictions and informs how much uncertainty is associated with the model prediction. The standard error result of the regression model shows that there is uncertainty in the predicted values. Table 4 presents the summary of the multiple correlation coefficient ( $R^2$ ), their significance and standard errors for the 41 catchments used in the regionalization. The non-parametric Spearman rank correlation was used (Seibert, 1999).

#### 4.3.2. Physical similarity method

For the single-donor type, Table 5 summarizes the smallest total rank used to select a donor catchment. For the pooling-group type, we analyzed different numbers of group members (3–20) to get an overview on the dependency of KGE values on the number of group members. The KGE values are slightly sensitive to the number of group members (Table 6). Table 7 presents the seven pooling-group members for test catchment 19.79, with Euclidian distance, the weights and the

weighted-average value (regionalized value) for celerity of river flow (rv).

#### 4.3.3. Combined method and comparison of methods

The DDD model parameters needing regionalization are two groups. The first group is estimated from calibration, and the second group is estimated from observed hydro-meteorological (described in detail under Section 3.4.3). Table 8 presents the regionalized model parameters using the three methods (physical similarity, multiple regression and combined) for one of the test catchments (ID 25.32) and compares with the calibrated parameters and parameters derived from recession.

The KGE and BIAS performance results for the three regionalization methods are presented in Table 9. KGE and BIAS values have an optimum value of 1. Fig. 9 presents the observed and predicted hydrographs using the three regionalization methods for two of the test catchments, and Table 10 compares the performance of calibration against regionalization methods.

## 5. Discussion

### 5.1. Model performance and parameters

The evaluation of calibration and validation results shows that the DDD model performs satisfactorily, but we have observed underestimation of floods caused by heavy precipitation events. The main reason for the underestimation of floods is likely an underestimation of the higher precipitations in the gridded data. Comparisons of the gridded precipitation with gauged data for the Svarttjønnbekken (ID 123.29 and area 3.6 km<sup>2</sup>) and Hokfossen (ID 123.28 and area 8.1 km<sup>2</sup>) catchments show that the gridded value is lower than the gauge-recorded data for several floods. Since we do not have rain gauges installed within the other small catchments used, we have to rely on the gridded data for the nationwide study. Another reason could be the assumption that the GIS-derived model parameters are constant during low, medium and high flows. The distance distributions of the marsh land and soil (non-marsh) land of hillslope and the distance distribution of the river network could be different during the three flow conditions. During heavy precipitation events (that can cause damaging floods), the river network transporting overland flow could increase and produce faster runoff generation, and it will be a topic for further investigation.



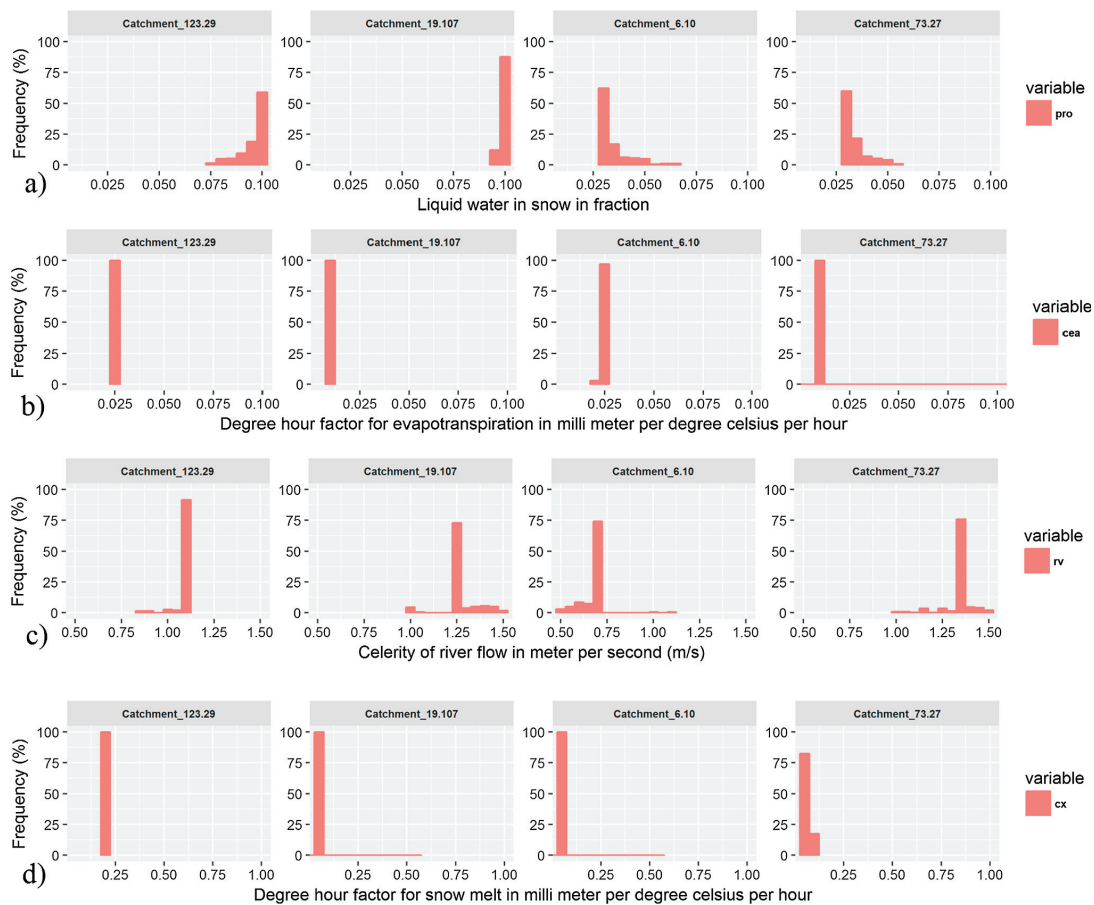


Fig. 5. Frequency histograms of liquid water in snow (pro), degree hour factor for evapotranspiration (cea), degree hour factor for snow melt (cx) and celerity of river flow (rv).

### 5.2. Uncertainty of calibrated parameters

Both the dot plots and the frequency histograms of the 5000 and 10,000 sample sizes have the same shape and distribution as the 500-sample size for the behavioral parameters. The histograms and dot plots of the river flow celerity for the catchment with ID 19.107 [Fig. 4(a) and (b)] show that the optimum celerity parameter is identifiable and has the same value (1.25 m/s) for sample sizes of 500, 5000 and 10000. Similar findings have been obtained using sample sizes of 500 and 2000 at another study catchment.

The calibrated parameters show one clear peak or most frequent value for almost all the study catchments even if the peak is at the extreme boundaries of the calibration interval for some parameters. The sharp and peaked distributions are associated with well-identifiable parameters, and the parameter estimates can unambiguously be inferred as modal values, while flat distributions indicate more parameter uncertainty (Blasone et al., 2008; Jin et al., 2010). The identifiability of the parameters and their small uncertainty resulted in the narrow width of uncertainty bounds (the difference between the maximum and minimum discharge for each hour). The small uncertainty of the calibrated model parameters reduces uncertainty in the model predictions at ungauged catchments. Two model parameters (degree hour factor for evapotranspiration and snow melt) show sharp, peaked and skewed

distribution to the lower boundary of the calibration intervals. Since the intervals are set based on experience, field results and literature, the skewness indicates that we can get a higher performance criteria (KGE) if we let the calibration parameters go beyond the specified intervals. However, we believe that gaining a higher KGE value in these cases comes with a cost of less realistic model parameters, and it was decided to keep the parameter intervals within a reasonable value.

### 5.3. Regionalization methods

#### 5.3.1. Multiple regression and physical similarity

The multiple regression performs satisfactorily in regionalizing the DDD model parameters, despite the uncertainty in the regression model. The pooling-group method also performs satisfactorily in regionalizing the model parameters despite the slight sensitivity of the method to the number of pooling-group members.

Significant correlations have been obtained between model parameters and CDs for the regression equations. Effective lake percentage, mean annual precipitation, specific discharge and mean elevation of the catchments are used to estimate the shape and scale parameters of  $\lambda$  and  $\Lambda$ . The scale parameter of  $\lambda$  is correlated with the effective lake percentage, the mean elevation and the specific discharge in the catchment. The shape and scale parameters of  $\Lambda$  are highly correlated

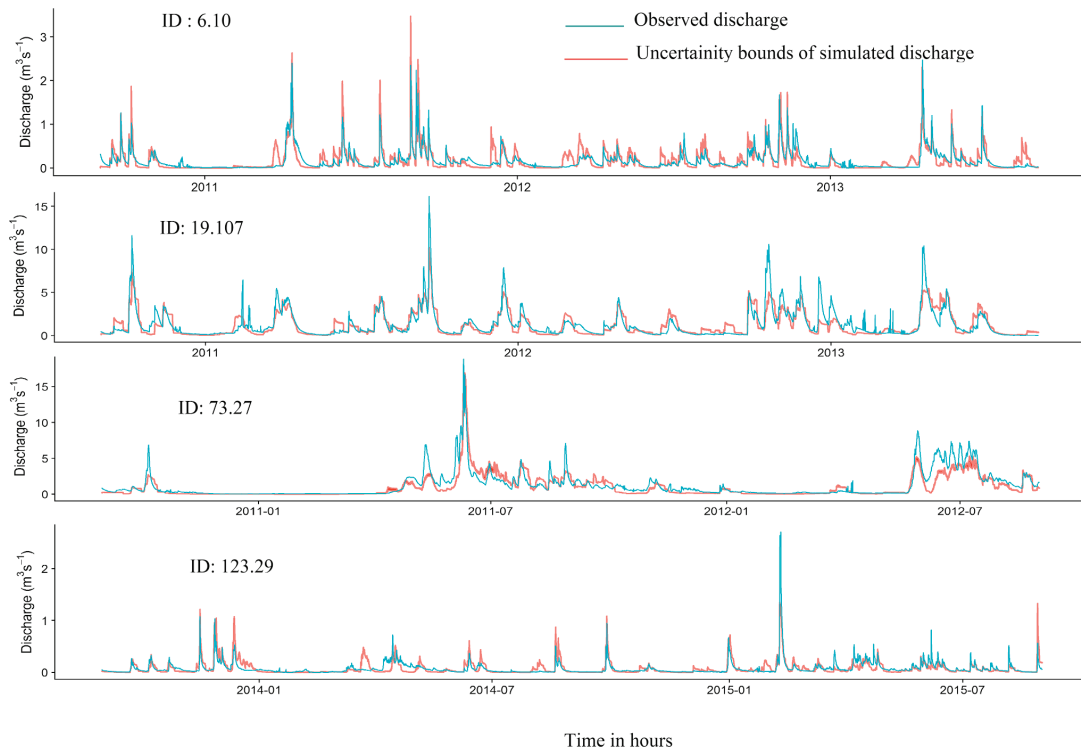


Fig. 6. Uncertainty bounds of DDD simulations due to calibrated parameters and observed discharges at four of the study catchments selected randomly.

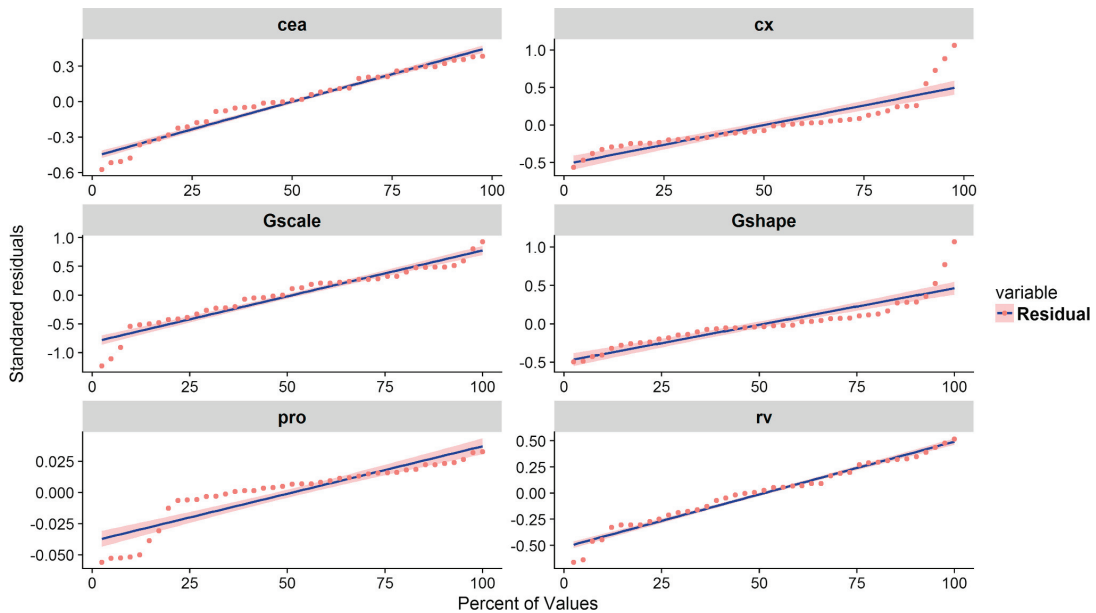


Fig. 7. Normal probability plots of the standard residuals of the multiple regression model.



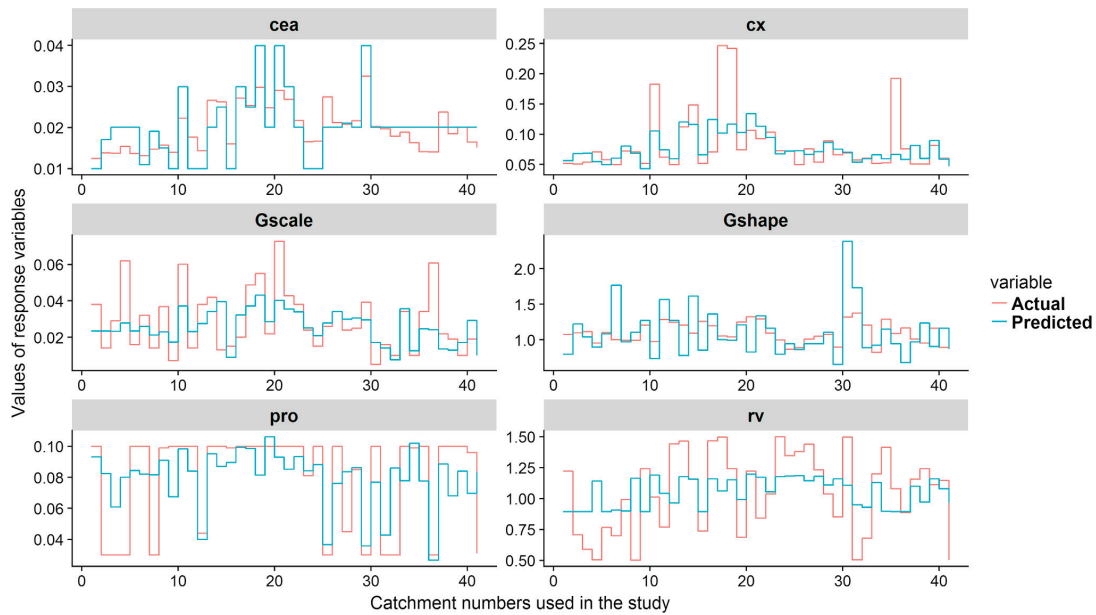


Fig. 8. Actual and predicted values of the response variables using the multiple regression model.

Table 4  
Summary of the multiple correlation coefficient of determination ( $R^2$ ), their significance ( $p$ -value) and standard error of the study catchments.

Parameter	Description of the parameter	$R^2$	Significance ( $p$ -value)	Standard Error
pro	Liquid water in snow	0.4	0.01	0.03
cx	Degree hour factor for snow melt	0.42	0.0001	0.35
cea	Degree hour factor for evapotranspiration	0.51	0.0001	0.28
rv	Celerity for river flow	0.14	0.06	0.3
Gshape	Shape parameter of $\lambda$	0.2	0.03	0.32
Gscale	Scale parameter of $\lambda$	0.43	0	0.5
GshInt	Shape parameter of $\Lambda$	0.97	0	0
GscInt	Scale parameter of $\Lambda$	0.98	0	0
CFR	Degree hour factor for refreezing	The regression model is statistically insignificant		

with the shape and scale parameters of  $\lambda$  (0.98 and 0.99, respectively). This correlation is expected since the latter is derived from the former (see Skaugen and Onof, 2014). Accordingly, we estimate the shape and scale parameters of  $\Lambda$  from the shape and scale parameters of  $\lambda$  with multiple linear regression.

The performance of the multiple-regression method in this study strengthens the statement that relating model parameters to catchment

characteristics offers a possibility for estimating hydrological model parameters to predict flow at ungauged catchments (Magette et al., 1976). The results obtained in this paper are consistent with what Magette et al. (1976) obtained using 21 catchments in USA in the regionalization of six selected parameters of the KWM hydrological model using hourly data. They found that the hydrological model with the regressed parameters was successful in predicting flow at ungauged small catchments. The satisfactory performance of the multiple regression equations is in agreement with the recent results of Skaugen et al. (2015) who used daily data on small and large catchments in Norway. The finding that multiple-regression method gives better regionalization is also supported by Young (2006) who compares multiple-regression against a nearest-neighbor-based method. The performance of the multiple-regression method is also supported by the study results of Post and Jakeman (1999). They regressed six IHACRES model parameters from six landscape attributes, and the predictions made at the daily stream flow at ungauged catchments gave very good results for some catchments.

The pooling-group type performs better than the single-donor type for group members ranging from 3 to 20. The pooling group performance is as good as the multiple regression if we vary the number of members in the pooling group (Table 6) for each test catchment (e.g. if we take catchment ID of 19.79 and 104.22, a pooling group of 17 and 7 members gives as good KGE as the multiple regression, respectively). If we select fixed number of group members, multiple regression performs

Table 5  
Summary of the smallest total rank and the donor catchments for the 7 test catchments.

Test catchments	ID	Area(km <sup>2</sup> )	Donor catchments	ID	Area(km <sup>2</sup> )	Smallest total rank
Gravå	19.79	6.3	Hangtjern	12.212	11.2	94
Knabåni	25.32	49.1	Jogla	26.26	31.1	123
Kjemåvatn	163.7	36.6	Viertjern	16.127	46.6	116
M.Mardalsvan	104.22	13.5	Nysetvatn	74.24	28.8	124
Fjellhaugen	42.16	7.3	Fjellanger	63.12	12.8	100
Tjellingtjernbekken	18.11	2.1	Gramstaddalen	29.7	1	98
Strandå	165.6	23.3	Laksåbru	168.3	26.8	108

**Table 6**  
KGE values of different numbers of members of the pooling-group based physical similarity.

ID	Multiple regression	Number of members of the pooling-group based physical similarity												
		3	4	5	6	7	8	9	10	12	15	17	20	Max KGE
18.11	0.44	0.36	0.35	0.35	0.39	0.41	0.41	0.41	0.42	0.42	0.42	0.41	0.41	0.42
19.79	0.67	0.44	0.41	0.61	0.64	0.63	0.64	0.65	0.64	0.65	0.69	0.67	0.69	0.69
25.32	0.74	0.7	0.71	0.71	0.72	0.72	0.7	0.69	0.69	0.68	0.68	0.68	0.68	0.72
42.16	0.75	0.71	0.72	0.72	0.72	0.72	0.73	0.73	0.73	0.72	0.72	0.72	0.72	0.73
104.2	0.65	0.56	0.58	0.61	0.61	0.62	0.59	0.56	0.55	0.53	0.53	0.61	0.51	0.62
163.7	0.75	0.71	0.73	0.7	0.65	0.66	0.67	0.68	0.67	0.67	0.68	0.68	0.67	0.73
165.6	0.57	0.6	0.6	0.61	0.6	0.6	0.62	0.61	0.61	0.62	0.62	0.62	0.62	0.62
<b>Mean</b>	<b>0.65</b>	<b>0.58</b>	<b>0.59</b>	<b>0.62</b>	<b>0.62</b>	<b>0.62</b>	<b>0.62</b>	<b>0.62</b>	<b>0.62</b>	<b>0.61</b>	<b>0.62</b>	<b>0.63</b>	<b>0.61</b>	<b>0.65</b>

**Table 7**  
Pooling-group based method of physical similarity for the celerity of river flow at test catchment with catchment identification number (Cat.ID) 19.79.

ID of Pooling group members	Euclidean distance (dist <sub>a,b</sub> )	Celerity of river flow(rv)	Linearly decreasing weights(S <sub>am</sub> )	Weights of the pooling group members(h <sub>am</sub> )	h <sub>am</sub> * rv
29.7	2.26	1.44	0.589	0.411	<b>0.594</b>
12.212	2.26	0.70	0.590	0.410	<b>0.286</b>
123.29	2.47	1.08	0.645	0.355	<b>0.384</b>
6.1	2.65	0.71	0.690	0.310	<b>0.219</b>
16.66	3.05	0.99	0.795	0.205	<b>0.203</b>
174.3	3.47	1.15	0.903	0.097	<b>0.111</b>
8.6	3.49	0.59	0.909	0.091	<b>0.053</b>
The weighted average of the estimated celerity of river flow will be the ratio between the two as stated in Eq. (11).				$\sum_{m=1}^{41} h_{am}rv$	<b>1.851</b>
Therefore, the regionalized value of rv using the pooling-group based physical similarity method is				$\sum_{m=1}^{41} h_{am}$	<b>1.880</b>
<b>1.851/1.88 = 0.99 m/s</b>					

slightly better than the pooling group method. We selected 5, 7 and 10 members for further analysis. A group of 7 members performs as well as a group of 10 members. The group of 5 members performs slightly lower than the groups of 7 and 10 members. Finally, the group of 7 members is considered an optimal size of the pooling-based physical similarity in this study.

The performance of the pooling-group method in this study adds to the confirmation that the method can be applied for regionalization in different regions with different rainfall-runoff hydrological models. Regionalization results from 119 catchments across England, Wales and Scotland (46 with hourly data, 73 with daily data and size ranging from 1 km<sup>2</sup> to 1200 km<sup>2</sup>), showed that pooling-group method performed best with the conceptual hydrological model Probability Distributed Model (PDM), (Kay et al., 2006). Bao et al. (2012) regionalized Variable Infiltration Capacity (VIC) model parameters using multiple-regression and multiple-donor (5 donors) physical-similarity methods at 55 catchments of China and found that the multiple donor performed better than multiple regression.

5.3.2. Combined method

Generally, the combined method (which uses recession parameters estimated from multiple regression and calibrated parameters from the pooling-group method of physical similarity) performs slightly better than multiple-regression and physical-similarity methods (Table 9). The better performance of the combined method shows that multiple-regression is slightly better than pooling-group method in estimating the recession parameters while the pooling method is slightly better than the regression method in estimating the calibrated model parameters.

The hydrographs are also used for evaluation of the performance of the regionalization methods in addition to the KGE and BIAS. The hydrographs in Fig. 9 show that the combined method predicted the magnitude and the shape of the observed hydrographs better than the multiple-regression and pooling-group methods of regionalization. The floods are underestimated in both the presented hydrographs. When we look at the hydrograph of the catchment with ID of 25.32, the combined method predicted the timing and magnitude of the 2014 summer flood better than the pooling-group method, but the pooling-group method of

**Table 8**  
Summary of model parameters estimated from three methods of regionalization for a test catchment ID 25.32. For combined method, values in italic are transferred with regression while the remainder is transferred using physical similarity.

Model Parameters	Calibration and runoff Recession analysis		Regression	Physical similarity		Combined (pooling and regression)
	Calibration	Recession		Single donor	Pooling group	
pro	0.1	...	0.1	0.1	0.09	0.09
cx	0.1	...	0.137	0.183	0.14	0.14
CFR	0.01	...	0.007	0.01	0.01	0.01
cea	0.02	...	0.014	0.03	0.02	0.02
rv	0.5	...	1.11	1.013	1.15	1.15
Gshape	...	1.139	1.187	0.735	0.9	<i>1.187</i>
Gscale	...	0.055	0.034	0.06	0.04	<i>0.034</i>
GshInt	...	1.521	1.771	0.899	1.2	<i>1.771</i>
GscInt	...	0.024	0.015	0.029	0.02	<i>0.015</i>

**Table 9**  
Summary of comparisons of the regionalization methods using KGE and BIAS. The green shows the best KGE values (close to 1) while the blue shows the best BIAS value (close to 1).

S.no	Test catchment	ID	Area (km <sup>2</sup> )	Regression method		Physical similarity method				Combined method								
						Recession parameters from regression		Recession parameters from physical similarity										
						Single donor		Pooling group (7 members)		Single donor		Pooling group		Single donor		Pooling group		
				BIAS	KGE	BIAS	KGE	BIAS	KGE	BIAS	KGE	BIAS	KGE	BIAS	KGE	BIAS	KGE	
1	Gravá	19.79	6.3	1.04	<b>0.67</b>	1.09	0.33	1.04	0.58	1.06	0.6	<b>1.03</b>	<b>0.67</b>	1.09	0.34	1.04	0.58	
2	Knabáni	25.32	49.1	<b>0.8</b>	0.74	0.75	0.66	0.77	0.72	0.75	0.66	0.77	0.7	0.75	0.66	<b>0.8</b>	<b>0.75</b>	
3	Kjemávatn	163.7	36.6	<b>0.9</b>	0.75	<b>0.9</b>	0.59	0.87	0.67	0.88	0.75	<b>0.9</b>	<b>0.76</b>	<b>0.9</b>	0.59	<b>0.9</b>	0.66	
4	M.Mardalsvatn	104.22	13.5	0.72	<b>0.65</b>	0.72	0.53	<b>0.74</b>	0.6	0.69	0.63	<b>0.74</b>	<b>0.65</b>	<b>0.74</b>	0.56	0.72	0.6	
5	Fjellhaugen	42.16	7.3	0.83	<b>0.75</b>	0.79	0.63	0.79	0.72	0.79	0.72	0.79	0.72	0.8	0.71	<b>0.84</b>	<b>0.75</b>	
6	Tjellingtjernbekken	18.11	2.1	1.47	0.44	1.51	0.2	1.46	0.34	1.46	0.45	<b>1.4</b>	<b>0.5</b>	1.49	0.26	1.49	0.31	
7	Stránda	165.6	23.3	1.13	0.57	<b>1.06</b>	<b>0.6</b>	<b>1.06</b>	<b>0.6</b>	1.07	0.58	1.08	0.59	<b>1.06</b>	0.6	1.12	0.58	
<i>Mean</i>					<i>0.98</i>	<i>0.65</i>	<i>0.97</i>	<i>0.51</i>	<i>0.96</i>	<i>0.60</i>	<i>0.96</i>	<i>0.63</i>	<i>0.96</i>	<i>0.66</i>	<i>0.98</i>	<i>0.53</i>	<i>0.99</i>	<i>0.60</i>
<i>Standard deviation</i>					<i>0.26</i>	<i>0.12</i>	<i>0.28</i>	<i>0.17</i>	<i>0.25</i>	<i>0.13</i>	<i>0.27</i>	<i>0.1</i>	<i>0.23</i>	<i>0.09</i>	<i>0.27</i>	<i>0.17</i>	<i>0.26</i>	<i>0.15</i>

regionalization has a KGE value of 0.72 while the combined method has a KGE value of 0.71.

The combined method combines the advantages from the two methods of regionalizations used in this study (physical similarity and multiple regression). Kokkonen et al. (2003) states that exploiting merely relationships between calibrated model parameters and CDs can result in a decrease in regionalization performance. Physical similarity has an advantage of transferring the entire calibrated model parameters from one or few gauged to ungauged catchments (Arsenault and

Brisette, 2014; McIntyre et al., 2005; Oudin et al., 2010; Parajka et al., 2005). The recession parameters describe the integrated information of how different factors influence the runoff process (Fiorotto and Caroni, 2013). Recession parameters are used in the DDD model to estimate the subsurface storage capacity (Skaugen and Mengistu, 2016), and they can also be used to model streamflow recession for regionalization and prediction (Stoelzle et al., 2013). Vogel and Kroll (1996) state that regression procedures for estimating hydrograph recession parameters generally work well, which is supported by our findings in that the

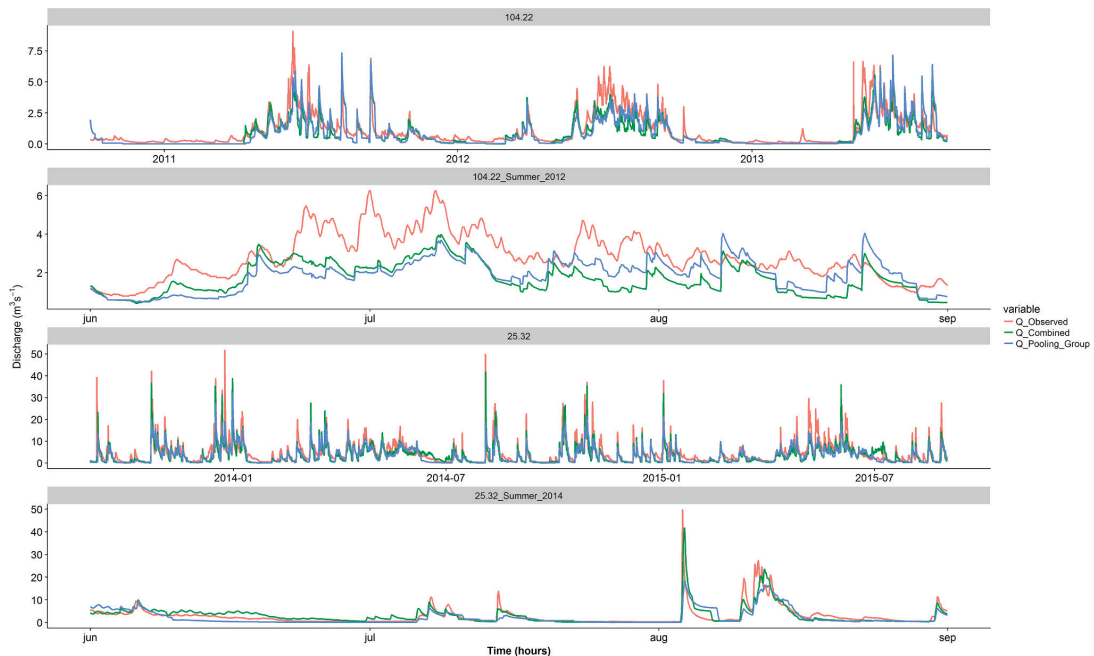


**Fig. 9.** Observed and predicted hydrographs using multiple regression, pooling group and combined methods of regionalization at two test catchments.

**Table 10**

Comparison of the KGE performance of calibration with the satisfactorily performing regionalization methods (the green shows KGE values of methods are better than calibration or the KGE values of calibration are better than methods).

S.no	Test catchment	ID	Area (km <sup>2</sup> )	Calibrated		Regression method		Physical Similarity method		Combined (recession parameters from regression and calibrated from pooling)	
				BIAS	KGE	BIAS	KGE	BIAS	KGE	Pooling group (7 members)	
										BIAS	KGE
1	Gravå	19.79	6.3	1.02	0.39	1.04	<b>0.67</b>	1.04	<b>0.58</b>	1.03	<b>0.67</b>
2	Knabåni	25.32	49.1	0.79	0.66	0.8	<b>0.74</b>	0.77	<b>0.72</b>	0.77	<b>0.7</b>
3	Kjemåvatn	163.7	36.6	0.86	<b>0.77</b>	0.9	0.75	0.87	0.67	0.9	0.76
4	M.Mardalsvatn	104.22	13.5	0.75	0.55	0.72	<b>0.65</b>	0.74	<b>0.6</b>	0.74	<b>0.65</b>
5	Fjellhaugen	42.16	7.3	0.82	0.7	0.83	<b>0.75</b>	0.79	<b>0.72</b>	0.79	<b>0.72</b>
6	Tjellingtjernbekken	18.11	2.1	1.22	<b>0.55</b>	1.47	0.44	1.46	0.34	1.4	0.5
7	Strånda	165.6	23.3	1.05	<b>0.63</b>	1.13	0.57	1.06	0.6	1.08	0.59
<i>Mean</i>				0.93	0.61	<i>0.98</i>	<i>0.65</i>	<i>0.96</i>	<i>0.60</i>	<i>0.96</i>	<i>0.66</i>
<i>Standard deviation</i>				0.17	0.12	<i>0.26</i>	<i>0.11</i>	<i>0.25</i>	<i>0.13</i>	<i>0.23</i>	<i>0.09</i>

recession parameters estimated using multiple regression are slightly better than those estimated by physical similarity. It must be noted, however, that the recession parameters derived from the regression method are estimated from hydrographs of 41 study catchments while that of the pooling-group method are derived from hydrographs of only 7 study catchments.

The regionalized recession parameters of DDD model (estimated by pooling-group, multiple regression and combined method) are, in some cases, better than the recession parameters estimated locally from a short period of hydro-meteorological data. This is the case for four of the test catchments and makes the performance of the regionalization methods better than the calibration result for the four catchments (Table 10). The main reason that the single-donor type of physical similarity performs the poorest is that the recession parameters in the single donor type are estimated from hydrographs of a single catchment while that of a pooling group and multiple regression are estimated from hydrographs of 7 and 41 catchments respectively. The other reason is probably the long distance between donor and test catchments.

The main limitation of this study is related to the precipitation data, mainly how heavy precipitation events are represented. As discussed previously, there are studies which show that the gridded data set has uncertainties and smooths out peaks (Lussana et al., 2018). To reduce the uncertainty in the precipitation, we have introduced a precipitation correction factor as mentioned in the methodology section, and we estimate the precipitation correction factor for ungauged catchments using a daily specific runoff map of Norway produced by NVE (<https://atlas.nve.no>). Another limitation is related to the use of the daily spatial variations of precipitation data for the gamma distributed snow parameters. Skaugen et al. (2015) used observed, daily precipitation data from rain gauges to estimate the snow distribution parameters of DDD. In this study, we assume that the daily spatial variation of precipitation is similar to that of hourly variation, and we used the parameters from the 84 calibrated catchments in Skaugen et al. (2015) due to the lack of sufficient rain gauges with hourly temporal resolution. One source of uncertainty in this study that is not yet quantified is the lack of long-term discharge data with hourly resolutions for estimating the runoff

recession parameters, as they are sensitive to the length of the time series.

## 6. Conclusions

The results of our study show that the DDD model performs satisfactorily both during the calibration and validation periods for small rural catchments in Norway (area < 50 km<sup>2</sup>) with hourly temporal resolution. The model underestimates floods generated by heavy precipitation events, and a method to improve the simulation of peak floods should be further investigated.

The calibrated parameters in the DDD model are identifiable and show small uncertainty in our analysis. The uncertainty bound of DDD simulations due to the calibrated parameters is narrow, which shows that the uncertainty due to calibrated parameters for predicting flow using hourly temporal resolution is small, and this also indicates that the model is suitable for regionalization.

Both the multiple-regression and pooling-group methods performed satisfactorily (except for one test catchment, both methods gave a KGE performance between 0.5 and 0.75). The combined method (which uses recession parameters estimated from multiple-regression and calibrated parameters from the pooling-group method of physical similarity) performed slightly better than the pooling-group and multiple-regression methods. Therefore, the combined method of regionalization is recommended as a method for estimation of flow at small rural ungauged catchments with hourly resolution in Norway. The recession parameters estimated by the three regionalization methods are, for some catchments, better than those estimated from a short period of hydro-meteorological data.

The parameter parsimonious rainfall-runoff hydrological model (DDD) has a capability of generating continuous flow data at ungauged small rural catchments with hourly temporal resolution using regionalized model parameters. The satisfactory performance of the combined method shows that regionalization of DDD model parameters is possible by combining multiple-regression and physical-similarity methods.

## Declaration of interests

None.

## Acknowledgments

The authors would like to acknowledge Cristian Lussana of the Norwegian Meteorological Institute for providing information on how to access and process the  $1 \times 1$  km spatial and 1-hour temporal resolution gridded precipitation and temperature data for Norway. We would like to acknowledge Abebe Girmay also for his support in processing the gridded data. The authors also acknowledge and appreciate the anonymous reviewers, despite their busy schedules, have taken out time to read the manuscript and give us feedback, which helped a lot for the improvement of the manuscript. Finally, the authors gratefully acknowledge the financial support by the Research Council of Norway and several partners through the Centre for Research-based Innovation “Klima 2050” (see [www.klima2050.no](http://www.klima2050.no)).

## References

- Arsenault, R., Brissette, F.P., 2014. Continuous streamflow prediction in ungauged basins: the effects of equifinality and parameter set selection on uncertainty in regionalization approaches. *Water Resour. Res.* 50 (7), 6135–6153. <https://doi.org/10.1002/2013WR014898>.
- Bao, Z., Zhang, J., Liu, J., Fu, G., Wang, G., He, R., et al., 2012. Comparison of regionalization approaches based on regression and similarity for predictions in ungauged catchments under multiple hydro-climatic conditions. *J. Hydrol.* 466–467, 37–46. <https://doi.org/10.1016/j.jhydrol.2012.07.048>.
- Bárdossy, A., 2007. Calibration of hydrological model parameters for ungauged catchments. *Hydrol. Earth Syst. Sci.* 11 (2), 703–710. <https://doi.org/10.5194/hess-11-703-2007>.
- Beldring, S., Engeland, K., Roald, L.A., Sælthun, N.R., Vokso, A., 2003. Estimation of parameters in a distributed precipitation-runoff model for Norway. *Hydrol. Earth Syst. Sci.* 7(3). <https://doi.org/10.5194/hess-7-304-2003>.
- Benke, K.K., Lowell, K.E., Hamilton, A.J., 2008. Parameter uncertainty, sensitivity analysis and prediction error in a water-balance hydrological model. *Math. Comput. Modell.* 47 (11), 1134–1149. <https://doi.org/10.1016/j.mcm.2007.05.017>.
- Bergström, S., 1976. Development and application of a conceptual runoff model for Scandinavian catchments. Department of Water Resources Engineering, Lund Institute of Technology, University of Lund, Lund.
- Berne, A., Krajewski, W.F., 2013. Radar for hydrology: Unfulfilled promise or unrecognized potential? *Adv. Water Resour.* 51 (Supplement C), 357–366.
- Beven, K.J., 2000. Uniqueness of place and process representations in hydrological modelling. *Hydrol. Earth Syst. Sci. Discuss.* 4 (2), 203–213.
- Beven, K.J., 2006. A manifesto for the equifinality thesis. *J. Hydrol.* 320 (1), 18–36. <https://doi.org/10.1016/j.jhydrol.2005.07.007>.
- Blasone, R.S., Madsen, H., Rosbjerg, D., 2008. Uncertainty assessment of integrated distributed hydrological models using GLUE with Markov chain Monte Carlo sampling. *J. Hydrol.* 353 (1), 18–32. <https://doi.org/10.1016/j.jhydrol.2007.12.026>.
- Blöschl, G., Sivapalan, M., 1995. Scale issues in hydrological modelling: a review. *Hydrol. Process.* 9 (3–4), 251–290. <https://doi.org/10.1002/hyp.3360090305>.
- Blöschl, G., Sivapalan, M., Wagener, T., Viglione, A., Savenije, H., 2013. *Runoff Prediction in Ungauged Basins: Synthesis across Processes, Places and Scales*. Cambridge University Press, Cambridge.
- Blöschl, G., Sivapalan, M., Wagener, T., Viglione, A., Savenije, H., 2013. *Runoff prediction in ungauged basins: synthesis across processes, places and scales*. Cambridge University Press, Cambridge.
- Borga, M., Boscolo, P., Zanone, F., Sangati, M., 2007. Hydrometeorological analysis of the 29 August 2003 flash flood in the eastern Italian Alps. *J. Hydrometeorol.* 8 (5), 1049–1067. <https://doi.org/10.1175/JHM593.1>.
- Bronstert, A., 2003. Floods and climate change: interactions and impacts. *Risk Anal.* 23 (3), 545–557.
- Creutin, Borga, M., 2003. Radar hydrology modifies the monitoring of flash-flood hazard. *Hydrol. Process.* 17 (7), 1453–1456. <https://doi.org/10.1002/hyp.5122>.
- Creutin, Obled, C., 1980. Modeling spatial and temporal characteristics of rainfall as input to a flood forecasting model. IAHS-AISH Publication 129 In: *Hydrological forecasting. Proc. Oxford symposium. International Association of Hydrological Sciences, Washington DC*, pp. 41–49.
- Devi, G. K., Ganasri, B. P., & Dwarakish, G. S., 2015. A review on hydrological models. International conference on water resources, coastal and ocean engineering (ICWRCOE'15) (Vol. 4).
- Fierz, C., R.L. A., Y. D., P. E., Greene, E., McClung, D., et al., 2009. The international classification for seasonal snow on the ground (UNESCO, IHP (International Hydrological Programme)-VII, Technical Documents in Hydrology, No 83; IACS (International Association of Cryospheric Sciences) contribution No 1).
- Fiorotto, V., Caroni, E., 2013. A new approach to master recession curve analysis. *Hydrol. Sci. J.* 58 (5), 966–975. <https://doi.org/10.1080/02626667.2013.788248>.
- Fleig, A. K., & Wilson, D., 2013. The Natural Hazards Project - 5 Flood and Surface Water Flooding Retrieved from Oslo, Norway.
- Frauenfelder, R., Solheim, A., Isaksen, K., Romstad, B., Dyrddal, A. V., Ekseth, K. H. H., et al., 2017. Impacts of extreme weather events on transport infrastructure in Norway. In: *Natural Hazards and Earth System Sciences Discussions*, 1–24. doi:10.5194/nhess-2017-437.
- Gupta, H.V., Kling, H., Yilmaz, K.K., Martinez, G.F., 2009. Decomposition of the mean squared error and NSE performance criteria: implications for improving hydrological modelling. *J. Hydrol.* 377 (1), 80–91. <https://doi.org/10.1016/j.jhydrol.2009.08.003>.
- Hailegeorgis, T.T., Abdella, Y.S., Alfredsen, K., Kolberg, S., 2015. Evaluation of regionalization methods for hourly continuous streamflow simulation using distributed models in boreal catchments. *J. Hydrol. Eng.* 20 (11). [https://doi.org/10.1061/\(ASCE\)HE.1943-5584.0001218](https://doi.org/10.1061/(ASCE)HE.1943-5584.0001218).
- Jin, X., Xu, C.-Y., Zhang, Q., Singh, V.P., 2010. Parameter and modeling uncertainty simulated by GLUE and a formal Bayesian method for a conceptual hydrological model. *J. Hydrol.* 383 (3), 147–155. <https://doi.org/10.1016/j.jhydrol.2009.12.028>.
- Kay, A.L., Jones, D.A., Crooks, S.M., Calver, A., Reynard, N.S., 2006. A comparison of three approaches to spatial generalization of rainfall-runoff models. *Hydrol. Process.* 20 (18), 3953–3973. <https://doi.org/10.1002/hyp.6550>.
- Kay, A.L., Jones, D.A., Crooks, S.M., Kjeldsen, T.R., Fung, C.F., 2007. An investigation of site-similarity approaches to generalisation of a rainfall-runoff model. *Hydrol. Earth Syst. Sci.* <https://doi.org/10.5194/hess-11-500-2007>.
- Kirchner, J.W., 2006. Getting the right answers for the right reasons: linking measurements, analyses, and models to advance the science of hydrology. *Water Resour. Res.* 42 (3), n/a-n/a. <https://doi.org/10.1029/2005WR004362>.
- Kokkonen, T., Jakeman, Anthony J., Young, Peter C., Koivusalo, Harri J., Blöschl, G., Vertessy, R., Zhang, L., 2003. Predicting daily flows in ungauged catchments: model regionalization from catchment descriptors at the Coweeta Hydrologic Laboratory, North Carolina. *Hydrol. Processes* 17 (11), 2219–2238. <https://doi.org/10.1002/hyp.1329>.
- Kuczera, G., Parent, E., 1998. Monte Carlo assessment of parameter uncertainty in conceptual catchment models: the Metropolis algorithm. *J. Hydrol.* 211 (1/4), 69–85. [https://doi.org/10.1016/S0022-1694\(98\)00198-X](https://doi.org/10.1016/S0022-1694(98)00198-X).
- Lamb, R., Kay, A.L., 2004. Confidence intervals for a spatially generalized, continuous simulation flood frequency model for Great Britain. *Water Resour. Res.* 40 (7), n/a-n/a. <https://doi.org/10.1029/2003WR002428>.
- Li, Z., 2014. Watershed modeling using arc hydro based on DEMs: a case study in Jackpine watershed. *Environ. Syst. Res.* 3 (1), 11. <https://doi.org/10.1186/2193-2697-3-11>.
- Lu, Q., Han, Q.-L., 2011. A probability particle swarm optimizer with information-sharing mechanism for odor source localization. *IFAC Proc.* 44 (1), 9440–9445. <https://doi.org/10.3182/20110828-6-IT-1002.00507>.
- Lussana, C., Ole Einar, T., & Francesco, U., 2016. seNorge v2.0: an observational gridded dataset of temperature for Norway. METReport, 108.
- Lussana, C., Saloranta, T., Skaugen, T., Magnusson, J., Einar Tveito, O., Andersen, J., 2018. SeNorge2 daily precipitation, an observational gridded dataset over Norway from 1957 to the present day. *Earth Syst. Sci. Data* 10 (1), 235–249. <https://doi.org/10.5194/essd-10-235-2018>.
- Magette, W.L., Shanholtz, V.O., Carr, J.C., 1976. Estimating selected parameters for the Kentucky Watershed Model from watershed characteristics. *Water Resour. Res.* 12 (3), 472–476. <https://doi.org/10.1029/WR012i003p0472>.
- Masih, I., Uhlenbrook, S., Maskey, S., Ahmad, M.D., 2010. Regionalization of a conceptual rainfall-runoff model based on similarity of the flow duration curve: a case study from the semi-arid Karkheh basin, Iran. *J. Hydrol.* 391 (1), 188–201. <https://doi.org/10.1016/j.jhydrol.2010.07.018>.
- McIntyre, N., Lee, H., Wheeler, H., Young, A., Wagener, T., 2005. Ensemble predictions of runoff in ungauged catchments. *Water Resour. Res.* 41 (12), n/a-n/a. <https://doi.org/10.1029/2005WR004289>.
- Merz, Blöschl, G., Parajka, J., 2006. In: *Regionalization Methods in Rainfall-runoff Modelling using Large Catchment Samples*. IAHS-AISH Publication, pp. 117–125.
- Merz, Blöschl, 2004. Regionalisation of catchment model parameters. *J. Hydrol.* 287 (1), 95–123. <https://doi.org/10.1016/j.jhydrol.2003.09.028>.
- Miao, Q., Yang, D., Yang, H., Li, Z., 2016. Establishing a rainfall threshold for flash flood warnings in China's mountainous areas based on a distributed hydrological model. *J. Hydrol.* 541, 371–386. <https://doi.org/10.1016/j.jhydrol.2016.04.054>.
- Montanari, A., 2011. Uncertainty of Hydrological Predictions (pp. 459–478).
- Nruthya, K., Srinivas, V.V., 2015. Evaluating methods to predict streamflow at ungauged sites using regional flow duration curves: a case study. *Aquat. Procedia* 4, 641–648. <https://doi.org/10.1016/j.aqpro.2015.02.083>.
- Oudin, L., Andréassian, V., Perrin, C., Michel, C., Le Moine, N., 2008. Spatial proximity, physical similarity, regression and ungauged catchments: a comparison of regionalization approaches based on 913 French catchments. *Water Resour. Res.* 44 (3), n/a-n/a. <https://doi.org/10.1029/2007WR006240>.
- Oudin, L., Kay, A., Andréassian, V., Perrin, C., 2010. Are seemingly physically similar catchments truly hydrologically similar? *Water Resour. Res.* 46 (11). <https://doi.org/10.1029/2009WR008887>. n/a-n/a.
- Parajka, J., Merz, R., Blöschl, G., 2005. A comparison of regionalisation methods for catchment model parameters. *Hydrol. Earth Syst. Sci. Discuss.* 2 (2), 509–542. <https://doi.org/10.5194/hessd-2-509-2005>.
- Parajka, J., Viglione, A., Rogger, M., Salinas, J.L., Sivapalan, M., Blöschl, G., 2013. Comparative assessment of predictions in ungauged basins &ndash; part 1: runoff-hydrograph studies. *Hydrol. Earth Syst. Sci.* 17 (5), 1783–1795. <https://doi.org/10.5194/hess-17-1783-2013>.
- Pathiraja, S., Westra, S., Sharma, A., 2012. Why continuous simulation? The role of antecedent moisture in design flood estimation. *Water Resour. Res.* 48 (6), n/a-n/a. <https://doi.org/10.1029/2011WR010997>.

- Pilgrim, D.H., Cordery, I., Baron, B.C., 1982. Effects of catchment size on runoff relationships. *J. Hydrol.* 58 (3), 205–221. [https://doi.org/10.1016/0022-1694\(82\)90035-X](https://doi.org/10.1016/0022-1694(82)90035-X).
- Post, D., Jakeman, A.J., 1999. Predicting the daily streamflow of ungauged catchments in S.E. Australia by regionalising the parameters of a lumped conceptual rainfall-runoff model. *Ecol. Model.* 123.
- R Core Team., 2017. R: A Language and Environment for Statistical Computing. doi:<http://www.R-project.org/>.
- Razavi, T., Coulibaly, P., 2013. Streamflow prediction in ungauged basins: review of regionalization methods. *J. Hydrol. Eng.* 18 (8), 958–975. [https://doi.org/10.1061/\(ASCE\)HE.1943-5584.0000690](https://doi.org/10.1061/(ASCE)HE.1943-5584.0000690).
- Reynolds, J.E., Halldin, S., Xu, C.Y., Seibert, J., Kauffeldt, A., 2017. Sub-daily runoff predictions using parameters calibrated on the basis of data with a daily temporal resolution. *J. Hydrol.* 550, 399–411. <https://doi.org/10.1016/j.jhydrol.2017.05.012>.
- Sæthun, N. R., 1996. The "Nordic" HBV model. Description and documentation of the model version developed for the project Climate Change and Energy production. (ISBN 82-410-0273-4). Retrieved from Oslo.
- Saloranta, T.M., 2012. Simulating snow maps for Norway: description and statistical evaluation of the seNorge snow model. *Cryosphere* 6 (6), 1323–1337. <https://doi.org/10.5194/tc-6-1323-2012>.
- Seibert, J., 1999. Regionalisation of parameters for a conceptual rainfall-runoff model. *Agric. For. Meteorol.* 98–99, 279–293. [https://doi.org/10.1016/S0168-1923\(99\)00105-7](https://doi.org/10.1016/S0168-1923(99)00105-7).
- Sivapalan, M., Takeuchi, K., Franks, S.W., Gupta, V.K., Karambiri, H., Lakshmi, V., Zehe, E., 2003. IAHS Decade on Predictions in Ungauged Basins (PUB), 2003–2012: shaping an exciting future for the hydrological sciences. *Hydrol. Sci. J.* 48 (6), 857–880. <https://doi.org/10.1623/hysj.48.6.857.51421>.
- Skaugen, T., Mengistu, Z., 2016. Estimating catchment-scale groundwater dynamics from recession analysis & enhanced constraining of hydrological models. *Hydrol. Earth Syst. Sci.* 20 (12), 4963–4981. <https://doi.org/10.5194/hess-20-4963-2016>.
- Skaugen, T., Onof, C., 2014. A rainfall-runoff model parameterized from GIS and runoff data. *Hydrol. Process.* 28 (15), 4529–4542. <https://doi.org/10.1002/hyp.9968>.
- Skaugen, T., Weltzien, I.H., 2016. A model for the spatial distribution of snow water equivalent parameterized from the spatial variability of precipitation. *Cryosphere* 10 (5), 1947. <https://doi.org/10.5194/tc-10-1947-2016>.
- Skaugen, T., Peereboom, I., Olaf, Nilsson, A., 2015. Use of a parsimonious rainfall-run-off model for predicting hydrological response in ungauged basins. *Hydrol. Process.* 29 (8), 1999–2013. <https://doi.org/10.1002/hyp.10315>.
- Skaugen, T., 1998. Studie av skilleteperatur for snø ved hjelp av samlokalisert snø pute, nedbør- og temperaturdata NVE RAPPORT nr. 11.
- Son, K., Sivapalan, M., 2007. Improving model structure and reducing parameter uncertainty in conceptual water balance models through the use of auxiliary data. *Water Resour. Manage.* 430.
- Spence, C., Whitfield, P.H., Pomeroy, J.W., Pietroniro, A., Burn, D.H., Peters, D.L., St-Hilaire, A., 2013. A review of the Prediction in Ungauged Basins (PUB) decade in Canada. *Can. Water Res. J./Revue canadienne des ressources hydriques* 38 (4), 253–262. <https://doi.org/10.1080/07011784.2013.843867>.
- Steinschneider, S., Yang, Y.-C.E., Brown, C., 2014. Combining regression and spatial proximity for catchment model regionalization: a comparative study. *Hydrol. Sci. J.* <https://doi.org/10.1080/02626667.2014.899701>.
- Stoelzle, M., Stahl, K., Weiler, M., 2013. Are streamflow recession characteristics really characteristic? *Hydrol. Earth Syst. Sci.* 17 (2), 817–828. <https://doi.org/10.5194/hess-17-817-2013>.
- Swain, J.B., Patra, K.C., 2017. Streamflow estimation in ungauged catchments using regionalization techniques. *J. Hydrol.* 554, 420–433. <https://doi.org/10.1016/j.jhydrol.2017.08.054>.
- Tegegne, G., Kim, Y.-O., 2018. Modelling ungauged catchments using the catchment runoff response similarity. *J. Hydrol.* 564, 452–466. <https://doi.org/10.1016/j.jhydrol.2018.07.042>.
- Thiemig, V., Rojas, R., Zambrano-Bigiarini, M., De Roo, A., 2013. Hydrological evaluation of satellite-based rainfall estimates over the Volta and Baro-Akobo Basin. *J. Hydrol.* 499, 324–338. <https://doi.org/10.1016/j.jhydrol.2013.07.012>.
- Viviroli, D., Mittelbach, H., Gurtz, J., Weingartner, R., 2009. Continuous simulation for flood estimation in ungauged mesoscale catchments of Switzerland – part II: parameter regionalisation and flood estimation results. *J. Hydrol.* 377 (1), 208–225. <https://doi.org/10.1016/j.jhydrol.2009.08.022>.
- Viviroli, D., Seibert, J., 2015. Can a regionalized model parameterisation be improved with a limited number of runoff measurements? *J. Hydrol.* 529, 49–61. <https://doi.org/10.1016/j.jhydrol.2015.07.009>.
- Vogel, R., Kroll, C., 1996. Estimation of baseflow recession constants. *Water Resour. Res.* 10.
- Vormoor, K., Skaugen, T., 2013. Temporal disaggregation of daily temperature and precipitation grid data for Norway. *J. Hydrometeorol.* 14 (3), 989–999. <https://doi.org/10.1175/JHM-D-12-0139.1>.
- Wagner, T., Wheeler, H. S., & Gupta, H. V., 2004. Rainfall-Runoff Modelling in Gauged and Ungauged Catchments.
- Wagner, T., Wheeler, H.S., 2006. Parameter estimation and regionalization for continuous rainfall-runoff models including uncertainty. *J. Hydrol.* 320 (1), 132–154. <https://doi.org/10.1016/j.jhydrol.2005.07.015>.
- Westerberg, I.K., Gong, L., Beven, K., Seibert, J., Smedo, A., Xu, C., Halldin, S., 2014. Regional water balance modelling using flow-duration curves with observational uncertainties. *Hydrol. Earth Syst. Sci.* 18 (8), 2993. <https://doi.org/10.5194/hess-18-2993-2014>.
- Wetterhall, F., Cloke, H., Pappenberger, F., Wetterhall, F., 2011. Effects of temporal resolution of input precipitation on the performance of hydrological forecasting. *Adv. Geosci.* 29, 21–25.
- Young, A.R., 2006. Stream flow simulation within UK ungauged catchments using a daily rainfall-runoff model. *J. Hydrol.* 320 (1), 155–172. <https://doi.org/10.1016/j.jhydrol.2005.07.017>.
- Young, A.R., Romanowicz, R.J., 2004. PUB and data-based mechanistic modelling: the importance of parsimonious continuous-time models. *International Environmental Modelling and Software Soc.(Proceedings for the iEMSs 2004 international congress: complexity and integrated resources management)*. 214–224.
- Zhang, Y., Chiew, F.H.S., 2009. Relative merits of different methods for runoff predictions in ungauged catchments. *Water Resour. Res.* 45 (7), n/a-n/a. <https://doi.org/10.1029/2008WR007504>.
- Zhang, Y., Vaze, J., Chiew, F.H.S., Teng, J., Li, M., 2014. Predicting hydrological signatures in ungauged catchments using spatial interpolation, index model, and rainfall-runoff modelling. *J. Hydrol.* 517 (Supplement C), 936–948. <https://doi.org/10.1016/j.jhydrol.2014.06.032>.



## **Paper II:**


**A dynamic river network method for the prediction of floods using a parsimonious rainfall-runoff model.**

Tsegaw, A. T., Alfredsen, K., Skaugen, T., & Muthanna, T. M. (2019). *Hydrology Research*, *nh2019003*. doi: <https://doi.org/10.2166/nh.2019.003>





## A dynamic river network method for the prediction of floods using a parsimonious rainfall-runoff model

Aynalem Tassachew Tsegaw, Thomas Skaugen, Knut Alfredsen and Tone M. Muthanna 


### ABSTRACT

Floods are one of the major climate-related hazards and cause casualties and substantial damage. Accurate and timely flood forecasting and design flood estimation are important to protect lives and property. The Distance Distribution Dynamic (DDD) is a parsimonious rainfall-runoff model which is being used for flood forecasting at the Norwegian flood forecasting service. The model, like many other models, underestimates floods in many cases. To improve the flood peak prediction, we propose a dynamic river network method into the model. The method is applied for 15 catchments in Norway and tested on 91 flood peaks. The performance of DDD in terms of KGE and BIAS is identical with and without dynamic river network, but the relative error (RE) and mean absolute relative error (MARE) of the simulated flood peaks are improved significantly with the method. The 0.75 and 0.25 quantiles of the RE are reduced from 41% to 23% and from 22% to 1%, respectively. The MARE is reduced from 32.9% to 15.7%. The study results also show that the critical support area is smaller in steep and bare mountain catchments than flat and forested catchments.

**Key words** | critical flux (FC), critical supporting area (AC), dynamic river network, floods

**Aynalem Tassachew Tsegaw** (corresponding author)

**Knut Alfredsen**

**Tone M. Muthanna** 

Civil and Environmental Engineering,  
Norwegian University of Science and Technology,  
SP Andersen Vei 5, Trondheim 7491,  
Norway  
E-mail: aynalem.t.tasachew@ntnu.no

**Thomas Skaugen**

Hydrology Department,  
Norwegian Water Resources and Energy  
Directorate (NVE),  
PO Box 5091, Oslo 0301,  
Norway

### INTRODUCTION

Floods are one of the major climate-related hazards and cause casualties and substantial damage on a global scale every year (Hirabayashi *et al.* 2013; Blaikie *et al.* 2014; Winsemius *et al.* 2015). Floods usually cause damage to agricultural land, infrastructure and buildings (Razi *et al.* 2010). Flood peak is one of the most important variables to be estimated as its magnitude and duration are responsible for the damage (Formetta *et al.* 2017; Gao *et al.* 2017). An accurate estimate of flood peak is a critical requirement for proposing appropriate flood damage mitigation

measures in order to reduce social and economic costs (Plate 2009).

The common hydrological tools for flood risk management are flood forecasting models and models used to estimate design floods (Plate 2009). The design flood, where the magnitude of the flood is associated with a return period and hence a level of risk, is important in the planning, design and operation of hydraulic structures and for protection of human life and property (Rahman *et al.* 1998; Reis & Stedinger 2005; Smithers 2012). Methods to estimate design floods are generally classified into three: (a) statistical flood frequency analysis; (b) event-based simulation; and (c) derived flood frequency simulation (Filipova *et al.* 2018).

Derived flood frequency analysis, using continuous rainfall-runoff models, is increasing in use for design flood

This is an Open Access article distributed under the terms of the Creative Commons Attribution Licence (CC BY-NC-ND 4.0), which permits copying and redistribution for non-commercial purposes with no derivatives, provided the original work is properly cited (<http://creativecommons.org/licenses/by-nc-nd/4.0/>)

doi: 10.2166/nh.2019.003

estimation (Cameron *et al.* 2000; Calver & Lamb 1995; Boughton & Droop 2003; Eschenbach *et al.* 2008). A rainfall-runoff model can be used to simulate several flow values under different conditions for extending and enhancing the observed flow record (Filipova *et al.* 2018). A stochastic weather generator is used to simulate long synthetic series of rainfall and temperature input data for the continuous simulation method. The long series of flow data derived from the simulation is then used to estimate the required return periods, usually using plotting positions (Camici *et al.* 2011; Haberlandt & Radtke 2014). There is a growing interest in continuous simulation method of flood estimation as an alternative to event-based method, and internationally the trend is to adopt the continuous method (Lamb & Kay 2004; Chetty & Smithers 2005; Pathiraja *et al.* 2012). The main advantages of the continuous simulation models are their ability to represent the antecedent moisture condition in the catchment and their capability to model future land use and climate changes impacts on the flood peaks (Brocca *et al.* 2011; Smithers *et al.* 2013). The other reason for using the continuous simulation approach is that precipitation records are more widely available and tend to have longer periods of records than stream flow data (Blazkova & Beven 2002). Continuous simulation can avoid the base flow estimation problem in the event-based method and avoid any need to associate return period of the flood with specific design precipitation because the frequency analysis of floods can be done directly.

Rainfall-runoff models are simplified representations of a complex physical system and therefore carry a certain amount of uncertainty in their applications (Bourdin *et al.* 2012). The performance of rainfall-runoff models depend on several factors which include the quality of precipitation input data and an appropriate model structure capable of simulating floods (Collier 2007). Therefore, the structure and performance of the rainfall-runoff models should be evaluated and improved for their capability in simulating flood peaks before using them in design flood estimation and flood forecasting.

There are several ways to classify rainfall-runoff models (Singh 1995). Rainfall-runoff models can be classified into lumped and distributed models. Lumped models consider the whole catchment as a single unit with state variables

that represent the average of the catchment (Beven 2001b). Distributed models make prediction at distributed locations, i.e., by discretizing the catchment into a number of elements with state variables representing local averages (Singh & Frevert 2006). When a rainfall-runoff model is used for design flood estimation, the model could underestimate the design flood. Thomas (1982) evaluated floods estimated by continuous simulation methods on 50 small streams in Oklahoma, and the result showed that the flood peaks were consistently underestimated. Pathiraja *et al.* (2012) used 45 catchments in the Murray–Darling basin in Australia to estimate design floods using the Australian water balance model. They found that the model underestimates the floods from 5% to 30% depending on how reasonably the antecedent moisture condition is simulated. The forecast of floods requires an accurate understanding of catchment characteristics and a precise determination of catchment's initial conditions before flooding (Rusjan *et al.* 2009).

There is a link between catchment morphology and a hydrologic response of a catchment (Rodríguez-Iturbe & Valdés 1979; D'Odorico & Rigon 2003; Rigon *et al.* 2011). Gupta *et al.* (1980) pointed out that the Geomorphic Instantaneous Unit Hydrograph (GIUH) is equivalent to the probability density function of travel times,  $f(t)$ , from any point in the catchment to the outlet. This permits the formulation of hydrologic response through the geomorphologic width function,  $W(x)$ . The GIUH and  $W(x)$  concepts represent the dependency of peak flows on the geomorphological properties of a catchment and provide a quantitative prediction of peak flows for engineering application (Rinaldo *et al.* 1991; Rinaldo *et al.* 1995; D'Odorico & Rigon 2003; Rigon *et al.* 2011). The form and extent of the stream network reflect the characteristics of the hillslope (Willgoose *et al.* 1991). The stream reflects the ground water dynamics and is often termed as perennial, intermittent and ephemeral streams (Dingman 1978; Bencala *et al.* 2011). Dynamic expansions and contractions of stream networks play an important role for hydrologic processes since they connect different parts of the catchment to the outlet (Nhim 2012). Stream networks in a catchment expand and contract as the catchment wets and dries, both seasonally and in response to individual precipitation events, and this dynamic of stream networks gives an

important information to the pattern and process of runoff generation (Godsey & Kirchner 2014; Ward *et al.* 2018). The mean of the distribution of distances from a point in the catchment to the nearest river reach ( $D_m$ ) and the drainage density ( $D_d$ ) are among the indexes used to describe a stream network. Horton (1945) defined the traditional  $D_d$  as the sum of lengths ( $L$ ) of all streams in a catchment divided by the catchment area ( $A$ ). The  $D_m$  reflects the spatial characteristics that affect the formation of streams and the response time of a catchment for a particular stream network (Wharton 1994; Tucker *et al.* 2009; Di Lazzaro *et al.* 2014; Skaugen & Onof 2014). The mean distance one has to walk from a random location in a hillslope before encountering a stream,  $D_m$  is related to the traditional definition of  $D_d$  (Horton 1932; Tucker *et al.* 2009; Di Lazzaro *et al.* 2014).

$$D_m \approx \frac{1}{2D_d} \quad (1)$$

Chorley & Morgan (1962) showed that the maximum flow is related to  $D_m$ . Day (1983) studied two catchments of New England (NSW, Australia) and found that the  $D_m$  is correlated with discharge. In these two catchments, the  $D_m$  was found to decrease for an increase in discharge, indicating that the stream network expands during the flooding events. During the expansion and contraction of streams, the critical supporting area ( $A_c$ ), which is the area needed to initiate and maintain streams, shows variations within a catchment and is an important variable for assessing geomorphometric characteristics (e.g.  $D_m$ ) (Papageorgaki & Nalbantis 2017). The relationship between  $D_d$  and  $A_c$  follows an inverse power law (Moglen *et al.* 1998) as shown in Equation (2).

$$D_d = kA_c^{-n} \quad (2)$$

where  $k$  and  $n$  are positive numbers. If we insert the value of  $D_d$  from Equation (2) into Equation (1), we will get a power relationship between  $D_m$  and  $A_c$  as shown in Equation (3).

$$D_m = aA_c^b \quad (3)$$

where  $a = 1/2k$  and  $b = n$ .

The Distance Distributions Dynamics (DDD) model is a parsimonious continuous rainfall-runoff model with a small number of calibration parameters recently developed by Skaugen & Onof (2014). Many of the model parameters can be estimated from catchment topography using GIS and recession characteristics. DDD is a semi-distributed model, i.e., lumped in model parameters and distributed input data (precipitation and temperature). The calibration and validation results for 41 small rural unregulated catchments in Norway (area  $<50 \text{ km}^2$ ) with hourly data showed that the DDD model, in most cases, underestimated flood peaks (Tsegaw *et al.* 2019). In the runoff dynamics of the DDD model, there is a single static river network forming the basis for the dynamics of water routing through the hillslopes and in the river network (Skaugen & Onof 2014). However, studies show that the river network has a dynamical nature, being more dense during high flows than at low or medium flows (Godsey & Kirchner 2014). The primary objective of this study is to investigate whether including a dynamic river network model into the DDD model will improve flood prediction in small rural catchments (area  $<50 \text{ km}^2$ ). The secondary objective is to improve the understanding of the stream development for different vegetation covers, catchment slopes and climate. The secondary objective helps us to assess whether there is a potential to relate a calibration parameter of the dynamic river network routine with the environmental factors so that there is a possibility for regionalizing the parameter.

## METHODOLOGY

### Study catchments and data

Fifteen gauged small rural catchments, which show significant underestimation of peak floods during the calibration and validation of 41 small catchments located in Norway (Tsegaw *et al.* 2019), are used in this study for testing the dynamic river network method. The catchments are selected from the Norwegian Water Resources and Energy Directorate (NVE) HYDRA II database. Figure 1 shows locations of the study catchments, and Table 1 shows the catchment characteristics. The definition of small catchment follows that of Fleig & Wilson (2013) with an upper area limit of

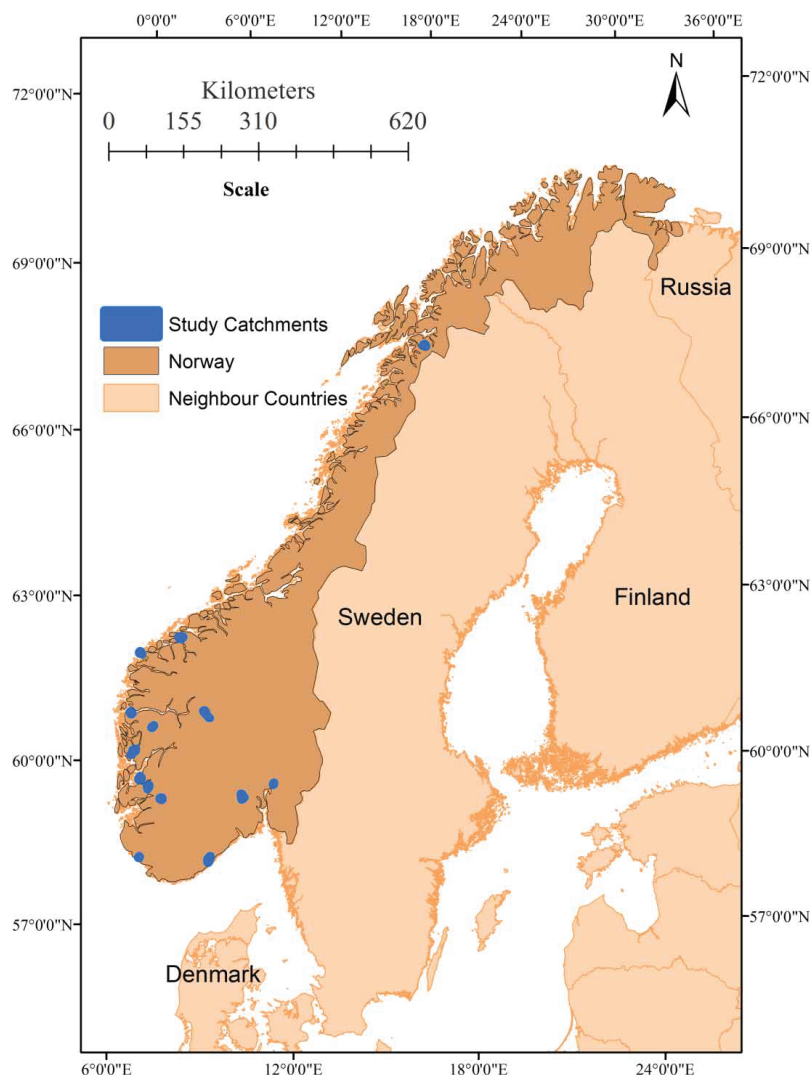


**Figure 1** | Locations of study catchments.

50 km<sup>2</sup>. We selected where the DDD model had a known history of underestimating floods so that the dynamic river network model could be tested and evaluated.

Precipitation, temperature and discharge are the main input data for running and calibrating the DDD model. We used hourly data of precipitation, temperature and discharge. Precipitation and temperature are based on

a 1 × 1 km gridded product of the Norwegian Meteorological Institute (<http://thredds.met.no/thredds/catalog.html>) (Lussana *et al.* 2016). We used a total of 5 years of data for calibration and validation. The DDD model uses distributed precipitation and temperature data as input for the model's 10 elevation zones extracted from the hypsographic curve of a catchment. The elevation of the center of each

Table 1 | Catchment characteristics of the study catchments

S.no	Cat_ID	Area (km <sup>2</sup> )	Lake (%)	Marsh land (%)	Forest (%)	Bare mountain (%)	Cultivated land (%)	Urban (%)	Mean elevation (m)	Mean annual precipitation (mm)	Mean annual temperature (°C)	Specific runoff (l/s/km <sup>2</sup> )	Mean hillslope slope (%)
1	6.10	7	2.7	1.6	94.3	0	0	0	302.9	886	4.1	20.6	18.3
2	12.195	50.7	1.3	3	88.4	0	4.3	0.5	306.5	840	3.8	17.5	15.3
3	19.107	41.5	4.8	1.4	86.4	0	4.2	0.8	88.4	1,158	4.2	24.2	14.7
4	26.64	9.7	7.2	2.2	38.8	46.2	1.1	0	203.9	1,688	6.7	45.8	28.3
5	36.32	20.9	2.5	0.9	13.5	81.4	0	0	1,039.4	2,377	0.2	105.2	34.1
6	41.8	27.4	7.7	0.4	8.8	82.2	0	0	836.8	2,955	2.7	126.4	37.5
7	42.2	31.1	2.8	1.4	40.7	52.1	0	0	573.3	2,361	4.8	108.3	40.4
8	55.4	50.6	3.7	1.3	51.8	30.7	2.8	0.2	361.3	2,593	5.4	100.4	41.9
9	63.12	12.8	4.5	0.3	5.8	86.1	0.6	0	886.2	2,579	1.1	94.8	34.4
10	68.2	20.9	4.3	0	20.2	50.3	2.5	0	402.4	2,736	5	125.2	43.6
11	73.21	25.8	7.4	2.2	2.2	88	0	0	1,292.5	946	-0.8	34.7	21.5
12	73.27	30.4	9.1	0.5	0.1	89.4	0	0	1,372	679	-2.5	33.5	14.8
13	91.2	25.8	10.1	3	3.7	66.5	1.3	0	261.9	2,072	6.1	63.5	29.9
14	101.1	40	11.3	1.6	61.3	11.3	6	0.1	232.9	1,704	5.5	54.9	23.9
15	172.8	21.2	10.7	0.5	1.4	82.5	0	0	659	1,465	1	46	17
Minimum		7	1.3	0	0.1	0	0	0	88.4	679	-2.5	17.5	14.7
Maximum		50.7	11.3	3	94.3	89.4	6	0.8	1,372	2,955	6.7	126.4	43.6

temperature and precipitation grid cell has been extracted from the  $10 \times 10$  m digital elevation model (DEM) of Norway. Discharge data have been obtained from the Norwegian Water Resources and Energy Directorates (NVE) HYDRA II database. The Norwegian Mapping Authority ([www.statkart.no](http://www.statkart.no)) is the source of the topography, observed river network and land use data.

### The DDD rainfall-runoff model

The DDD model currently runs operationally with daily and three-hourly time steps at the Norwegian flood forecasting service. It has two main modules: the subsurface and the dynamics of runoff. In DDD, the distribution of distances between points in the catchment and their nearest river reach (distance distributions of a hillslope) is the basis for describing the flow dynamics of the hillslope. The distribution of distances between points in the river network and the outlet forms the basis for describing the flow dynamics of the river network. The hillslope and river flow dynamics of DDD is hence described by unit hydrographs (UHs) derived from distance distributions from a GIS and celerity derived from recession analysis (Skaugen & Onof 2014; Skaugen & Mengistu 2016). When the distance distributions are associated with flow celerity of the hillslope and rivers, we obtain the distributions of travel times which constitute the time area concentration curve (Maidment 1993). The derivative of the time area concentration curve gives the instantaneous UH (Bras 1990), which is basically a set of weights distributing the input (precipitation and snowmelt) in time to the outlet.

### Subsurface

The volume capacity of the subsurface water reservoir,  $M$  (mm), is shared between a saturated zone with volume  $S$  (mm) and an unsaturated zone with volume  $D$  (mm). If the volume of the saturated zone is high, the unsaturated volume has to be correspondingly small (Skaugen & Onof 2014; Skaugen & Mengistu 2016). The actual water volume present in the unsaturated zone is described as  $Z$  (mm). The subsurface state variables are updated after evaluating whether the current soil moisture,  $Z(t)$ , together with the input of rain and snowmelt,  $G(t)$ , represent an excess of

water over the field capacity,  $R$ , which is fixed at 30% ( $R = 0.3$ ) of  $D(t)$  (Skaugen & Onof 2014). If  $G(t) + Z(t) > R * D(t)$ , then the excess water  $X(t)$  is added to  $S(t)$ .

$$\text{Excess water (mm/h)} \quad X(t) = \text{Max} \left\{ \frac{G(t) + Z(t)}{D(t)} - R, 0 \right\} D(t) \quad (4)$$

$$\text{Ground water (mm/h)} \quad \frac{dS}{dt} = X(t) - Q(t) \quad (5)$$

$$\text{Soil water content (mm/h)} \quad \frac{dZ}{dt} = G(t) - X(t) - E_a(t) \quad (6)$$

$$\text{Soil water zone (mm/h)} \quad \frac{dD}{dt} = -\frac{dS}{dt} \quad (7)$$

$$\text{Potential evapotranspiration (mm/h)} \quad E_p = C_{ea} * T \quad (8)$$

$$\text{Actual evapotranspiration (mm/h)} \quad E_a = E_p * \frac{S + Z}{M} \quad (9)$$

$Q(t)$  is runoff, and  $E_a(t)$  is the actual evapotranspiration which is estimated as a function of potential evapotranspiration and the level of storage.  $C_{ea}$  is a degree hour factor which is positive for positive temperature ( $T$ ) and zero for negative temperature.  $E_a$  is drawn from  $Z$ . The degree hour approach is a simplification but experiences from Skaugen & Onof (2014) show that the evapotranspiration routine in DDD calculates similar values to the approach used in the well-known rainfall-runoff model HBV (Bergström 1976). A recession analysis of observed runoff from the catchment is used to estimate the catchment-scale fluctuations of storage and the capacity of the subsurface water reservoir ( $M$ ) (see Skaugen & Mengistu 2016).

### Runoff dynamics

The dynamics of runoff in DDD has been derived from the catchment features using a GIS combined with runoff recession analysis. The method for describing the runoff dynamics of a catchment is built on the distance distribution derived from the catchment topography. The distances from the points in the catchment to the nearest river reach are calculated as Euclidean distance for the marsh and soil parts of a hillslope. Previous studies in more than 120 catchments in

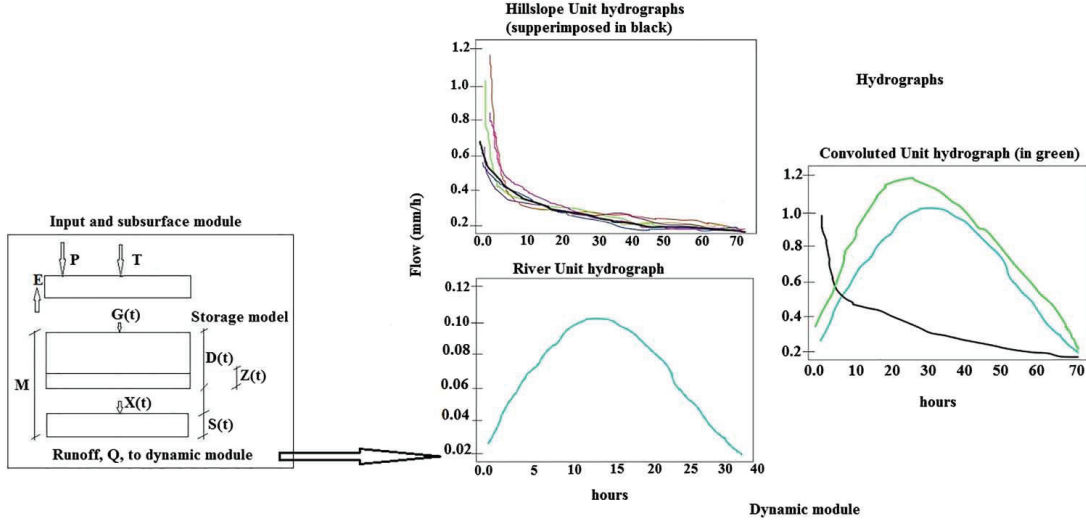


Figure 2 | Structure of distance distribution dynamics (DDD) rainfall-runoff model.

Norway showed that the exponential distribution describes the hillslope distance (Euclidean distance from the nearest river reach) distribution well, and the normal distribution describes well the distances between points in the river network and outlet of a catchment (Skaugen & Onof 2014). Figure 2 shows the structure of the DDD model. The model is written in the R programming language. All GIS work is done with ArcGIS 10.3 (ESRI 2014), and the recession analysis is done using an R script (R Core Team 2017).

Water is conveyed through the soils to the river network by waves with celerity determined by the actual storage,  $S(t)$ , in the catchment (Skaugen & Onof 2014; Skaugen & Mengistu 2016). The celerity associated with the different levels of subsurface storage is estimated by assuming exponential recessions with parameter  $\Lambda$  in the equation  $Q(t) = Q_0 \Lambda e^{-\Lambda(t-t_0)}$ , where  $Q_0$  is the peak discharge immediately before the recession starts.  $\Lambda$  is the slope per  $\Delta t$  of the recession in the log-log space.

$$\Lambda(t) = \log(Q(t)) - \log(Q(t + \Delta t)) \quad (10)$$

The distribution of  $\Lambda$  is modeled using a two-parameter gamma distribution.

The celerity,  $v$ , is calculated as a function of  $\Lambda$  using Equation (11).

$$v = \frac{\Lambda D_m}{\Delta t} \quad (11)$$

where,  $D_m$  is the mean of the distances from points in the catchment (hillslope) to the nearest river. The capacity of the subsurface reservoir  $M$  (mm) is divided into five storage levels,  $i$ , corresponding to the quantiles of the distribution of  $\Lambda$  under the assumption that the higher the storage, the higher the value of  $\Lambda$ . Each storage level is further assigned a celerity  $v_i = \frac{\lambda_i D_m}{\Delta t}$  (see Equation (11)), where  $\lambda_i$  is the parameter of the UH for the individual storage level  $i$ , and estimated such that the runoff from several storage levels will give a UH equal to the exponential UH with a parameter  $\Lambda_i$ . With the assumption that the recession and its distribution carries information on the distribution of catchment-scale storage, we can consider that the temporal distribution of catchment-scale storage,  $S(t)$ , is a scaled version to that of  $\Lambda$ .  $S(t)$  is calculated using Equation (12), and its distribution is modeled using a two-parameter gamma distribution.

$$S(t) = \frac{Q(t)}{1 - e^{-\Lambda(t)}} \quad (12)$$



The DDD model has five storage levels ( $i = 1, \dots, 5$ ). Four storage levels are subsurface level, whereas the fifth one is an overland flow level with unlimited capacity (Skaugen & Onof 2014; Skaugen & Mengistu 2016). The five levels have five-UHs (four for subsurface flow and one for overland flow) and each of them has different temporal scales as they have been assigned different celerities. The UH is modeled as follows:

$$UH_i(t) = \lambda_i e^{-\lambda_i(t-t_0)} \quad (13)$$

where  $t_0$  is the time of input, and  $\lambda_i$  is the parameter of the exponential distribution estimated from recession analysis for each level,  $i$ .

### Model parameters and calibration

The model parameters are divided into three main groups. The first group are those estimated from observed hydro-meteorological data (Table 2), the second group are those estimated by model calibration against observed discharge

(Table 3), and the third group are those estimated from digitized maps using a GIS (Table 4). The snow routine in DDD has two parameters estimated from the spatial distribution of observed precipitation data (Skaugen & Weltzien 2016). The shape parameter ( $a_0$ ) and the decorrelation length ( $d$ ) of the gamma distribution of snow and snow water equivalent (SWE) are estimated from a previous calibration for 84 catchments in Norway (Skaugen *et al.* 2015). The calibration of the model is performed using the probability particle swarm optimization (PPSO) algorithm (Lu & Han 2011). The Kling-Gupta efficiency criteria (KGE) have been used as objective function for the calibration (Gupta *et al.* 2009), and we used KGE, the BIAS (ratio of the mean of simulated to observed discharge) and visual inspection of hydrographs to evaluate the performance of the model.

### Dynamic river network routine

We introduce a dynamic river network concept into the DDD model so that the scale of the overland unit hydrograph (OUH) will be dynamic while keeping the four

**Table 2** | List of DDD rainfall-runoff model parameters estimated from observed hydro-meteorological data

Parameters	Description of the parameter	Method of estimation	Unit
$d$	Parameter for spatial distribution of SWE, decorrelation length	From spatial distribution of observed precipitation	Positive real number
$a_0$	Parameter for spatial distribution of SWE, shape parameter	From spatial distribution of observed precipitation	Positive real number
MAD	Long-term mean annual discharge	From long-term observed mean annual flow data	$m^3/s$
Gshape	Shape parameter of $\lambda$	Recession analysis of observed runoff	Positive real number
Gscale	Scale parameter of $\lambda$	Recession analysis of observed runoff	Positive real number
GshInt	Shape parameter of $\Lambda$	Recession analysis of observed runoff	Positive real number
GscInt	Scale parameter of $\Lambda$	Recession analysis of observed runoff	Positive real number

**Table 3** | List of DDD rainfall-runoff model parameters needing calibration

Parameters	Description of the parameter	Method of estimation	Unit	Intervals of calibration
pro	Liquid water in snow	Calibration	fraction	0.03–0.1
cx	Degree hour factor for snow melt	Calibration	$mm \cdot C^{-1} h^{-1}$	0.05–1.0
CFR	Degree hour factor for refreezing	Calibration	$mm \cdot C^{-1} h^{-1}$	0.001–0.01
Cea	Degree hour factor for evapotranspiration	Calibration	$mm \cdot C^{-1} h^{-1}$	0.01–0.1
rv	Celerity for river flow	Calibration	m/s	0.5–1.5

**Table 4** | List of DDD rainfall-runoff model parameters estimated from geographical data using GIS

Symbol of parameters	Description of the parameter
Area	Catchment area
maxLbog	Maximum distance of marsh land portion of hillslope
midLbog	Mean distance of marsh land portion of hillslope
bogfrac	Areal fraction of marsh land from the total land uses
zsoil	Areal fraction of DD for soils (what area with distance zero to the river)
zbog	Areal fraction of distance distribution for marsh land (what area with distance zero to the river)
midFl	Mean distance (from distance distribution) for river network
stdFL	Standard deviation of distance (from distance distribution) for river network
maxFL	Maximum distance (from distance distribution) for river network
maxDL	Maximum distance (from distance distribution) of non-marsh land (soils) of hill slope
midDL	Mean distance (from distance distribution) of non-marsh land (soils) of hill slope
midGl	Mean distance (from distance distribution) for glaciers
stdGl	Standard deviation of distance (from distance distribution) for glaciers
maxGl	Maximum distance (from distance distribution) for glaciers
Hypsographic curve	11 values describing the quantiles 0, 10, 20, 30, 40, 50, 60, 70, 80, 90, 100

subsurface UHs constant during the simulation period. The methodology, we used in estimating the dynamic OUHs of a hillslope, is similar to that of GIUH and of the width function, i.e., the travel time probability density function of a unit amount of water draining from a catchment. However, the approaches used in estimating the parameters of the distribution are different, i.e., the approach in calculating the celerity and distances of a flow from the points in the hillslope to the nearest river reach. Further, we assumed that the scale of the travel time distribution in a hillslope is dynamic for generating dynamic OUHs while the shape is held constant. In DDD, the dynamic OUHs are turned on and off according to saturation of the subsurface thus giving a dynamic travel time distribution.

The river network indicates where the subsurface water flow becomes surface water flow. The network system governs the dynamics of runoff for conditions where we have no overland flow from the hillslope in that there is a significant (orders of magnitude) difference in water celerity for flow through the soils and flow in the river network (Robinson *et al.* 1995). In case of overland flow, however, we can imagine a dynamic river network (and hence dynamic distance distributions) as a function of overland flow (OF). We made three assumptions to derive such algorithm.

1. The mean celerity of the overland flow ( $v_{OF}$ ) is constant, i.e., independent of the subsurface saturation and river network.
2. The overland flow unit hydrograph (OUH) is exponential determined from  $D_m$  and  $v_{OF}$ .
3. The  $D_m$  of a river network is a function of volume of water per area per unit time, i.e., OF. If we assume a critical flux,  $F_c$  of  $10 \text{ m}^3/\text{h}$  is necessary to create a stream, then OF of 10 mm for an hour over  $A_c = 1000 \text{ m}^2$ , will provide such a flux, whereas the same flux is obtained for OF of 100 mm over  $100 \text{ m}^2$ . The two cases have different critical supporting area ( $A_c$ ), and these cases will provide us with two different river networks where the latter has smaller  $D_m$  than the former.

The physical mechanisms underpinning the above three assumptions are:

1. The variable contributions of saturation excess overland flow of a hillslope develops along the existing river network following the concept of Dunne's overland flow (Dunne 1978).
2. The critical supporting area ( $A_c$  defines the minimum catchment area from which the generated runoff is sufficient to initiate and maintain river development

(Schaefer *et al.* 1979)). The expansion and contraction of the stream network is governed by the amount of saturation excess overland flow.

3. The hillslope travel time probability density function of overland flow is estimated from the distance distributions at any point from the hillslope to the river network and the celerity of flow in the hillslope (D'Odorico & Rigon 2003; Rigon *et al.* 2011).

In order to compute the OUH, we need the mean ( $D_m$ ) and the maximum ( $D_{max}$ ) of the hillslope distance distribution and the mean overland flow celerity,  $v_{OF}$ . Using assumption (3), we can derive a dynamic  $A_c$  after introducing a critical flux ( $F_c$ ) as shown in Equation (14), which needs to be determined.

$$F_c (m^3/h) = A_c(m^2) * OF (m/h) \quad (14)$$

where OF is saturation excess overland flow and is estimated from the DDD model output at each simulation time step. When the subsurface is saturated and there is overland flow ( $OF > 0$ ), the dynamic river network routine is activated and the corresponding  $A_c$  will be calculated in the model using Equation (14).

We need to compute the coefficients  $a$  and  $b$  of the general power relation between  $D_m$  and  $A_c$  of each of the study catchments (see Equation (3)) for computing a dynamic  $D_m$  during simulation. For computing  $a$  and  $b$ , we have used the following procedure:

1. The  $10 \times 10$  m DEM of a catchment has been reconditioned to the observed river network using the DEM reconditioning tool from Arc Hydro and a raster flow accumulation map has been prepared using GIS.
2. We wrote a python script that can loop through several thresholds of flow accumulation ( $A_c$ ) to define stream and create several stream networks. From the distance distributions derived from each stream networks, the  $D_m$  is calculated.
3. A regression curve is fitted to the synthetically derived  $A_c$  and  $D_m$  of a catchment to estimate  $a$  and  $b$  (Figure 3 shows the fitted curves for six sample catchments). The values of  $a$  and  $b$  are unique for each catchment and are listed in Table 5 for all study catchments.

After we have obtained the coefficients of the relationship between  $A_c$  and  $D_m$ , the  $A_c$  estimated from Equation (14) will be used to estimate  $D_m$  using Equation (3). We estimated  $D_{mx}$  from the exponential distribution with parameter  $D_m$ , as a distance where 99% of the catchment area is accounted for. From the recession analysis for estimating celerities, we already have an estimate of  $v_{OF}$  in the DDD model (Skaugen & Onof 2014). We estimate a dynamic OUH for every time step when overland flow is estimated.

When the  $D_m$  calculated using Equation (3) is greater than the  $D_m$  of the observed river network, the dynamic river network degenerates to the observed river network. The observed river network is the basis network for all cases where the subsurface capacity is unsaturated, saturated but no overland flow and when there is overland flow but not sufficient to expand the observed (existing) stream network. When the subsurface capacity is saturated and there is sufficient OF, the observed stream network starts to expand. The extent of expansion is determined by the magnitude of the estimated OF and  $F_c$ .

We have tested the performance of the DDD model with and without the dynamic river network routine. We calibrated and validated the DDD model as described in the model parameter and calibration section, and we implemented the dynamic river routine into the model and calibrated  $F_c$ . We have calibrated  $F_c$  manually after calibrating automatically DDD parameters without dynamic river network. The procedures we have followed in calibrating are as follows:

1. The  $F_c$  parameter is adjusted by trial and error to fit the observed flood peaks, which had been underestimated by DDD without dynamic river network.
2. We have visually compared the observed flood hydrographs and flood hydrographs simulated with and without dynamic river network.
3. While calibrating DDD with  $F_c$  (with dynamic river network module), the KGE and BIAS values obtained should not be less than the KGE and BIAS values of DDD without dynamic river network method (earlier calibration result).
4. Using the visual inspection of observed hydrographs, KGE and BIAS, the  $F_c$  which fits the observed flood peaks well is taken as a calibrated value.

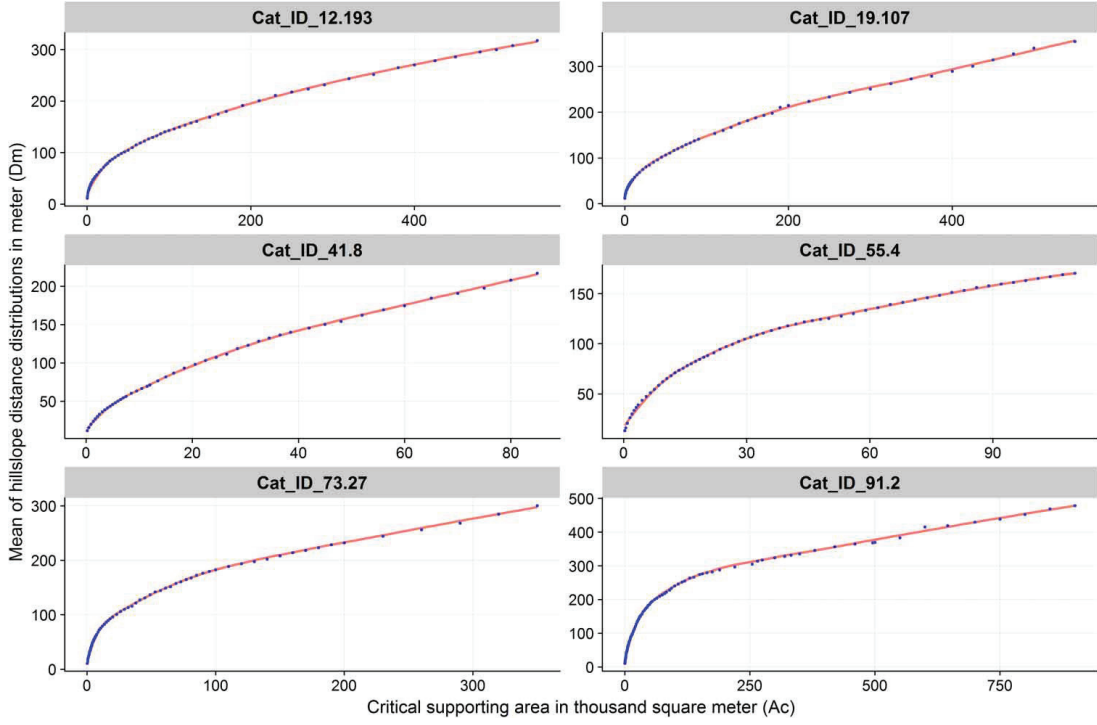


**Figure 3** | Curves fitted to the relation between mean distance distribution of hillslope, i.e.,  $D_m$  and critical supporting area, i.e.,  $A_c$  for six sample study catchments with a relation,  $D_m = aA_c^b$ .

As for the previous case, we used KGE, BIAS and hydrographs to evaluate the performance of the model with dynamic river network routine. We have also analyzed the mean absolute relative error (MARE, Equation (15)) of 91 flood peaks with and without river dynamics.

$$\text{MARE}(\%) = \frac{1}{N} \sum_{i=1}^N \left| \frac{(O_i - S_i)}{O_i} * 100 \right| \quad (15)$$

where  $O_i$  is the observed flood peak and  $S_i$  is the predicted flood peak with and without dynamic river network.  $N$  is the number of flood peaks (91 in this study). We have also analyzed the quantiles of the distribution of relative errors (RE, Equation (16)) of the flood peaks prediction.

$$\text{RE}(\%) = \frac{(O_i - S_i)}{O_i} * 100 \quad (16)$$

where  $O_i$  is the observed flood peak and  $S_i$  is the predicted flood peak with and without dynamic river network.

#### Correlation between $A_c$ and $F_c$ with environmental factors

We have done a correlation analysis between the parameters  $A_c$  and  $F_c$  and environmental factors to improve the understanding on how the dynamic river network develops and to assess the potential for relating  $F_c$  to environmental factors. The environmental factors included in the correlation analysis are mean annual precipitation, mean hillslope slope, bare mountain and forest land covers of the study catchments. We have used the Pearson correlation coefficient for the analysis. The  $A_c$  derived from observed river network has a spatial variation within a catchment; therefore, we have estimated the mean  $A_c$  for

**Table 5** | The coefficient of determination ( $R$ -squared) and the coefficients of the power relation between  $D_m$  and  $A_c$ , i.e.,  $D_m = aA_c^b$  for all the study catchments

cat_ID	a	b	R <sup>2</sup>
6.1	2.17	0.37	0.99
12.193	1.16	0.42	1
19.107	1.04	0.43	1
26.64	1.23	0.42	1
36.32	1.18	0.42	1
41.8	0.61	0.51	0.99
42.2	0.92	0.45	1
55.4	1.1	0.44	1
63.12	1.05	0.45	1
68.2	0.86	0.49	1
73.21	0.82	0.48	1
73.27	1.19	0.44	0.99
91.2	0.68	0.51	0.99
101.1	1.1	0.45	0.98
172.8	1.08	0.44	1

each of the study catchments before the correlation analysis using the following two steps. First, the  $D_m$  of the observed stream network is estimated using GIS. Second, the mean  $A_c$  of the observed river network is calculated using Equation (3). To assess the potential for relating  $F_c$  with the environmental factors, correlation analysis between the calibrated  $F_c$  and the environmental factors has also been performed. We have also done a stepwise method of multiple linear regression between  $F_c$  and the four environmental factors mentioned above to see if there is a possibility for regionalizing  $F_c$ .

## RESULTS

### Performance of DDD with and without dynamic river network

The calibration and validation results of the DDD model without a dynamic river network show that the model performs satisfactorily with KGE values between 0.55 and 0.9 and BIAS between 0.75 and 1.25. As stated by Thiemig *et al.* (2013),  $0.75 \leq KGE < 0.9$  is considered good,

$0.5 \leq KGE < 0.75$  is intermediate and  $0.0 \leq KGE < 0.5$  is poor. Seven catchments show good and eight catchments show intermediate performance both during the calibration and validation periods. Even if the KGE performance is satisfactory, the visual inspection of the hydrographs shows that several observed flood peaks are underestimated.

We added the dynamic river network routine into the DDD model and calibrated the critical flux ( $F_c$ ) parameter of the routine manually for the whole simulation period. The KGE and BIAS performance of the model are similar as before, i.e., without dynamic river network for all study catchments except one, where the KGE is slightly lower. However, the inspection of the hydrographs clearly shows that the predication of several underestimated flood peaks has been improved after the addition of the dynamic river network routine. The dynamic OUHs that resulted from the dynamic river network have higher peaks and narrower width during the flooding events, and these OUHs, added with the subsurface UHs, helped in improving the previously underestimated floods. Figure 4 shows the hillslope distance distributions for variable  $A_c$  for catchment 73.27. Figure 5 shows the empirical cumulative distance distributions functions as an example for the dynamic distance distribution presented in Figure 4, and Figure 6 shows the four dynamic OUHs which resulted from the corresponding distance distributions functions. Table 6 shows OF,  $A_c$  and  $D_m$  for a catchment 12.193 during a flooding event.

Figure 7 shows the hydrographs during the flooding periods with and without the dynamic river network routine for six sample study catchments. Table 7 shows the observed floods, simulated floods, KGE and BIAS performance of DDD model with and without dynamic river network routine for five sample study catchments selected randomly.

The results of the statistical analysis (mean absolute relative errors and quantiles of relative errors), for the 91 observed peak floods from the 15 study catchments, show that the dynamic river network method improved the prediction of peak floods significantly. The 0.75 quantile of the relative errors of the simulated peaks reduced from 41% to 23%, and the 0.25 quantile of the relative errors reduced from 22% to 1%. Figure 8 shows box plots of the relative errors with and without river dynamics. The MARE of the magnitude of the underestimated peak floods is reduced from 32.9% to 15.7%.

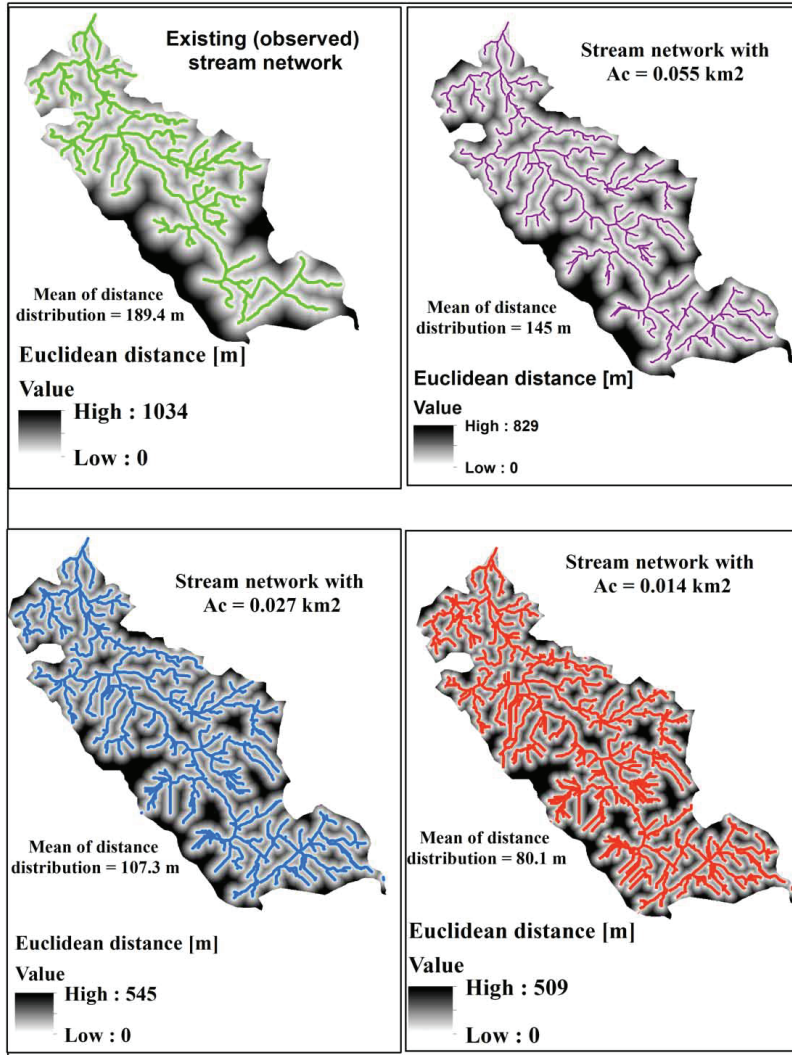


Figure 4 | Map of sample dynamic distance distributions of hillslope generated from dynamic critical supporting area, i.e.,  $A_c$  during flooding events for catchment 73.27.

### Correlation between $A_c$ and $F_c$ with environmental factors

The critical supporting area,  $A_c$ , of an observed stream network of a catchment shows spatial variation within the catchment (Figure 9 shows the distributions for five

sample catchments); therefore, the mean value of a catchment is used for the correlation analysis. The mean  $A_c$  for the observed river networks is correlated with environmental factors, i.e., vegetation cover, topography and climate. The correlation with vegetation cover is stronger than that of topography and climate. The mean



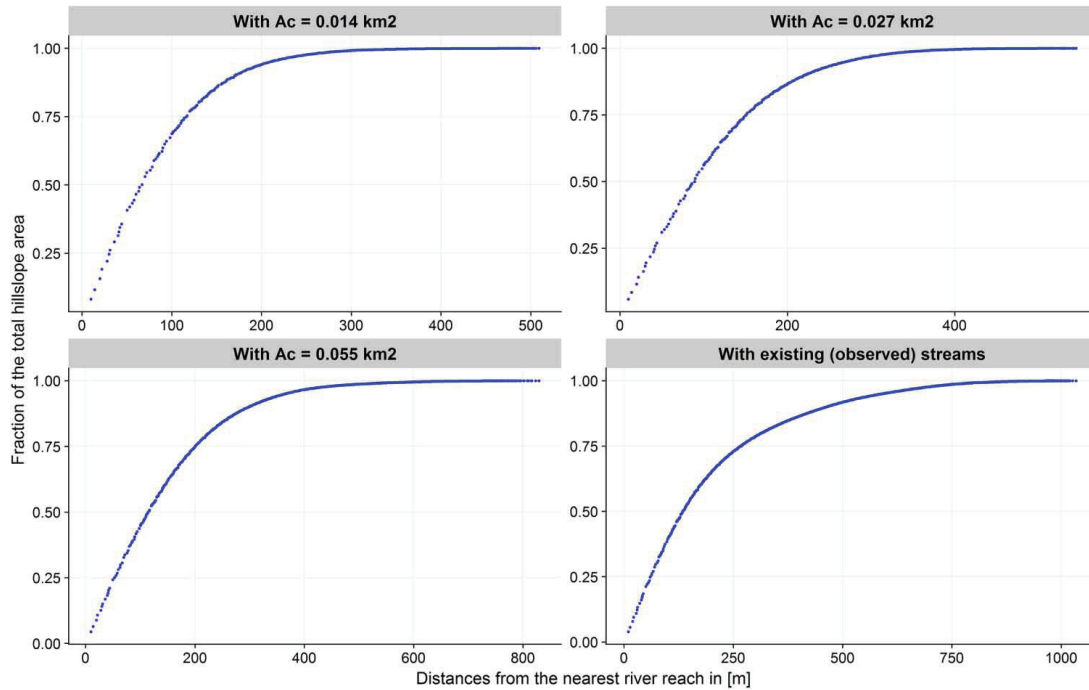


Figure 5 | Cumulative distance distributions functions of the dynamic hillslope distance distributions of Figure 4 for catchment 73.27.

$A_c$  has a positive correlation with the forest cover in a catchment, but it has a negative correlation with mean

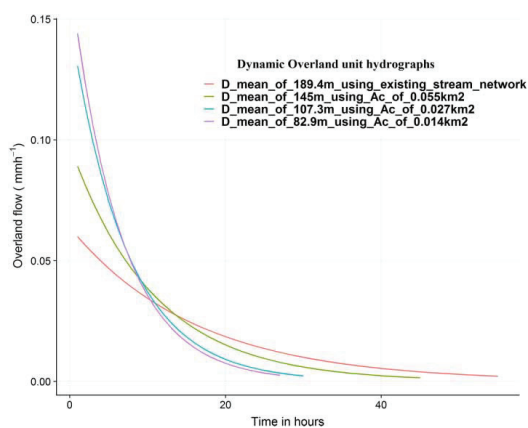


Figure 6 | Dynamic overland unit hydrographs of the cumulative distance distributions functions under Figure 5 during a flooding event for catchment 73.27.

annual precipitation, bare mountain cover and mean hillslope slope of a catchment. Table 8 shows the correlation between the mean  $A_c$  and  $F_c$  and the environmental factors.

The calibrated critical flux,  $F_c$ , of the dynamic river network routine is correlated with the environmental factors. The correlation between  $F_c$  and the vegetation cover is stronger than the correlation between  $F_c$  and topography and mean annual precipitation.  $F_c$  shows positive correlation with forest and negative correlation with bare mountain, mean annual precipitation and mean hillslope slope of a catchment. Table 9 shows the environmental factors used in the correlation analysis, the  $D_m$  and mean  $A_c$  of observed river network and the calibrated  $F_c$  of the dynamic river network routine of the study catchments.

The result of stepwise multiple linear regression shows that there is a potential to estimate  $F_c$  from the environmental factors as shown in Equation (17). Bare mountain is the only environmental factor contributing significantly to the regression with a significant level of 0.1. The multiple

**Table 6** | Dynamic mean distance of the hillslope distance distributions estimated and used for generating dynamic overland unit hydrograph during flooding event at catchment 12.193 with a calibrated critical flux of 90 m<sup>3</sup>/h

OF (mm/h)	$A_c$ (m <sup>2</sup> )	$D_m$ (m) estimated using Equation (3)	$D_m$ (m) used in deriving OUH
0.144	1,319,444.4	429.08	<i>301.1</i>
2.19	86,758	137.58	137.58
2.22	85,585.6	136.79	136.79
0.94	202,127.7	196.26	196.26
10.9	17,431.2	70.12	70.12
1.4	135,714.3	166.02	166.02
2.7	70,370.4	126	126
1.19	159,663.9	177.75	177.75
0.19	1,027,027	388.44	<i>301.1</i>
1.27	149,606.3	172.96	172.96
0.2	950,000	375.93	<i>301.1</i>
1.33	142,857.1	169.64	169.64
1.28	148,902.8	172.61	172.61
0.17	1,117,647.1	402.48	<i>301.1</i>
0.14	1,319,444.4	431.54	<i>301.1</i>
0.64	296,875	230.64	230.64
0.34	558,823.5	302	<i>301.1</i>
0.31	612,903.2	312.72	<i>301.1</i>
0.83	228,915.7	206.79	206.79

Italic numbers are rounded to two significant figures.

coefficient of determination ( $R^2$ ) of the multiple regression is 0.3 and the significant level ( $P$ ) is 0.06.

$$F_c \text{ (m}^3\text{/h)} = 160.7 - 1.4 * \text{bare mountain (\%)} \quad (17)$$

## DISCUSSION

### Dynamic river networks

Dynamic river networks and hence dynamic OUHs are introduced and implemented in the DDD rainfall-runoff model to improve the simulation of floods. The dynamic river network method expands the observed river networks during OF events. The expansion means that the  $A_c$  required to initiate and maintain a stream decrease. Smaller  $A_c$  results in smaller  $D_m$  (see Table 5). The smaller  $D_m$  value

indicates shorter travel times from points in the catchment to the nearest river reach. The shorter travel time distribution generates OUHs with a higher peak and shorter scale for the hillslopes (Figure 6). The dynamic OUHs are superpositioned with the other four subsurface UHs of DDD to give a single dynamic UH of a catchment during flooding events. The results of the method are supported by the previous study of D'Odorico & Rigon (2003) who found that shorter hillslope distances result in shorter travel times and hence higher flood peaks. The smaller  $D_m$  results, obtained during the flooding events using the dynamic river network method, are also supported by the study of Humbert (1990) who found that a good correlation exists between the runoff coefficient of flooding events and  $D_d$ , and hence the  $D_m$ , for 45 French catchments. Lazzaro *et al.* (2015) also found that the variability of runoff due to higher  $D_d$  (lower  $D_m$ ) creates a faster concentration of flow that implies shorter travel times and higher peak floods. The results in this study are also supported by the results of Lee *et al.* (2008) who found that a UH of a catchment is dynamic during different precipitation intensities, i.e., the higher the precipitation intensity, the higher the peak and shorter the temporal scale of the UHs. The results of this study also show that a dynamic river network method could be a solution for rainfall-runoff models which face challenges in predicting flood peaks through continuous simulation. Improving the prediction of peak floods in a continuous simulation is very important because the hydrograph consisting of this peak flow is mainly responsible for the damage caused by floods. Therefore, a dynamic river network is a method to be conceptualized and included as one routine in continuous rainfall-runoff models which underestimate predictions of floods.

We analyzed statistically 91 underestimated flood peaks to evaluate the performance of the dynamic river network. The MARE and quantiles of RE of the prediction with and without dynamic river network show that the overall performance of the method has improved the prediction of the peaks satisfactorily. The dynamic river network overestimated 17 of the 91 flood peaks and still underestimates the remaining 74 floods but with a significant improvement in the prediction of flood peaks compared to the results obtained without a dynamic river network.



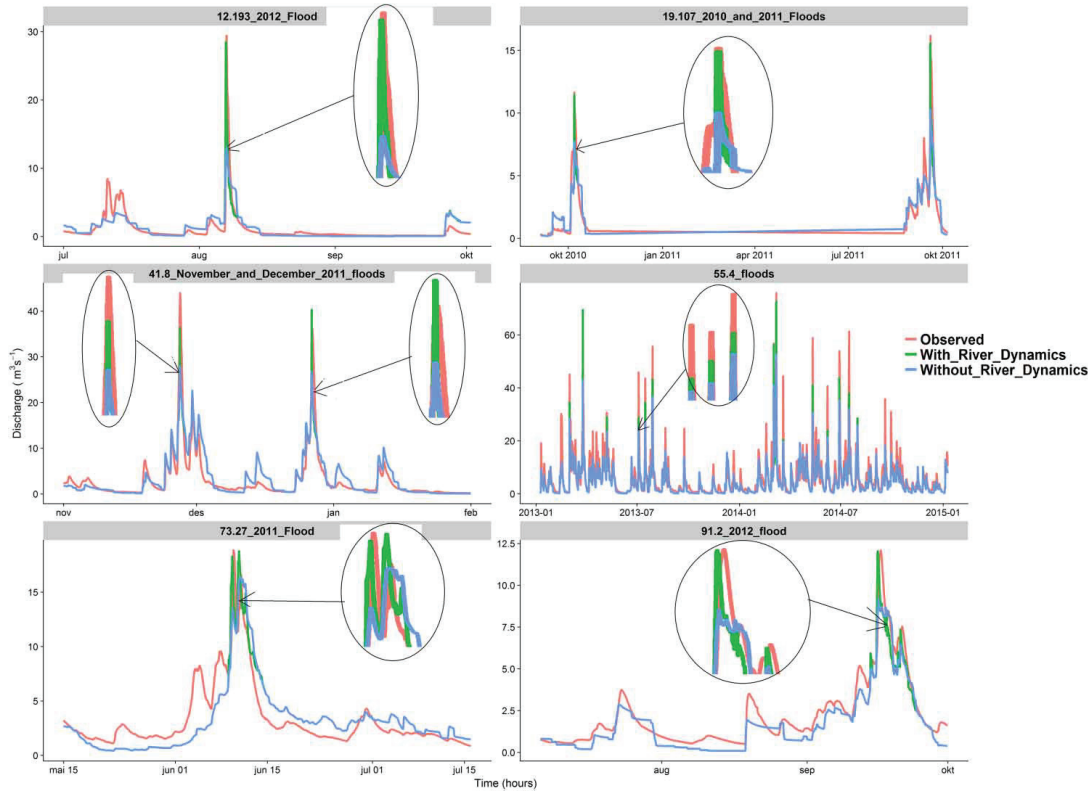


**Figure 7** | Hydrographs of continuous simulations results of DDD rainfall-runoff models with flood peaks, i.e. observed, simulated with and without dynamic river network.

**Table 7** | Observed and simulated floods using DDD with and without dynamic river network and the corresponding performance of the model for five sample catchments

Cat_ID	Observed flood(s) in m <sup>3</sup> /s	Simulation period	Simulated value(s) of flood without river dynamics in m <sup>3</sup> /s	Performance of DDD model without river dynamics in calibration		Simulated value(s) of flood with river dynamics in m <sup>3</sup> /s	Performance of DDD model with river dynamics	
				KGE	BIAS		KGE	BIAS
12.193	29.42	2 years	12.97	0.64	1.2	28.78	0.65	1.2
19.107	11.65 and 16.2	3 years	7.64 and 10.3	0.8	0.93	9.42 and 16.1	0.81	0.94
41.8	43.96 and 36.13	2 years	28.02 and 26.74	0.77	0.84	36.3 and 40.3	0.77	0.84
73.27	18.85	3 years	13.3	0.71	0.76	18.3	0.71	0.76
91.2	12.06	2 years	8.34	0.71	0.8	12.04	0.71	0.8

Italic numbers are rounded to two significant figures.

A single calibrated critical flux,  $F_c$ , improves the prediction of several underestimated floods significantly, but it also overestimates a few flood peaks (Figure 7). Reasons for

overestimation could be that a single calibrated  $F_c$  could not represent the different precipitation patterns, overland flow patterns and initial conditions prior to flooding

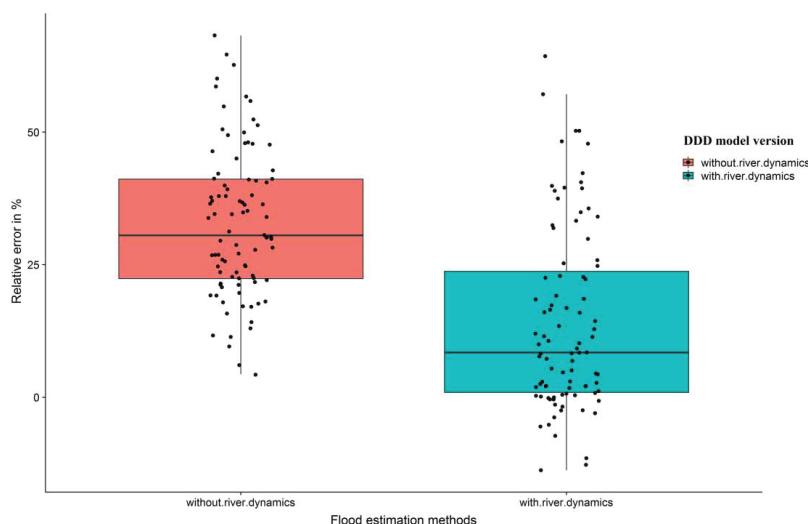


**Figure 8** | Distributions of relative errors (%) of prediction of 91 flood peaks with and without dynamic river network.

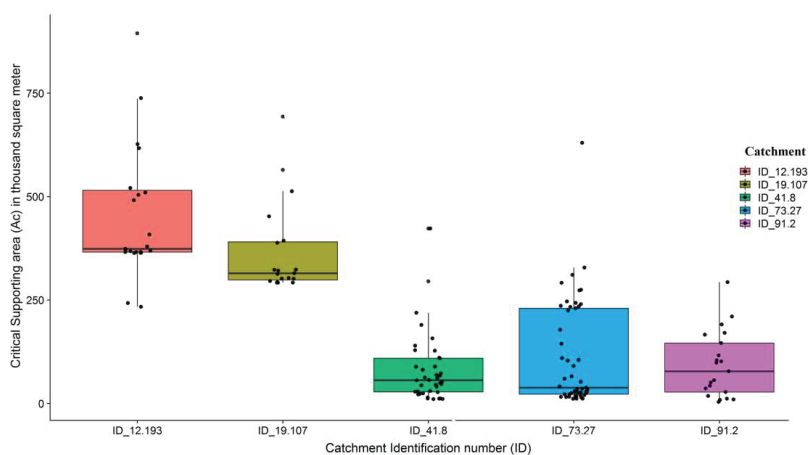


**Figure 9** | Distributions of critical supporting area, i.e.,  $A_c$  of observed stream networks for five of sample study catchments.

**Table 8** | Correlation between calibrated critical flux,  $F_c$  of the dynamic river network with environmental variables, and correlation between mean critical area,  $A_c$  of the observed river network with some environmental variables

	Forest (%)	Bare mountain (%)	Mean hillslope slope (%)	Mean annual precipitation (mm)
Mean $A_c$ ( $m^2$ )	0.63	-0.63	-0.56	-0.49
$F_c$ ( $m^3/h$ )	0.46	-0.5	-0.29	-0.18

events. Another reason for such overestimation could be that the dynamic  $D_m$  estimated using Equation (3) is not always an accurate representation of the reality during a flood event. The limitations of manual calibration include subjectivity and time consuming. Manual calibration methods are subjective in the evaluation of model fit and the final choice of optimal parameters. [Ndiritu \(2009\)](#)

**Table 9** | The environmental factors used in the correlation analysis, the mean distance distribution, and mean critical area,  $A_c$ , of observed river network, and the calibrated critical flux,  $F_c$ , of the dynamic river network routine

Cat_ID	Environmental factors				Observed river network		Dynamic river network
	Forest (%)	Bare mountain (%)	Mean annual precipitation (mm)	Mean hillslope slope (%)	$D_m$ (m)	Mean $A_c$ (m <sup>2</sup> )	$F_c$ (m <sup>3</sup> /h)
6.1	94.3	0	886	18.3	149.2	92,406	15
12.193	88.4	0	840	15.3	301.1	560,042	190
19.107	86.4	0	1,158	14.7	336.9	689,123	370
26.64	38.8	46.2	1,688	28.3	181.6	146,146	5
36.32	13.5	81.4	2,377	34.1	168.6	135,213	120
41.8	8.8	82.2	2,955	37.5	157.2	53,418	15
42.2	40.7	52.1	2,361	40.4	175.9	117,477	30
55.4	51.8	30.7	2,593	41.9	155.1	76,715	15
63.12	5.8	86.1	2,579	34.4	181.2	93,596	80
68.2	20.2	50.3	2,736	43.6	211.3	75,573	150
73.21	2.2	88	946	21.5	298.4	216,464	15
73.27	0.1	89.4	679	14.8	189.4	100,964	60
91.2	3.7	66.5	2,072	29.9	283.8	137,481	90
101.1	61.3	11.3	1,704	23.9	334.0	328,354	150
172.8	1.4	82.5	1,465	17	168.1	95,972	10

pointed out that manual calibration may be more prone to obtaining suboptimal parameter sets than automatic calibration. Studies also show that manual calibration is more subjective than automatic calibration because it largely depends on visual hydrograph inspection and the personal judgment of the hydrologist. Substantial amount of time is also required to adjust  $F_c$  so that the observed and simulated flood peaks agreed well. A separate automatic calibration of  $F_c$  (which is not included in this study) after defining and writing appropriate objective function could improve the limitations of the manual calibration. However, since we have only one manually calibrated parameter and we have enough experience of using DDD model, the manual calibration result of  $F_c$  could be very good. In addition, the results of our study show that the manually calibrated  $F_c$  resulted in a significant improvement in predicting flood peaks using dynamic river network method.

The hydrograph in Figure 7 shows that the two floods of the catchment 41.8 could not be estimated well using a single calibrated  $F_c$  of magnitude 15 m<sup>3</sup>/h even if the overall prediction of the flood peaks is improved. When we look at the flood hydrographs, the 27 November flood of 43.96 m<sup>3</sup>/s

(at 8 A.M), had been preceded by a 1-day precipitation of 68.9 mm (from 26 November 2011 09:00 to 27 November 2011 08:00). The precipitation was again preceded by a 3-day precipitation of magnitude 86.1 mm, i.e., the 4-day precipitation preceded the flooding event was 154.9 mm. When  $F_c$  is fitted to this single flooding event, 5 m<sup>3</sup>/h is required. After 1 month, another heavy precipitation event happened (56.9 mm/day) and the event was preceded by 82.2 mm of 3-day precipitation, i.e., the 4-day precipitation preceded the flooding event was 139.7 mm. The magnitude of the flood was 36.13 m<sup>3</sup>/s. When  $F_c$  is fitted to this single flooding event, 25 m<sup>3</sup>/h is required. The variation in the fitted values of  $F_c$  for different flooding events in a catchment shows that we could have an overestimation of flooding events when we use a single calibrated  $F_c$  for the whole simulation period as a representative for a catchment. Accordingly, a single  $F_c$  of 15 m<sup>3</sup>/h for the catchment 41.8 has overestimated the December 2011 flood, i.e., 36.13 m<sup>3</sup>/s, but it has improved the overall prediction of the flood peaks in the catchment.

The spatial variability of  $A_c$  during flooding events, which is not considered in this study, could also be another

factor for the overestimation of floods using a single calibration value of  $F_c$  for a catchment. We have derived the coefficients of Equation (3) ( $a$  and  $b$ ) with the assumption of constant  $A_c$  using the DEM, which considers only the topography of a catchment. However, the  $A_c$  of observed stream networks clearly shows that there is a spatial variability of  $A_c$  within a catchment. Geological and land use factors play significant roles in initiating and maintaining a stream, and these factors control the spatial variability of  $A_c$  in a catchment (Montgomery & Dietrich 1989; Ogden *et al.* 2011; Sjöberg 2016; Ward *et al.* 2018) in addition to the topography. The correlation results between  $A_c$  and vegetation cover, which is done in this study and explained in the next section, also confirm that the land use affects the spatial variability of  $A_c$ . Figure 7 shows box plots of the spatial distributions of  $A_c$  of observed stream network for five sample catchments. For flooding events preceded by short duration and higher values of OF, Equation (3) gives very low values of  $D_m$ . The very low  $D_m$  gives OUHs of sharp peak and short scales which overestimated the floods. However, if we had calculated the actual  $D_m$  using the spatial variability of  $A_c$ , we could have found higher values of  $D_m$  than the value calculated using Equation (3) and the overestimation could have been avoided.

For estimating the parameters of travel time distributions of overland flow of a hillslope, we followed the original approach used in DDD (e.g. the distance from any point in the catchment to the nearest river network is calculated using the Euclidean distance and the celerity is determined from recession analysis). The GIUH and of width function estimates the distribution of travel times at the outlet of a catchment combining the hillslope and river network travel times using the steepest descent path from any point in the catchment to the outlet and the shape and scale parameters of the travel time distribution could change with the extent of hillslope saturation. Therefore, further investigation, i.e., comparison assessment is required before concluding as one method is better than the other.

#### Correlation of $A_c$ and $F_c$ with environmental factors

Environmental factors such as vegetation cover, topography and climate, affect  $A_c$  and hence  $D_m$ . Land use (e.g. vegetation cover) affects the hydrology and can affect

subsurface as well as overland flow which in turn can cause changes in the stream network, i.e.,  $A_c$  (Jonathan & Dennis 2001). The correlation results show that the denser the vegetation cover in a catchment the higher the  $A_c$  is required for initiating and maintaining a stream and vice versa, i.e., positive correlation with forest and negative correlation with bare mountain. The correlation result confirms the findings that a decrease in vegetation causes a decrease in surface resistance and critical shear stress, which result in an increase of drainage density (a reduction in  $D_m$ ), i.e., streams form easier in less vegetated catchments (Willgoose *et al.* 1991; Prosser & Dietrich 1995; Magnuson *et al.* 1997; Tucker & Slingerland 1997). Field observations also show that higher  $D_m$  and hence higher  $A_c$  is generally observed in denser vegetation cover (Morisawa 1985).

The steepness of a catchment is one of the topographical factors controlling  $A_c$  and hence  $D_m$ . In this study, we used the mean hillslope slope of a catchment and found that a catchment hillslope slope has negative correlation with  $A_c$ , i.e., the higher the steepness, the lower the  $A_c$  required to initiate and maintain stream. This finding is supported by Montgomery & Dietrich (1989) who found that stream initiation on steep slopes shows a negative relationship between valley gradient at the stream head and  $A_c$ , i.e., the higher the stream head slope the lower the  $A_c$  (lower  $D_m$ ).

The positive correlation between  $F_c$  and vegetation cover in a catchment shows that the denser the vegetation covers, the higher the  $F_c$ .  $F_c$  shows negative correlation with bare mountain, mean hillslope slope and mean annual precipitation of a catchment. The  $A_c$  and hence  $F_c$  depend on several factors, which include geology, precipitation, vegetation, morphology, soils and land uses, and one factor may be more important than another (see Table 8). Therefore, a more detailed investigation supported by field work (e.g. mapping of the slope, geology, vegetation cover and soil of a catchment at the head of first-order streams of observed river networks and mapping of the pattern of expansion of first-order streams during flooding events) should be carried out to assess how the combination of these factors control  $A_c$  and hence  $F_c$ .

We have done a simple multiple linear regression analysis using the four environmental factors as predictors, i.e., forest, bare mountain, slope and mean annual precipitation,

to estimate the response variable  $F_c$ . The result shows that only bare mountain is contributing significantly in estimating  $F_c$  with a significance level of 0.1, and the coefficient of determination of the regression ( $R^2$ ) is 0.3. The objective of the regression analysis, done in this study, is to assess a preliminary method for regionalization that can predict  $F_c$  for ungauged catchments from environmental factors and to lay a foundation for further studies.

A dynamic river network method could be implemented in rainfall-runoff models as shown for DDD for prediction of floods for catchments with a wide range of topography and land uses (Table 1). In this study, the effect of steep hills is reflected in the dynamic river networks as the steepness of a catchment is one of the factors that govern the initiation of streams. As shown in Table 8, the mean hillslope slope has a negative correlation with  $A_c$ , i.e., we need a smaller  $A_c$  to initiate and maintain streams in steep topography than in a flat topography. Table 9 also shows that the mean  $A_c$  of an observed stream network decreases as the mean hillslope slope of a catchment increases. The fundamental theory behind the method is the expansion of river networks during flooding events, i.e., whether the critical flux,  $F_c$ , which is required to initiate and maintain a stream, is satisfied or not. The magnitude of  $F_c$  depends on the magnitude of saturation excess overland flow, OF, and the critical support area,  $A_c$ . The study results also show that the critical support area, required to initiate and maintain a stream, is smaller in steep and bare mountain catchments than flat and forested catchments. Therefore, the method could be applicable at different catchments with different characteristics.

## CONCLUSIONS

The dynamic river network method, introduced in Distance Distribution Dynamics (DDD) rainfall-runoff model, can improve the prediction of flood peaks in continuous simulation satisfactorily. The performance of the DDD model is the same with and without dynamic river network in terms of KGE and BIAS. The statistical analysis on 91 flood peaks, underestimated by DDD without dynamic river network method, shows that the MARE of the prediction reduced from 32.9% to 15.7% using the dynamic river

network method. With a dynamic river network method, the 0.75 quantile of the relative errors reduced from 41% to 23%, and the 0.25 quantile of the relative errors reduced from 22% to 1%. The visual inspection of the hydrographs also shows an improvement in the prediction of flood peaks for several flooding events. Therefore, we recommend the use of a dynamic river network method in the prediction of floods. The next step in the development of the method is to investigate the applicability of the method from gauged to ungauged catchments and find a way to address the limitations identified in this study.

The critical flux,  $F_c$ , the calibration parameter introduced in the method, has been formulated as the product of critical supporting area ( $A_c$ ) and the saturated excess overland flow (OF).  $F_c$  shows stronger correlation with vegetation cover than topographical and climate factors. The parameter shows positive correlation with forest cover of catchments, and negative correlation with bare mountain, mean hillslope slope and mean annual precipitation. The simple multiple linear regression, using the four environmental factors as predictors and  $F_c$  as a response variable, shows that there is a potential to estimate  $F_c$  from environmental factors and regionalize it for using the method without calibration. The value of the calibrated  $F_c$  could be different for the same catchment of different flood magnitudes, and it could be different for the same type of vegetation cover for different catchments. This difference shows that  $F_c$  could depend on several environmental factors and further investigations should be carried out.

## ACKNOWLEDGEMENTS

The authors would like to acknowledge Cristian Lussana of the Norwegian Meteorological Institute for providing information on how to access and process the  $1 \times 1$  km spatial and 1-h temporal resolution gridded precipitation and temperature data for Norway. Finally, the authors gratefully acknowledge the financial support by the Research Council of Norway and several partners through the Centre for Research-based Innovation 'Klima 2050' (see [www.klima2050.no](http://www.klima2050.no)).

## REFERENCES

- Bencala, K. E., Gooseff, M. N. & Kimball, B. A. 2011 Rethinking hyporheic flow and transient storage to advance understanding of stream-catchment connections. *Water Resources Research* **47**, 3. doi:10.1029/2010WR010066.
- Bergström, S. 1976 *Development and Application of a Conceptual Runoff Model for Scandinavian Catchments*. Department of Water Resources Engineering, Lund Institute of Technology, University of Lund, Lund.
- Beven, K. 2011b *Rainfall-Runoff Modelling: The Primer*. John Wiley and Sons, Chichester, UK, pp. 1–360.
- Blaikie, P., Cannon, T., Davis, I. & Wisner, B. 2014 *At Risk: Natural Hazards, People's Vulnerability and Disasters*. Routledge, London.
- Blazkova, S. & Beven, K. 2002 Flood frequency estimation by continuous simulation for a catchment treated as ungauged (with uncertainty). *Water Resources Research* **38** (8), 14-11–14-14. doi:10.1029/2001WR000500.
- Boughton, W. & Droop, O. 2003 Continuous simulation for design flood estimation – a review. *Environmental Modelling & Software* **18**, 309–318. https://doi.org/10.1016/S1364-8152(03)00004-5.
- Bourdin, D. R., Fleming, S. W. & Stull, R. B. 2012 Streamflow modelling: a primer on applications, approaches and challenges. *Atmosphere-Ocean* **50** (4), 507–536. doi:10.1080/07055900.2012.734276.
- Bras, R. L. 1990 *Hydrology: An Introduction to Hydrologic Science*. Addison-Wesley, Reading, MA.
- Brocca, L., Melone, F. & Moramarco, T. 2011 Distributed rainfall-runoff modelling for flood frequency estimation and flood forecasting. *Hydrological Processes* **25** (18), 2801–2813. doi:10.1002/hyp.8042.
- Calver, A. & Lamb, R. 1995 Flood frequency estimation using continuous rainfall-runoff modelling. *Physics and Chemistry of the Earth* **20** (5), 479–483. doi:10.1016/S0079-1946(96)00010-9.
- Cameron, D., Beven, K., Ja, T. & Naden, P. 2000 Flood frequency estimation by continuous simulation (with likelihood based uncertainty estimation). *Hydrology and Earth System Sciences* **4**, 23–34.
- Camici, S., Tarpanelli, A., Brocca, L., Melone, F. & Moramarco, T. 2011 Design soil moisture estimation by comparing continuous and storm-based rainfall-runoff modeling. *Water Resources Research* **47**, 5. doi:10.1029/2010WR009298.
- Chetty, K. & Smithers, J. 2005 Continuous simulation modelling for design flood estimation in South Africa: preliminary investigations in the Thukela Catchment. *Quarterly Journal of the Royal Meteorological Society* **30**, 3–23.
- Chorley, R. J. & Morgan, M. A. 1962 Comparison of morphometric features, Unaka Mountains, Tennessee and North Carolina, and Dartmoor, England. *GSA Bulletin* **73** (1), 17–34. doi:10.1130/0016-7606(1962)73[17:COMFUM]2.0.CO;2.
- Collier, C. G. 2007 Flash flood forecasting: what are the limits of predictability? *Quarterly Journal of the Royal Meteorological Society* **133** (622), 3–23. https://doi.org/10.1002/(SICI)1099-1085(19970630)11:8<825::AID-HYP509>3.0.CO;2-G.
- Day, D. G. 1983 Drainage density variability and drainage basin outputs. *Journal of Hydrology (New Zealand)* **22** (1), 3–17.
- Di Lazzaro, M., Zarlenga, A. & Volpi, E. 2014 A new approach to account for the spatial variability of drainage density in rainfall-runoff modelling. *Boletín Geológico y Minero* **125** (3), 301–313.
- Dingman, S. L. 1978 Drainage density and streamflow: a closer look. *Water Resources Research* **14** (6), 1183–1187. doi:10.1029/WR014i006p01183.
- D'Odorico, P. & Rigon, R. 2003 Hillslope and channel contributions to the hydrologic response. *Water Resources Research* **39**, 5. doi:10.1029/2002WR001708.
- Dunne, T. 1978 Field studies of hillslope flow processes. In: *Hillslope Hydrology*, Vol. 9 (M. J. Kirkby ed.), *Geographical Research Letters* **9**, 227–293.
- Eschenbach, D., Haberlandt, U., Buchwald, L. & Belli, A. 2008 Derived flood frequency analysis using rainfall runoff modelling and synthetic precipitation data. *Wasserwirtschaft* **98** (11), 19–23.
- ESRI 2014 *ArcGISDesktop Help 10.3 Geostatistical Analyst*. https://www.esri.com/en-us/home.
- Filipova, V., Lawrence, D. & Skaugen, T. 2018 A stochastic event-based approach for flood estimation in catchments with mixed rainfall/snowmelt flood regimes. *Natural Hazards and Earth System Sciences Discussion* **2018**, 1–30. doi:10.5194/nhess-2018-174.
- Fleig, A. K. & Wilson, D. 2013 *Flood Estimation in Small Catchments: Literature Study* Naturfareprosjektet, Rapport (Norges Vassdrags-og Energidirektorat: Online) (Vol. no. 60-2013). Norwegian Water Resources and Energy Directorate, Oslo.
- Formetta, G., Prosdoci, I., Stewart, E. & Bell, V. 2017 Estimating the index flood with continuous hydrological models: an application in Great Britain. *Hydrology Research* **49**, 23–33.
- Gao, H., Cai, H. & Duan, Z. 2017 Understanding the impacts of catchment characteristics on the shape of the storage capacity curve and its influence on flood flows. *Hydrology Research* **49** (1), 90–106. doi:10.2166/nh.2017.245.
- Godsey, S. E. & Kirchner, J. W. 2014 Dynamic, discontinuous stream networks: hydrologically driven variations in active drainage density, flowing channels and stream order. *Hydrological Processes* **28** (23), 5791–5803. doi:10.1002/hyp.10310.
- Gupta, V. K., Waymire, E. & Wang, C. T. 1980 A representation of an instantaneous unit hydrograph from geomorphology. *Water Resources Research* **16** (5), 855–862. doi:10.1029/WR016i005p00855.
- Gupta, H. V., Kling, H., Yilmaz, K. K. & Martinez, G. F. 2009 Decomposition of the mean squared error and NSE performance criteria: implications for improving



- hydrological modelling. *Journal of Hydrology* **377** (1), 80–91. doi:10.1016/j.jhydrol.2009.08.003.
- Haberlandt, U. & Radtke, I. 2014 Hydrological model calibration for derived flood frequency analysis using stochastic rainfall and probability distributions of peak flows. *Hydrology and Earth System Sciences* **18** (1), 353–365. doi:10.5194/hess-18-353-2014.
- Hirabayashi, Y., Mahendran, R., Koirala, S., Konoshima, L., Yamazaki, D., Watanabe, S. & Kanae, S. 2013 Global flood risk under climate change. *Nature Climate Change* **3**, 816. doi:10.1038/nclimate1911. <https://www.nature.com/articles/nclimate1911#supplementary-information>
- Horton, R. E. 1952 Drainage-basin characteristics. *Eos, Transactions American Geophysical Union* **13** (1), 350–361. doi:10.1029/TR013i001p00350.
- Horton, R. E. 1945 Erosional development of streams and their drainage basins: hydrophysical approach to quantitative morphology. *Bulletin of the Geological Society of America* **56**, 275–370. *Progress in Physical Geography: Earth and Environment* **19** (4), 535–554. doi:10.1177/030913339501900406.
- Humbert, J. 1990 Interet de la densite de drainage pour regionaliser les donnees hydrologiques en zone montagneuse. In: *Hydrology in Mountainous Regions I, Hydrological Measurements, the Water Cycle*. IAHS Publisher, Strasbourg, pp. 373–380.
- Jonathan, L. L. M. & Dennis, P. L. 2001 Effects of forest roads on flood flows in the Deschutes river. *Earth Surface Processes and Landforms* **26**, 115–134, Vol. **26**. Washington.
- Lamb, R. & Kay, A. L. 2004 Confidence intervals for a spatially generalized, continuous simulation flood frequency model for Great Britain. *Water Resources Research* **40** (7). doi:10.1029/2003WR002428.
- Lazzaro, D. M., Zarlenga, A. & Volpi, E. 2015 Hydrological effects of within-catchment heterogeneity of drainage density. *Advances in Water Resources* **76**, 157–167. doi:10.1016/j.advwatres.2014.12.011.
- Lee, K. T., Chen, N.-C. & Chung, Y.-R. 2008 Derivation of variable IUH corresponding to time-varying rainfall intensity during storms/Dérivation d'un HUI variable correspondant à l'évolution temporelle de l'intensité pluviométrique durant les averse. *Hydrological Sciences Journal* **53** (2), 323–337. doi:10.1623/hysj.53.2.323.
- Lu, Q. & Han, Q.-L. 2011 A probability particle swarm optimizer with information-sharing mechanism for odor source localization. *IFAC Proceedings Volumes* **44** (1), 9440–9445. doi:10.3182/20110828-6-IT-1002.00507.
- Lussana, C., Ole Einar, T. & Francesco, U. 2016 Senorge v2.0: an observational gridded dataset of temperature for Norway. *METreport* **108**, 75–86.
- Magnuson, J., Webster, K., Assel, R., Bowser, C., Dillon, P., Eaton, J. & Mortsch, L. 1997 Potential effects of climate changes on aquatic systems: Laurentian Great Lakes and Precambrian Shield region. *Hydrological Processes* **11**. doi:10.1002/(SICI)10991085(19970630)11:8<825::AID-HYP509>3.3.CO;2-7.
- Maidment, D. R. 1993 *Developing A Spatially Distributed Unit Hydrograph by Using GIS*. IAHS Publication, Austin, TX, 211, pp. 181–192.
- Moglen, G. E., Eltahir, E. A. B. & Bras, R. L. 1998 On the sensitivity of drainage density to climate change. *Water Resources Research* **34** (4), 855–862. doi:10.1029/97WR02709.
- Montgomery, D. R. & Dietrich, W. E. 1989 Source areas, drainage density, and channel initiation. *Water Resources Research* **25** (8), 1907–1918. doi:10.1029/WR025i008p01907.
- Morisawa, M. 1985 *Rivers. Form and Process*. Longman Inc, New York.
- Ndiritu, J. 2009 A comparison of automatic and manual calibration using the Pitman Model. *Engineering* **34**, 62–63.
- Nhim, T. 2012 *Variability of Intermittent Headwater Streams in Boreal Landscape: Influence of Different Discharge Conditions*. 248 Student Thesis. Available from: <http://urn.kb.se/resolve?urn=urn:nbn:se:uu:diva-183137>; DiVA database.
- Ogden, F. L., Raj Pradhan, N., Downer, C. W. & Zahner, J. A. 2011 Relative importance of impervious area, drainage density, width function, and subsurface storm drainage on flood runoff from an urbanized catchment. *Water Resources Research* **47** (12). doi:10.1029/2011WR010550.
- Papageorgaki, I. & Nalbantis, I. 2017 Definition of critical support area revisited. *European Water* **57**, 273–278.
- Pathiraja, S., Westra, S. & Sharma, A. 2012 Why continuous simulation? The role of antecedent moisture in design flood estimation. *Water Resources Research* **48**, 6. doi:10.1029/2011WR010997.
- Plate, E. J. 2009 Classification of hydrological models for flood management. *Hydrology and Earth System Sciences* **13** (10), 12. doi:10.5194/hess-13-1939-2009.
- Prosser, I. P. & Dietrich, W. E. 1995 Field experiments on erosion by overland flow and their implication for a digital terrain model of channel initiation. *Water Resources Research* **31** (11), 2867–2876. doi:10.1029/95WR02218.
- Rahman, A., Hoang, T. M. T., Weinmann, P. E. & Laurenson, E. M. 1998 *Joint Probability Approaches to Design Flood Estimation: A Review Report 98/8*. CRC for Catchment Hydrology, Clayton, VIC.
- Razi, M., Ariffin, J., Tahir, W. & Arish, N. A. M. 2010 Flood estimation studies using hydrologic modeling system (HEC-HMS) for Johor river. *Journal of Applied Sciences* **10**, 930–939. doi:10.3923/jas.2010.930.939.
- R Core Team 2017 *R: A Language and Environment for Statistical Computing*. Available from: <http://www.R-project.org/>
- Reis, D. S. & Stedinger, J. R. 2005 Bayesian MCMC flood frequency analysis with historical information. *Journal of Hydrology* **313** (1), 97–116. doi:10.1016/j.jhydrol.2005.02.028.
- Rigon, R., D'Odorico, P. & Bertoldi, G. 2011 The geomorphic structure of the runoff peak. *Hydrology and Earth System Sciences* **15** (6), 1853–1863. doi:10.5194/hess-15-1853-2011.
- Rinaldo, A., Marani, A. & Rigon, R. 1991 Geomorphological dispersion. *Water Resources Research* **27** (4), 513–525.

- Rinaldo, A., Vogel, G. K., Rigon, R. & Rodriguez-Iturbe, I. 1995 Can one gauge the shape of a basin? *Water Resources Research* **31** (4), 1119–1127. doi:10.1029/94WR03290.
- Robinson, J. S., Sivapalan, M. & Snell, J. D. 1995 On the relative roles of hillslope processes, channel routing, and network geomorphology in the hydrologic response of natural catchments. *Water Resources Research* **31** (12), 3089–3101. doi:10.1029/95WR01948.
- Rodríguez-Iturbe, I. & Valdés, J. B. 1979 The geomorphologic structure of hydrologic response. *Water Resources Research* **15** (6), 1409–1420. doi:10.1029/WR015i006p01409.
- Rusjan, S., Kobold, M. & Mikoš, M. 2009 Characteristics of the extreme rainfall event and consequent flash floods in W Slovenia in September 2007. *Natural Hazards and Earth System Sciences* **9**, 3. doi:10.5194/nhess-9-947-2009.
- Schaefer, M., Elifrits, D. & Barr, D. 1979 *Sculpturing Reclaimed Land to Decrease Erosion, Paper Presented at the Symposium on Surface Mining Hydrology, Sedimentology and Reclamation*. University of Lexington, Kentucky.
- Singh, V. P. 1995 *Computer Models of Watershed Hydrology*. Water Resources Publications, Littleton, CO.
- Singh, V. P. & Frevert, D. K. 2006 Watershed models. *Experimental Agriculture* **42** (3), 370. doi:10.1017/S0014479706293797.
- Sjöberg, O. 2016 *The Origin of Streams: Stream Cartography in Swiss Pre Alpine Headwater*. 16003 Student Thesis. Available from: <http://urn.kb.se/resolve?urn=urn:nbn:se:uu:diva-277377> DiVA database.
- Skaugen, T. & Mengistu, Z. 2016 Estimating catchment-scale groundwater dynamics from recession analysis – enhanced constraining of hydrological models. *Hydrology and Earth System Sciences* **20** (12), 4963–4981. doi:10.5194/hess-20-4963-2016.
- Skaugen, T. & Onof, C. 2014 A rainfall-runoff model parameterized from GIS and runoff data. *Hydrological Processes* **28** (15), 4529–4542. doi:10.1002/hyp.9968.
- Skaugen, T. & Weltzien, I. H. 2016 A model for the spatial distribution of snow water equivalent parameterized from the spatial variability of precipitation. *The Cryosphere* **10** (5), 1947. doi:10.5194/tc-10-1947-2016.
- Skaugen, T., Peerebom, I. O. & Nilsson, A. 2015 Use of a parsimonious rainfall-run-off model for predicting hydrological response in ungauged basins. *Hydrological Processes* **29** (8), 1999–2013. doi:10.1002/hyp.10315.
- Smithers, J. 2012 Methods for design flood estimation in South Africa. *Water SA* **38**, 633–646.
- Smithers, J., Chetty, K., Frezghi, M., Knoesen, D. & Tewelde, M. 2013 Development and assessment of a daily time-step continuous simulation modelling approach for design flood estimation at ungauged locations: ACUR model and Thukela Catchment case study. *Water SA* **39**, 00–00.
- Thiemig, V., Rojas, R., Zambrano-Bigiarini, M. & De Roo, A. 2013 Hydrological evaluation of satellite-based rainfall estimates over the Volta and Baro-Akobo Basin. *Journal of Hydrology* **499**, 324–338. doi:10.1016/j.jhydrol.2013.07.012.
- Thomas, W. O. 1982 An evaluation of flood frequency estimates based on rainfall/runoff modeling. *JAWRA Journal of the American Water Resources Association* **18** (2), 221–229. doi:10.1111/j.1752-1688.1982.tb03964.x.
- Tsegaw, A. T., Alfredsen, K., Skaugen, T. & Muthanna, T. M. 2019 Predicting hourly flows at ungauged small rural catchments using a parsimonious hydrological model. *Journal of Hydrology*. doi:10.1016/j.jhydrol.2019.03.090.
- Tucker, G. E. & Slingerland, R. 1997 Drainage basin responses to climate change. *Water Resources Research* **33** (8), 2031–2047. doi:10.1029/97WR00409.
- Tucker, G. E., Catani, F., Rinaldo, A. & Bras, R. L. 2001 Statistical analysis of drainage density from digital terrain data. *Geomorphology* **36** (3), 187–202. doi:10.1016/S0169-555X(00)00056-8.
- Ward, A. S., Schmadel, N. M. & Wondzell, S. M. 2018 Simulation of dynamic expansion, contraction, and connectivity in a mountain stream network. *Advances in Water Resources* **114**, 64–82. doi:10.1016/j.advwatres.2018.01.018.
- Wharton, G. 1994 Progress in the use of drainage network indices for rainfall-runoff modelling and runoff prediction. *Progress in Physical Geography: Earth and Environment* **18** (4), 539–557. doi:10.1177/030913339401800404.
- Willgoose, G., Bras, R. L. & Rodriguez-Iturbe, I. 1991 A coupled channel network growth and hillslope evolution model: 1. Theory. *Water Resources Research* **27** (7), 1671–1684. doi:10.1029/91WR00935.
- Winsemius, H., Aerts, J., van Beek, L. P. H., Bierkens, M. F. P., Bouwman, A., Jongman, B. & Ward, P. 2015 Global drivers of future river flood risk. *Nature Climate Change* **6**, 381–385.





**Paper III:**

**Hydrological impacts of climate change on small ungauged catchments-  
results from a GCM-RCM-hydrologic model chain**

Tsegaw, A.T., Kristvik, Erle, Pontoppidan, M., Alfredsen, K., Muthanna, T. M.

*Manuscript*

This article is awaiting publication and is not included in NTNU Open

## **Appendix B: Statements from co-authors**



NTNU

Encl. to application for assessment of PhD thesis

## STATEMENT FROM CO-AUTHOR

(cf. section 10.1 in the PhD regulations)

Aynalem Tassachew Tsegaw applies to have the following thesis assessed:

### **Predicting flows in ungauged small rural catchments using hydrological modelling**

\*) The declaration should describe the work process and division of labor, **specifically identifying the candidate's contribution**, as well as give consent to the article being included in the thesis.

\*) Statement from co-author Knut Alfredsen

I hereby declare that I am aware that the work entitled as follows, of which I am co-author, will form part of the PhD Thesis by the PhD candidate who made a significant contribution to the work in the planning phase, research phase and writing phase:

- Predicting hourly flows at ungauged small rural catchments using a parsimonious hydrological model
- A dynamic river network method for the prediction of floods using a parsimonious rainfall-runoff model
- Hydrological impacts of climate change on small ungauged catchments-results from a GCM-RCM-hydrologic model chain

*Trollin 27/8-19*

Place, date

*Knut Alfredsen*

Signature co-author



NTNU

Encl. to application for assessment of PhD thesis

## STATEMENT FROM CO-AUTHOR

(cf. section 10.1 in the PhD regulations)

Aynalem Tassachew Tsegaw applies to have the following thesis assessed:

### **Predicting flows in ungauged small rural catchments using hydrological modelling**

\*) The declaration should describe the work process and division of labor, **specifically identifying the candidate's contribution**, as well as give consent to the article being included in the thesis.

\*) Statement from co-author **Tone M. Muthana**

I hereby declare that I am aware that the work entitled as follows, of which I am co-author, will form part of the PhD Thesis by the PhD candidate who made a significant contribution to the work in the planning phase, research phase and writing phase:

- Predicting hourly flows at ungauged small rural catchments using a parsimonious hydrological model
- A dynamic river network method for the prediction of floods using a parsimonious rainfall-runoff model
- Hydrological impacts of climate change on small ungauged catchments-results from a GCM-RCM-hydrologic model chain

Tjordheim, 23.08.19

Place, date

Signature co-author



NTNU

Encl. to application for assessment of PhD thesis

## STATEMENT FROM CO-AUTHOR

(cf. section 10.1 in the PhD regulations)

Aynalem Tassachew Tsegaw applies to have the following thesis assessed:

**Predicting flows in ungauged small rural catchments using hydrological modelling**

\*) The declaration should describe the work process and division of labor, **specifically identifying the candidate's contribution**, as well as give consent to the article being included in the thesis.

\*) Statement from co-author Thomas Skaugen

I hereby declare that I am aware that the work entitled as follows, of which I am co-author, will form part of the PhD Thesis by the PhD candidate who made a significant contribution to the work in the planning phase, research phase and writing phase:

- Predicting hourly flows at ungauged small rural catchments using a parsimonious hydrological model
- A dynamic river network method for the prediction of floods using a parsimonious rainfall-runoff model

Oslo, 26/8/2019  
.....  
Place, date

Thomas Skaugen  
.....  
Signature co-author



NTNU

Encl. to application for assessment of PhD thesis

## STATEMENT FROM CO-AUTHOR

(cf. section 10.1 in the PhD regulations)

Aynalem Tassachew Tsegaw applies to have the following thesis assessed:

### **Predicting flows in ungauged small rural catchments using hydrological modelling**

\*) The declaration should describe the work process and division of labor, **specifically identifying the candidate's contribution**, as well as give consent to the article being included in the thesis.

\*) Statement from co-author **Marie Pontoppidan**

I hereby declare that I am aware that the work entitled as follows, of which I am co-author, will form part of the PhD Thesis by the PhD candidate who made a significant contribution to the work in the planning phase, research phase and writing phase:

- Hydrological impacts of climate change on small ungauged catchments-results from a GCM-RCM-hydrologic model chain

Bergen d. 23. aug 2019  
Place, date

*Marie Pontoppidan*  
Signature co-author





NTNU

Encl. to application for assessment of PhD thesis

## STATEMENT FROM CO-AUTHOR

(cf. section 10.1 in the PhD regulations)

Aynalem Tassachew Tsegaw applies to have the following thesis assessed:

### **Predicting flows in ungauged small rural catchments using hydrological modelling**

\*) The declaration should describe the work process and division of labor, **specifically identifying the candidate's contribution**, as well as give consent to the article being included in the thesis.

\*) Statement from co-author **Erle Kristvik**

I hereby declare that I am aware that the work entitled as follows, of which I am co-author, will form part of the PhD Thesis by the PhD candidate who made a significant contribution to the work in the planning phase, research phase and writing phase:

- Hydrological impacts of climate change on small ungauged catchments-results from a GCM-RCM-hydrologic model chain

Oslø, 27/08-19  
Place, date

Erle Kristvik  
Signature co-author